HOLOCENE FLOODPLAIN DEVELOPMENT OF THE LOWER SYCAN RIVER, OREGON

by

POLLYANNA LIND

A THESIS

Presented to the Department of Geography
and the Graduate School of the University of Oregon
in partial fulfillment of the requirements
for the degree of
Master of Science

December 2009

"Holocene Floodplain Development of the Lower Sycan River, Oregon," a thesis prepared by Pollyanna Lind in partial fulfillment of the requirements for a Master of Science degree in the Department of Geography. This thesis has been approved and accepted by:

Dr. Patricia McDowell, Chair of the Examining Committee

Dec 1, 2009

Date

Committee in Charge: Dr. Patricia McDowell, Chair
Dr. Jim E. O'Connor
Dr. Andrew Marcus

Accepted by:

Dean of the Graduate School

An Abstract of the Thesis of

Pollyanna Lind for the degree of Master of Science

in the Department of Geography to be taken December 2009

Title: HOLOCENE FLOODPLAIN DEVELOPMENT OF THE LOWER SYCAN RIVER, OREGON

Approved: ____

Dr. Patricia McDowell

Water and pumice accumulated behind a dam that, upon failure, scoured the clay-dominated floodplain and deposited pumice sands across the Sycan Valley. The pumice originated from the eruption of Mount Mazama (approximately 7660 ybp), and dam failure occurred very shortly afterwards. In response to the flood the lower Sycan River underwent episodes of channel aggradation and degradation. This study presents the history of channel evolution for the lower Sycan River from 11,000 years ago to present, based on floodplain stratigraphy and radiocarbon chronology. Seven primary periods of channel and floodplain development are identified: I. Early Holocene Dynamic Equilibrium; II. Sycan Outburst Flood; III. Initial Channel Formation; IV. Degradation & Widening; V. Aggradation & Lateral Migration; VI. (Secondary) Degradation & Widening; VII. Modern Dynamic Equilibrium. The active floodplain of the modern lower Sycan River is flanked by terraces of the rapidly abandoned Sycan Outburst Flood deposits.

CURRICULUM VITAE

NAME OF AUTHOR: Pollyanna Lind

PLACE OF BIRTH: Lookingglass, Oregon

DATE OF BIRTH: April 26, 1970

GRADUATE AND UNDERGRADUATE SCHOOLS ATTENDED:

University of Oregon, Eugene

DEGREES AWARDED:

Master of Science, Geography, 2009, University of Oregon
Bachelor of Science, General Science, 1993, University of Oregon

AREAS OF SPECIAL INTEREST:

Fluvial Geomorphology
Geology and Physical Geography

PROFESSIONAL EXPERIENCE:

Regional Project Coordinator, Salmon Safe Program, Northwest Coalition for Alternatives to Pesticides, Eugene, Oregon, 1999-2004

GRANTS, AWARDS AND HONORS:

Research Scholarship, North Umpqua Foundation, 2005

ACKNOWLEGEMENTS

I thank my advisers Patricia McDowell, Jim E. O'Connor, and Andrew Marcus for the many hours they each invested in my evolution as a scientist and a geographer. It is difficult to imagine a better set of mentors or colleagues. I am ever grateful for their contributions and for the friendships forged in the process. This research also rests on the kindness of the landowners of the Sycan Valley and their interest in the river. To each of them I extend a warm and appreciative thank you! Access to 90% of my study area would not have been possible without them: Shields family; Phillips; Kornnelson; Kronenberger; Walkers; Hyde; Buscher; Haydn-Meyer; and Flinn. My family, friends, and co-graduate students deserve special acknowledgement. Many times throughout this process I have leaned on you and received valuable support. Thank you.

DEDICATION

I stepped on to their wide porch overlooking the Sycan Valley to ask if I could study their river. From that first moment Terry and Jessi Shields and their family opened their home and land to us. This gesture of good-will expresses this incredible family's desire to create an opportunities for people to explore and learn about the natural world. On summer nights, after a long day's work in the field, I sat around a campfire in the Shield's lower field with other students, scientists, ranchers, watershed managers, and others sharing perspectives on the landscape of the Klamath Basin. These are the true classrooms. And for this, I dedicate this research to Terry and Jessi Shields.

TABLE OF CONTENTS

Chapter | Page

Chapter Page

LIST OF FIGURES

Figure Page

LIST OF TABLES

Table | Page

Table Page

CHAPTER I

INTRODUCTION

Comprehending a region's geologic and geomorphic history is necessary to establish a context for current river processes. A channel's floodplain alluvium reflects the geologic and hydrologic history of a watershed. The type and quantity of sediment delivered "to a valley can determine the type of channel found there, as well as the variable morphology and behavior of the channel" (Schumm 2005, 60). Preserved within the stratigraphy of a floodplain are periods of aggradation that reveal the evolution of a system's available sediment (quantity and type), stream energy conditions, and the range of floodplain forming processes (Brierly and Fryirs 2005). Without such historic information on a system, river management and restoration decisions are often misguided (Thorne *et al.* 1996; Lane and Richards 1997).

This research contributes quantitative data and geomorphic interpretation to the understanding of approximately 11 ky of channel evolution, including response to large-scale environmental change, on the lower Sycan River, Oregon. The history of the lower Sycan River's channel and floodplain development is based primarily on valley morphology and stratigraphic analysis of alluvial deposits in the Sycan Valley. This is a common technique for reconstructing channel history (McDowell 1983; Gerrard 1992; Hagedorn and Rother 1992; Lane and Richards 1997; Knighton 1998; Passmore and Macklin 2000; Boggs 2001; Ogden et al. 2001; Houben 2007).

The stratigraphy of the alluvial floodplains of the lower Sycan River reveals that this system has undergone extraordinary landscape alteration and channel adjustments during the Holocene. Contributing environmental forces of channel adjustment have included changes in climatic and hydrologic conditions and the aerial deposition of pumice-rich tephra from the volcanic eruptions of Mount Mazama (7660 cal *yr* BP). This research reveals that shortly after the eruption of Mount Mazama, at approximately 7580 cal *yr* BP (Beta-252116), up to 3.5 m of Mazama pumice sands buried the Sycan Valley and lower Sycan River as a result of a landscape-altering outburst flood event.

Today, the lower Sycan River and three distinct, pumice-rich floodplain surfaces are inset below the outburst flood terraces. To understand the Holocene evolution of the lower Sycan River this thesis will address the following set of questions:

1. When did the major flood event(s) that deposited Mazama pumice sands in the lower Sycan River occur and what was the minimum flood magnitude?
2. What do the stratigraphic record and landforms in the lower Sycan River Valley reveal about the distribution of the flood-event deposits of Mazama pumice sands and the nature of the flood?
3. What sequence of geomorphic processes occurred after the flood event that resulted in the modern Sycan River system?

4. What is the character of the current channel morphology of the lower Sycan River?
5. How do the modern floodplain sediments and channel form of the Sycan differ from the pre-flood influenced river?

The evolutionary history of the Sycan River through the Holocene is unique but also comparatively valuable. Many semi-arid streams across Idaho and eastern Oregon and Washington were forced to respond to the aerial deposition of Mount Mazama tephra, as well as shifts in hydrologic regimes caused by regional climate change. This thesis determines the distribution and source of the fluvially deposited pumice sands in the Sycan Valley, presents a model of the seven major periods of geomorphic adjustment the river has undergone during the Holocene, describes potential mechanisms that initiated channel adjustments, and examines modern channel and floodplain characteristics. This research will be a vital tool for ongoing restoration efforts in the area as it will aid in understanding the geomorphic relationship of the modern lower Sycan River to its landscape.

Thesis Organization

Chapter I introduces the goals of this study, including research questions developed during the course of work. The chapter concludes with a discussion of the major geomorphic concepts related to channel response and recovery, and then offers a summary of the region's climate history during the Holocene. A description of the region and watershed characteristics are provided in Chapter II. Chapter III presents the methods used to address the research questions. The results of this study are given in Chapter IV, including: 1) descriptions of the major floodplain units of the lower Sycan River, 2) findings regarding the Sycan Outburst Flood, 3) the channel and floodplain development model of the lower Sycan River through the Holocene, and 4) a description of the geomorphic characteristics of the modern lower Sycan River. A discussion of the interpretation of climate history in relation to the geomorphic evolution of the lower Sycan River, including the role of extrinsic and intrinsic geomorphic thresholds, is provided in Chapter V. Chapter VI presents the study's conclusions.

Geomorphic Concepts of Fluvial Dynamics

Fluvial systems are inherently dynamic, adjusting in response to environmental change. However, there is limited quantitative documentation of the time scales and pathways for response and recovery of fluvial systems to environmental change (Knox 2006), in part because the range of environmental changes experienced by fluvial systems is vast. Reconstructing the channel and floodplain evolution of a river thus offers valuable insights to how a specific system responds to environmental change, while also offering an examples to compare with similar fluvial environments.

Interpretations of the geomorphic processes that formed the floodplains of the lower Sycan River are based on the characteristics of the preserved floodplain stratigraphy. A model of Holocene channel and floodplain development of the lower Sycan River (presented in detail in Chapter IV) contains seven main periods of channel and floodplain evolution. Each period represents a shift in the channel's dominant geomorphic process.

Basic concepts of fluvial geomorphology were utilized in the creation of the Holocene model of channel and floodplain development of the lower Sycan River. These concepts include equilibrium, channel relaxation rates, and geomorphic thresholds. To account for the cycles of short-term channel evolution within each period, the model relies upon concepts of complex channel response and draws on examples of decade-scale channel evolution models. These concepts are discussed below as they underlie the interpretations presented in this study.

Equilibrium

The tendency towards a state of equilibrium is key to channel evolution. Natural fluvial systems adjust to equilibrate themselves in response to change. In theory, streams evolve so that minimal energy loss is expended to sustain a channel's geometry (width, depth, and slope) given water and sediment transfer requirements (Richards 1982; Knighton 1988; USGS 1999).

However, fluvial systems are not static. Richards (1982, 254) states, "No comprehensive quantitative process-related model of channel adjustment exists because of the multivariate and indeterminate nature of river equilibrium" (Richards 1982, 254). Rivers thus are "inherently unstable" dynamic systems driven by a continually changing morphology (Lane and Richards 1997). As described by both Richards (1982) and Graf (1988a), a natural channel is in a continual flux of force (stream energy) vs. resistance (available sediment). This inherent internal process creates a negative feedback relationship that results in spatial variance of channel form (Richards 1982). To be in a steady state of equilibrium the depositional and erosional rates of a channel are relatively equal over time at a decade or century scale.

Graf (1977) states that equilibrium is typically assumed to exist in a fluvial geomorphic system if no visible change is observed in a three to four decade time frame. However, field observations, modeling, and flume based studies (Schumm et al. 1987; Simon 1992; Simon and Downs 1995; Simon and Darby 1999; Doyle and Harbor 2003; Simon and Rinaldi 2006) show that the rate and degree of channel adjustment in response to environmental change depends on the system's characteristics and the magnitude of change to which it is responding. In some channels response and recovery to a new state of equilibrium can be rapid (Knighton 1998, Fig. 5.3). In simulated modeling of channel disturbance at a low head dam, Doyle and Harbor (2003) confirmed a year to a decade "equilibrium time" for a channel to evolve to a similar bed gradient after disturbance.

In the case of large scale change or a catastrophic disturbance, channel response and recovery usually occur over longer time scales (Simon 1992). Where vast amounts of sediment are deposited, channel recovery can be substantially longer (Knighton 1998; Simon and Rinaldi 2006). If the disturbance is large enough the system will be forced to adjust to a new position of equilibrium that reflects the altered characteristics of the landscape. Issues of disturbance magnitude and response time were considered in the development of the channel and floodplain development model presented in this thesis for the lower Sycan River.

Channel Relaxation Rates

The time it takes a channel to adjust back to a state of equilibrium is considered the relaxation rate. Graf's rate law in fluvial geomorphology (1977, 189) concisely states that "geomorphic systems approach new steady states very rapidly at first, but that adjustment becomes progressively slower." And that "the form of adjustment may be explained by the distribution of available energy in the stream system." Figure 1-1 is a copy of Graf's rate law model (1977, Fig 1: 179). Knox (1972) presented a similar model for geomorphic adjustment patterns in response to abrupt climate change. A similar relaxation concept to channel evolution as a relationship between available stream energy (kinetic) and the maximum rate of energy dissipation is presented by Simon (1992), and Simon and Rinaldi (2006). They state that maximum adjustment reduces excess stream energy "by an amount proportional to the available energy and critical conditions for entrainment..." (Simon and Rinaldi 2006, 378). As a result, smaller changes will occur as the amount of excess stream energy is diminished over time. All of the models mentioned above represent a non-linear pattern of channel recovery that, depending on the disturbance, may extend throughout the fluvial system.

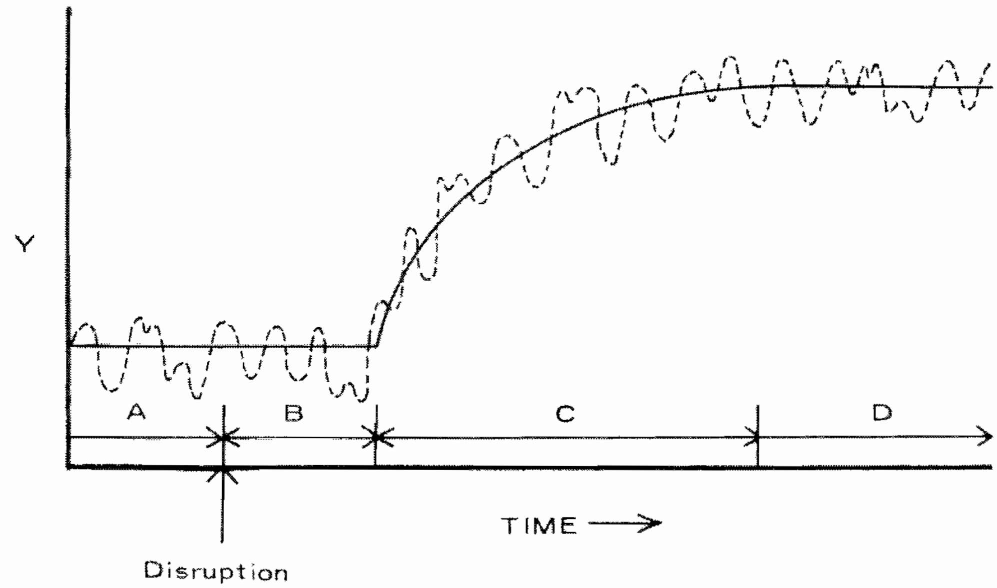

Fig. 1. Graphic representation of the response of a geomorphic system subjected to disruption. Solid line indicates mean condition, dashed line represents actual values. A system parameter, Y (some dimensional or spatial charactersitic of the system such as length or width), is in a steady state during period A. After the climatic or human disruption, new conditions are internalized by the system during period B, the reaction time. During relaxation time, period C, the system adjusts to the new conditions. The rate law provides a model for the system change during this period. A new steady state is established in period D, resulting in new dimensional characteristics as signified by a new mean value for Y.

Not all systems experience steady states. In some cases the initial condition might be in dynamic equilibrium and be drawn as a sloping line in times A and B. After a threshold value is passed, system adjustments in period C would be the same as shown in the diagram. The new conditions in time D might also be represented by a sloping line indicating dynamic equilibrium.

Figure 1-1. Relaxation curve from Graf (1977).

Represented in Graf's channel relaxation trajectory (Figure 1-1) is both the system average (solid line) and the inherent oscillations of complex channel response (dashed line). In the model of channel and floodplain development of the lower Sycan River a third element of channel evolution is also implied. The model considers the possibility of additional disturbances imposed onto an already adjusting system. As a result, a single relaxation rate trajectory toward a new state of equilibrium can be altered – shifting the trajectory of the system towards a different state of equilibrium.

Geomorphic Thresholds and Complex Channel Response

A geomorphic threshold is a "threshold of landform stability that is exceeded either by intrinsic change of the landform itself, or by a progressive change of an external variable" over time (Schumm 1979, 488). Adjustment or failure will not occur until the system has evolved or been disturbed to a critical situation of instability. When instability is reached and a geomorphic threshold is crossed, the system is put in a state of disequilibrium that produces a series of complex systematic changes as the channel responds (Shumm 1973).

As described above, stream channels are dynamic systems that evolve through varying their geometry, hydraulics, and sediment load to minimize stream energy and obtain equilibrium. It is these inherent variations and over-adjustments of fluvial systems that can create the negative feedback cycle of complex channel response. A typical complex response includes repeated periods of incision moving upstream, widening through mass-wasting at the area of maximum disturbance, and aggradation in a previously incised section downstream (Schumm 1979; Schumm et al. 1987). Headward migrating incision (knick-points or knick-zones) result in successive waves of increased local channel slope and downstream aggradation (Simon and Darby 1999; Schumm 2005). Channel evolution models for river systems responding to a variety of intrinsic and/or extrinsic landform changes have demonstrated similar complex channel response over short-term (decade scale) time frames (Womack and Schumm 1977; Simon and Hupp 1986; Simon 1989; Simon 1992; Simon and Downs 1995; Simon and Darby 1999; Simon et al. 2000; Simon and Thomas 2002; Simon and Rinaldi 2006).

The model of channel and floodplain development presented in this research for the lower Sycan River identifies seven main periods of geomorphic evolution over 10 ky. At such a large temporal scale, this channel evolution model does not attempt to capture details on the rate and scale of decadal oscillations of complex response within each major period. Instead, the model relies on the decadal channel evolution models of complex response applied from other similar river systems combined with Sycan valley floodplain stratigraphic interpretations to hypothesize episodes of complex response that the channel has likely undergone.

Climate History

Variations in climate conditions have been shown to result in both aggradation and degradation of channels (Knox 1972; McDowell 1983; Brakenridge 1988; Hagedorn and Rother 1992; Welcher 1993; Tucker and Slingerland 1997). Environmental variables associated with climate conditions that have the potential to influence a channel's geomorphology are precipitation, temperature, and vegetation. The degree of influence these environmental variables have on a fluvial system depends on the duration of the condition (e.g. extended vs. short term drought) and the geography of the landscape (e.g. stability of hillslopes).

Vegetation coverage and type is a product of an area's soil type and aridity/humidity. Vegetation acts as a stabilizer of surfaces and channel banks, and adds a roughness (resistance) to streams and floodplains that can lessen flow velocity (Knighton 1998). Vegetation is also important in soil development and it can reduce erosive processes on surfaces by providing foliage cover (Lavee et al. 1998).

Precipitation directly influences the hydrology of river systems. Quantity, timing, and type of precipitation determine a channel's discharge regime. Quantity and timing of precipitation affects stream power and activation of available sediment, which in turn are connected to channel network extension (increased runoff) or retraction (decreased runoff). When precipitation increases channel network extension it reactivates sediment from hillslopes and floodplains. As a result, a system's transport capacity is increased while simultaneously having access to more sediment. Tucker and Slingerland's (1997) study showed that an increased runoff is expected to cause a channel response of initial rapid aggradation in the alluvial portions of the river system, followed by degradation as upstream sediment supply is diminished. A decrease in runoff will retract the channel network, but geomorphic response will be more gradual. A similar system response to abrupt changes in climate was presented by Knox (1972). Climate trends of the Holocene thus are considered in this study as a potential forcing environmental variable in geomorphic processes.

Holocene Climate Reconstruction

Climate trends of the northwestern Great Basin and surrounding areas during the Holocene have been reconstructed primarily through pollen, charcoal, macrofossils, animal middens, tree ring records, lake level variations, diatom concentrations, and area lithologies. Table 1-1 contains a summary of climate reconstructions related to effective moisture and annual precipitation from studies done throughout the region.

The climate history of the northwestern Great Basin shows some spatial variation but overall trends in climate conditions overshadow them. Still, interpretations of the constructed climate data of lakes in close proximity to the Sycan River (Klamath, Patterson, and Lily) are emphasized in this research. As a primary source of surface water discharge to Klamath Lake the climate data from Bradbury et al. (2004) is given greatest priority when interpreting shifts in discharge of the Sycan River.

During the early Holocene (10-5 ka yr BP) the area experienced drier, warmer conditions than present. This extended dry and warm period led to intensified droughts in some studies at approximately 7.5- 6.0 ka (Mohr et al. 2000; Wigand and Rhode 2002; Bradbury et al. 2004). Imposed upon the early Holocene drought trend was the eruption of Mount Mazama (7660 cal *yr* BP). Inputs of mass quantities of pumice-rich tephra across the northwestern United States appear to have exaggerated arid conditions in places such as Dead Horse Lake, Oregon (Minckley et al. 2007), Klamath Lake (Bradbury et al. 2004); Flathead Lake, Montana (Hofman 2005), and Long Valley, Idaho (Doerner and Carrara 2001). Bradbury et al. (2004) showed that lake levels in Klamath Lake were at their lowest between 7.5 – 5.0 ka yr BP.

Age (cal yr BP x 1,000)	Northwestern Great Basin				Klamath Mountains, CA			Southeastern Cascades, CA
	Klamath Lakes	**Patterson & Lily Lake**	**Summary**	**Summary**	**Bluff Lake**	**Cedar Lake**	**Crater Lake**	**Medicine Lake**
0	Higher lake levels, increased precip	Present conditions	Climate variability across region	Coolest and most moist				
			Drought					
1–3	Increased precip and Q into Upper Klamath Lake; cooling, moist trend; ample Q to lakes by 4 ka yr BP; at 1-0.2 ka years lake levels lowered	Higher than present	Increase in winter precip: water table reaches Holocene max by 3.7 ka yr BP	Cooler and more moist than previous; increased effective moisture	Cooler	Summer droughts		Increasing precip; decrease in available moisture at 2 ka yr BP
3		Lower				Cooler and wetter		
4		Higher than present	Increase in winter rainfall; minimal droughts				Cooler trend; increased precip	
5–7	Drier climate than present; reduced winter storms; lower Q inputs -- low seasonal water levels; 7.5-5 ka yr BP lowest lake levels -- low Q and high sediment loading , 6-5 ka yr BP lakes begin to rise with a slight increase in precip	Lower than present	Severe regional drought; aeolian dune development	Hot and dry; reduced effective moisture; drought begins to end ~ 5.3 ka yr BP	Cooling trend but warmer and drier than present	Warmer and drier than present; increased drought conditions		
8			Dry and warm with potential summer monsoons		Intensified summer drought		Warmer and drier than present	Drier than present; precip began to increase at 7 ka yr BP (snow/rain)
9–10				Dry, cool summers				
		ANNP						
	Bradbury et al., 2004	Minckley et al., 2007	Wigand and Rhode, 2002	Grayson, 1993	Mohr et al., 2000			Starratt et al., 2002

Q = Discharge, precip = precipitation; ANNP = annual precipitation

Table 1-1. Holocene climate reconstruction of the NW Great Basin, Klamath Mountains, CA and Southeastern Cascades, CA.

Increasing precipitation and cooler temperatures are the prevailing trend through the later half of the Holocene (5.0 ka yr BP to present). According to evidence of gradually rising lake levels, a shift towards a wetter, cooler climate began in the Klamath Lake area at 6.0-5.0 ka (Bradbury et al. 2004) with increasing precipitation. By 5.0 ka yr BP, much of the region's climate conditions were experiencing the trend of cooler temperatures and increased precipitation. At Patterson and Lily Lakes (Minckley et al. 2007) annual precipitation was higher than present from the mid Holocene. This was also expressed at Bluff, Cedar, and Crater Lakes in the Klamath Mountains of California (Mohr et al. 2000).

A short period of decreased precipitation and cooling is reflected in some of the climate reconstruction records of the late Holocene. At Klamath Lake this is noted as occurring between 1.0 – 0.2 ka (Bradbury et al. 2004). Wigand and Rhode (2002) describe this period as a drought in the northwestern Great Basin beginning at ~ 1.0 ka. In the Siskiyou Mountains, west of the Cascade Mountains, Briles et al. (2008) reports a cooling period between 1.2 – 0.3 ka yr BP. All of these climate shifts are attributed to a cooling episode known as the "Little Ice Age." In the last ~ 500 years the climate has trended overall toward a wetter climate that defines the present conditions of the region with relative warming and drying occurring in the last ~150 years.

CHAPTER II

REGIONAL SETTING

Regional Description

The Sycan River is the largest tributary of the Sprague River, which is located in the upper Klamath Basin of south-central Oregon (Figure 2-1). The upper Klamath Basin lies at the northwestern most boundary of the Basin and Range province and along the eastern edge of Oregon's southern Cascade Mountains. The Basin and Range province is dominated by tectonic extension that is expressed as north-northwest trending horst and graben faults throughout the upper Klamath Basin. Along the eastern boundary of the Klamath Basin, the development of the Cascade Mountains has resulted in a complex volcanic history that includes, but is not limited to, faulting and periodic inputs of volcanic materials. Bedrock materials across upper Klamath Basin and the Sycan River watershed are mostly basalts and rhyolites from the upper Miocene and Pliocene with lacustrine sedimentary rocks locally layered within the bedrock (Sherrod and Pickthorn 1992).

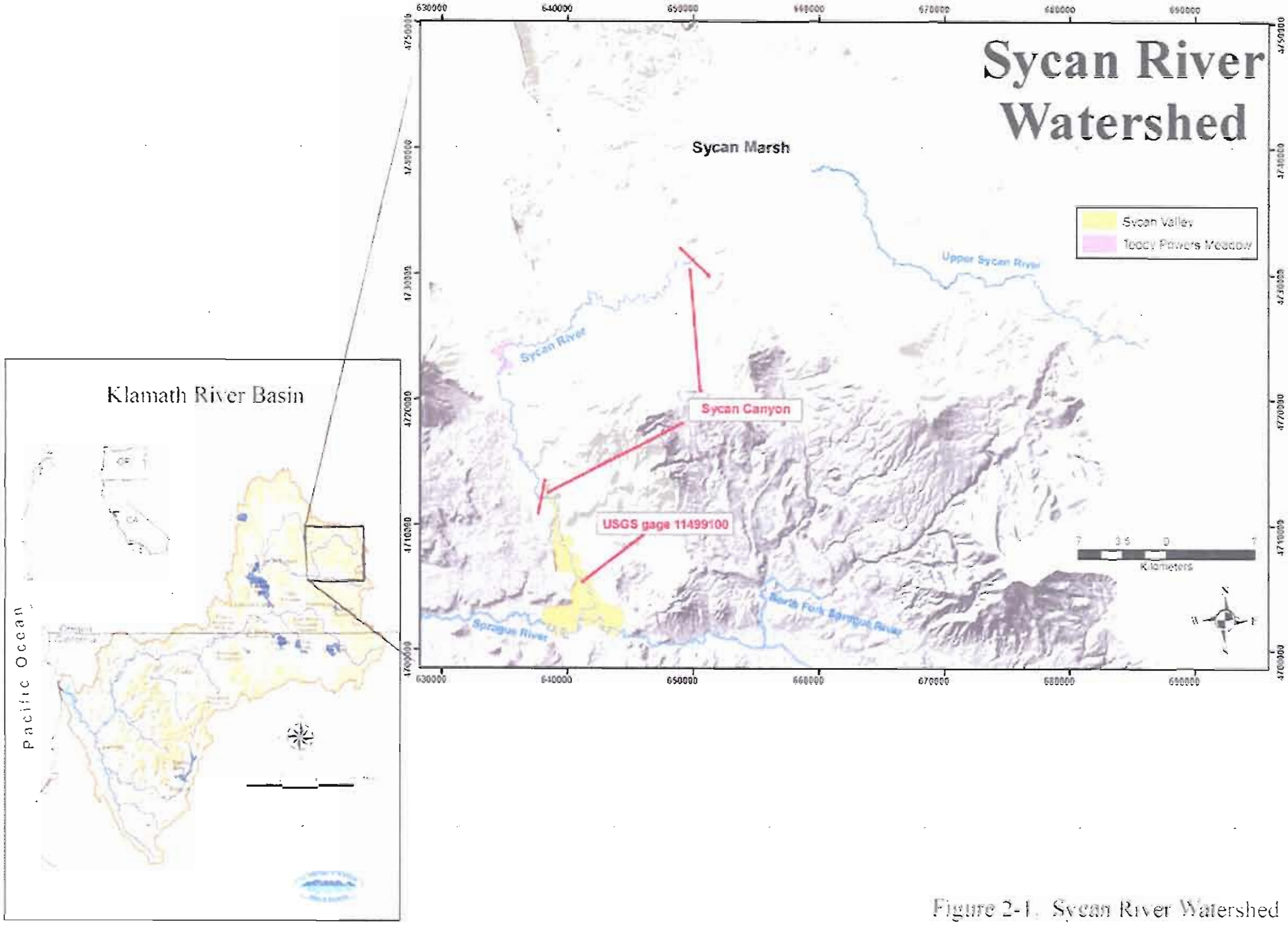

Figure 2-1. Sycan River Watershed

The Cascade Mountains create a rain shadow on the eastern side of the range. The upper Klamath Basin is considered a semi-arid region with annual precipitation in the Sprague River basin averaging approximately 38 to 64 cm per year with 30 to 50 percent received as snowfall during the winter months (Loy et al. 2001). A small portion of the annual precipitation is received in the summer months as thunderstorms.

Only 56 km from Crater Lake, the Sycan River watershed received an abundance of volcanic tephra as a result of Mount Mazama's massive pyroclastic eruptions approximately 7660 cal *yr* BP. The tephra plume traveled northeastward from Mount Mazama. As a result, airfall tephra was deposited, ranging from approximately 50 cm thick in the northern part of the Sycan Basin (Sherrod and Pickthorn 1992) to five cm in the more southern lower Sycan Valley. Today the watershed is dominated by non-cohesive pumice rich soils either as alluvium in the valleys or as a mantle over the Miocene and Pliocene basalt flows (NRCS 2005).

Characteristics of the Sycan River Watershed

The Sycan River originates on the northern flank of Gearhart Mountain (peak at 2,551 m above sea level) located at the eastern margin of the watershed. The Sycan flows over the volcanic plateau, then enters the Sycan Marsh, an 88 km^2 depression historically occupied by extensive wetlands. The Sycan River exits the marsh at the southwest end and flows through Sycan Canyon for roughly 45 river km. Sycan Canyon is a basalt-walled canyon just 35 m wide at its most narrow points. The least confined area of the canyon is at Teddy Powers Meadow where the canyon opens for 3.5 km river-length with a floodplain that stretches up to 360 m across. Downstream from Teddy Powers Meadow is the steepest 13 km of Sycan Canyon, known as Coyote Bucket. Upon exiting Sycan Canyon the lower Sycan River meanders at a low gradient for 16 river km through the southward widening Sycan Valley to its confluence with the Sprague River. A photo gallery of the river is provided in Appendix A.

The basin area of the Sycan River is 1,470 km^2 with an elevation drop of 1,140 m over its 92 river km. Except through the lowermost thirteen kilometers of Sycan Canyon, the Sycan River maintains a relatively low gradient for 62.21 km from the mouth of Sycan Marsh at 1514 m to its confluence with the Sprague River at 1312 m (Figure 2-2).

The Sycan Valley widens southward for 12 km from the mouth of Sycan Canyon toward its confluence with the Sprague River. The lower Sycan River is a moderately meandering system with a sinuosity of 1.4. Channel slope from the head of Sycan Valley to the confluence with the Sprague River is just 0.000238. Generous perennial springs emerging along the margins of the valley sustain tributaries and subsurface hydrologic inputs. Pumice-rich horizontal terraces composed of Sycan Flood deposits flank the lower Sycan River and its active floodplain. The modern lower Sycan River through Sycan Valley has characteristics most similar to Nanson and Croke's (1992) medium to low energy floodplain, of partially-cohesive materials, with lateral migration and a scrolled floodplain.

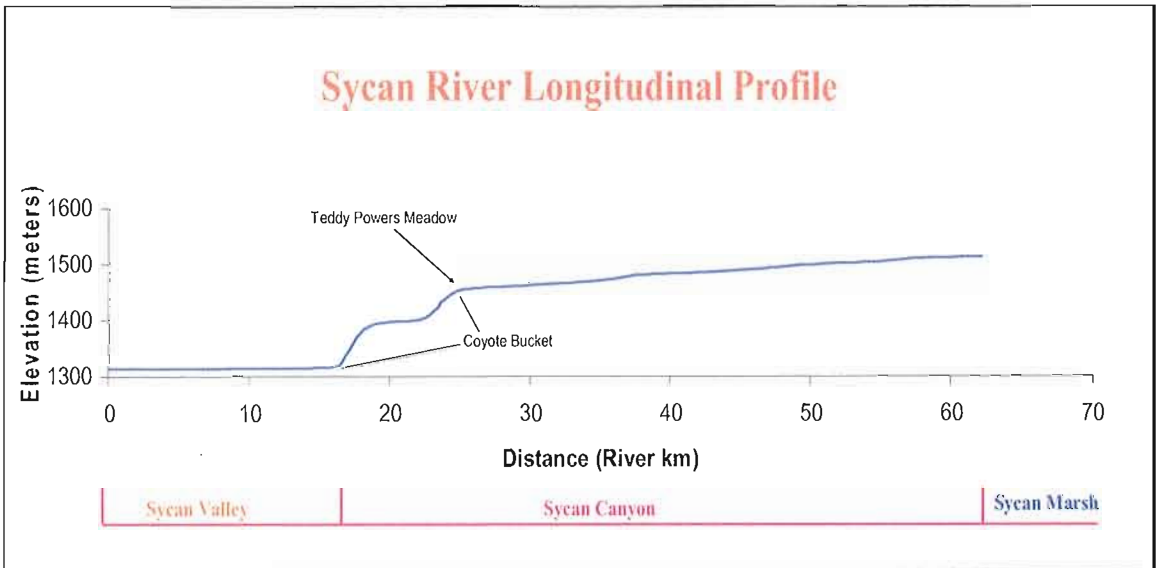

Channel Slope:

Sycan Valley = 0.000238
Coyote Bucket = 0.0113
Upper Sycan Canyon = 0.00173

Figure 2-2. Longitudinal profile and channel slope of Sycan River from the mouth of Sycan Marsh to the confluence with the Sprague River.

The lower Sycan River from 1978 to 2007 had an average daily discharge of 4.3 cms, with peak flows during seasonal snow melt events of up to 28 cms (USGS 2008). Dry summer months return the river's base flow to a mean flow of 0.68 cms, fed primarily from perennial springs (USGS 2007). Figure 2-3 depicts the seasonally fluctuating hydrograph of the Sycan River from the mean monthly discharge data of 1978 to 1991.

The majority of the Sycan watershed is within the Winema and Fremont National Forests. Only the lower Sycan Valley and small in-holdings upstream are privately owned and managed. Parts of Sycan Marsh have been owned and managed by the Nature

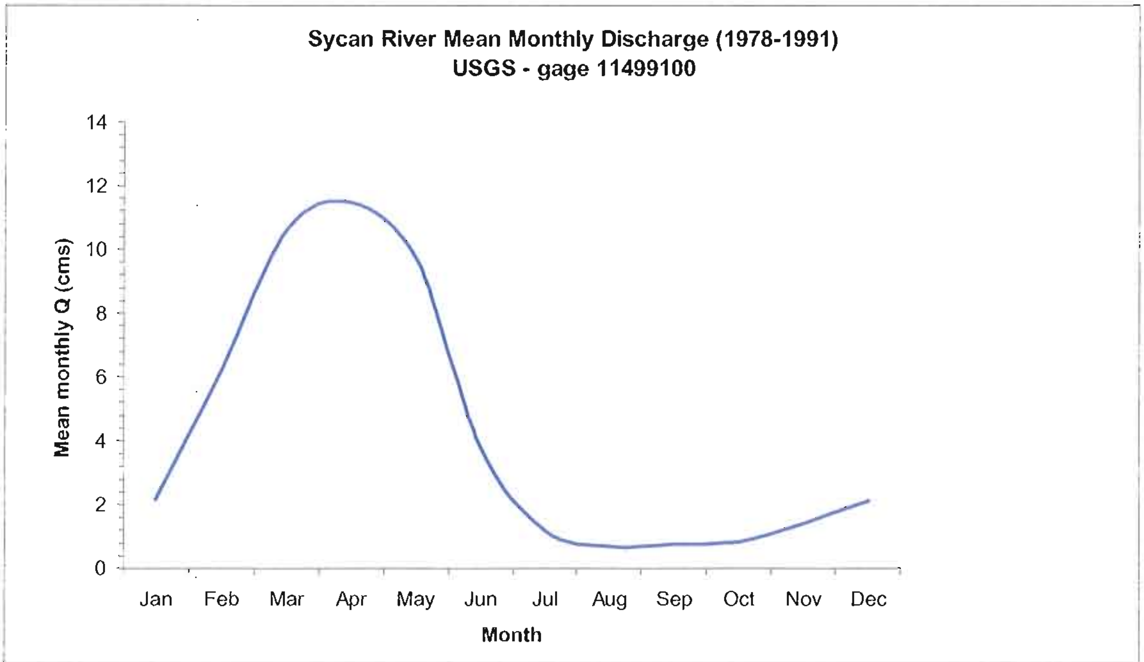

Figure 2-3. Hydrograph of the mean monthly discharge of the lower Sycan River (1978 – 1991). Discharge gage 11499100 located on the Sycan River below Snake Creek.

Conservancy since 1980. Cattle ranching is the main land use on private lands while timber harvest and cattle grazing leases are permitted on the public lands of the national forests.

The Sycan Marsh is vegetated with wetland grasses and forbs. Ponderosa and lodgepole pine forests dominate the landscape in the uplands of the Sycan watershed, while sage and sparse juniper and pine trees vegetate the terraced floor of the valley (NRCS 2005). Grasses, rabbit brush, sage, and the occasional currant or wild rose have established themselves across the surfaces of the inset floodplain terraces. Riparian vegetation species such as willow, rush and sedge commonly occur along the channel margin or spring outlets (Massingill et al. 2008).

CHAPTER III

METHODOLOGY

Data Collection and Analysis

Diverse data collection and analysis were required to document the complex set of geomorphic adjustments the Sycan River has undergone during the Holocene. Observations of surface morphology and deposits were made from the mouth of Sycan Marsh to the terminus of the Sycan River, with the majority of data collected from the floodplain of the Sycan Valley. Composition of floodplain deposits and their location were mapped in conjunction with channel form. Mapping and analysis of the data combined field based and digital imagery techniques.

Locations of field sites were recorded with resource-grade Trimble GPS units that have horizontal accuracies of 10 cm to a few meters and vertical accuracies of 1 m depending on the availability and positioning of satellites, and instrument programming parameters. For this research a maximum pdop (dilution of precision) of 5.0 was programmed on the instruments to restrict the collection of 3D GPS data. This restriction ensured that the probability of 3D accuracy was kept to approximately 1-3 m. Accuracy of GPS points was further enhanced by post-processing the data.

All digital analysis and mapping were done in ArcGIS. The remotely sensed data, aerial imagery and maps used included historic black and white aerial photos from the U.S. Department of Agriculture (1940 and 1968) that I rectified in ArcMap using the protocol defined by Hughes et al. (2006) for highest accuracy. Other imagery include black and white digital orthoquads created by the U.S. Geological Survey (2000); 7.5 minute U.S. Geological Survey topographic maps (multiple year sets) both paper and digital (rectified); color digital orthoquads created by the U.S. Geological Survey (2005); and rectified color photos collected in conjunction with LiDAR imagery. The high resolution digital elevation data (LiDAR) were collected and processed by Watershed Sciences, Inc, for the Klamath Tribes in 2004.

Reconstruction of Floodplain Development

Stratigraphy

Reconstruction of the Holocene channel evolution and floodplain development of the lower Sycan River is based primarily on detailed stratigraphic descriptions of floodplain deposits. The primary field sites for collecting detailed stratigraphic data in the Sycan Valley are mapped in Figure 3-1. The sites consist of two soil pits (PIT), 19 bank exposures (BE), and seven augers holes (AUG). All primary sites are located in the Sycan Valley except one soil pit (PIT-02) at river km 60.7 and one bank exposure

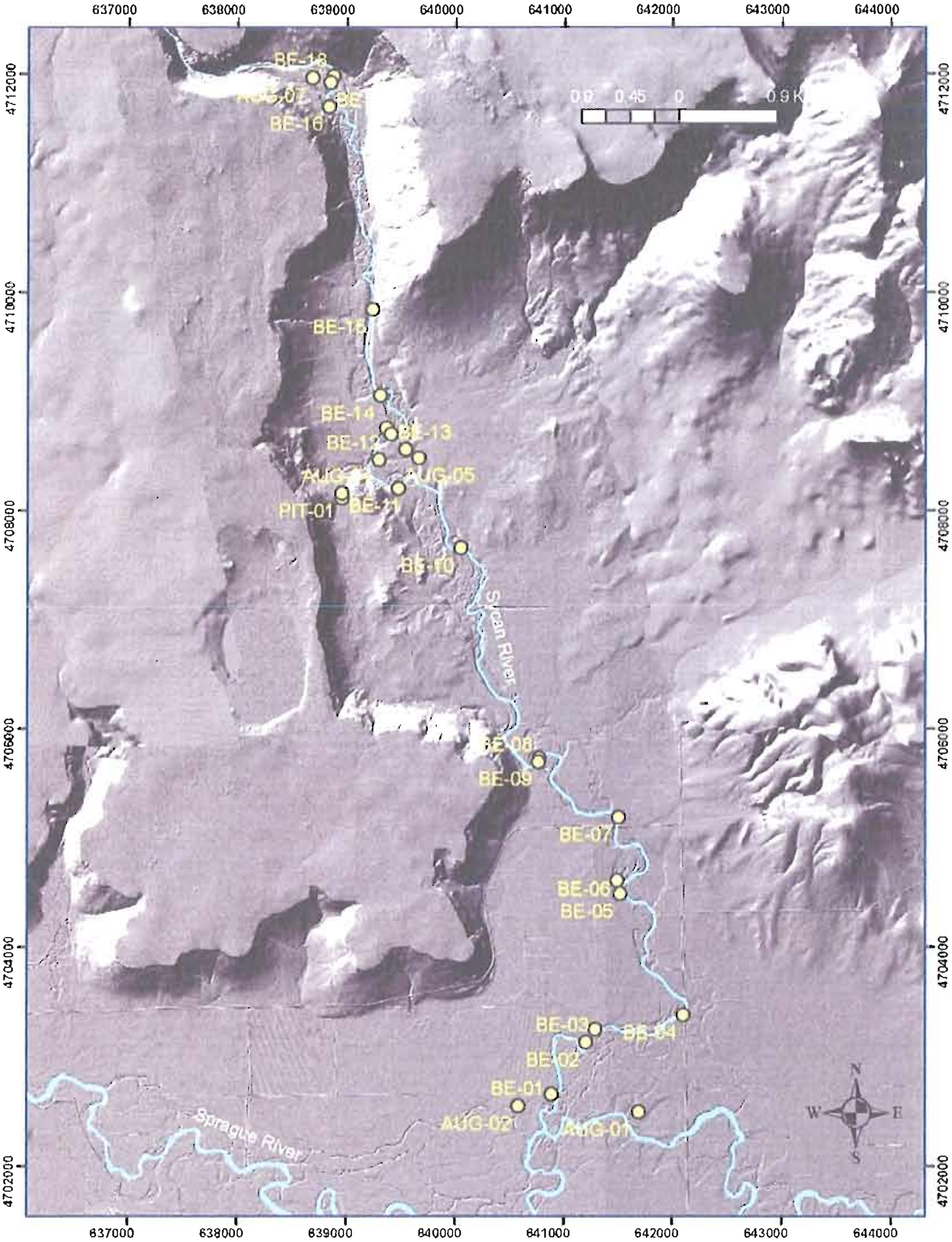

Figure 3-1. Stratigraphic sites in the lower Sycan Valley:
BE (bank exposure); AUG (auger hole); PIT (soil pit)

(BE-19) at river km 53 located in upper Sycan Canyon. All pits and bank exposures were excavated with shovel and trowel. A hand operated 3 ¾ inch diameter bucket-head auger with extension arms was utilized for augering. In addition to the primary sites, numerous soil probes and site-based morphology observations of the floodplain surfaces and composition support channel history reconstruction and surface mapping.

Utilizing the architecture of a floodplain to reconstruct channel history is a conventional technique in geomorphology. A few examples of such reconstructions include McDowell (1983) on Brush Creek in Wisconsin; Hagedorn and Rother (1992) in Lower Saxony Germany; Passmore and Macklin (2000) on the South Tyne in England; and Houben (2007) on the river Wetter in Germany. On the Sycan River, material composition, physical characteristics, and erosional unconformities of the stratigraphic sequences were recorded. Interpretation of the fluvial processes associated with each stratum was done on site. The descriptions were done in vertical sequence with relative depth of each layer measured from the surface of the floodplain. These data facilitated the correlation of depositional sequences within disparate terraces across the floodplain. The stratigraphic diagrams and descriptions for each primary site are available as Appendix B.

Chronology

A chronology of the formation of the geomorphic units was constructed from calibrated radiocarbon dating of organic materials (i.e. seeds, charcoal, wood stems) collected from in situ stratigraphic layers. The organic samples were processed through

Beta Analytic and the U.S. Geological Survey (USGS) laboratories. Beta Analytic utilizes Accelerator Mass Spectrometry (AMS) radiocarbon dating procedures through the International Consortium of Accelerator Laboratories (ICAL). A full description of their sample processing and radiocarbon dating protocol is available on their website at http://www.radiocarbon.com/international.htm. USGS process samples at their laboratory in Reston, Virginia, and ^{14}C ages were determined at the Center for Accelerator Mass Spectrometry (CAMS), Lawrence Livermore National Laboratory, Livermore, California.

To simplify the channel development chronology a single adjusted date for each sample was derived from the probable mean of the calendric age-spans at the 2-sigma error range in years before present. Table 3-1 presents the calibrated and adopted ages of the samples utilized in this research. All ^{14}C dates were calibrated using the program CALIB REV5.0.2 (Copyright 1986-2005, M Stuiver and PJ Reimer) that is used in conjunction with Stuiver and Reimer (1993) and available publically at http://calib.qub.ac.uk/calib/calib.html.

Calibration with CALIB REV5.0.2 produces a probability curve of the age range possible for each calibrated date (calibrated years before present -- cal *yr* BP). An adopted age was derived by selecting the age of highest probability nearest the reported median (p50), as depicted on the probability curves created in the calibration process. For example, at BE-18 an adopted age closest to the mean by a decade, but with higher probability than the calibrated median age of 601 cal *yr* BP, was selected because the median date occurs at a point of low probability on the curve (see Appendix Figure C-2).

Strat Site	Material	Lab	Lab Sample Code	Corrected Conventional 14C age BP	14C age error (+/-) years	$\delta^{13}C$*	Calibrated Age [2 sigma range] - cal yr BP	Median Age (p50) - cal yr BP	** Adopted Age - cal yr BP	Floodplain Unit
BE-13	charcoal	USGS	WW6097	516	33	-25	604 - 627	534	530	T1
BE-18	wood	USGS	WW5422	630	35	-25	551-663	601	590	T1
BE-12	charcoal	USGS	WW6096	1399	33	-25	1277-1358	1311	1300	***
BE-06	willow stem	Beta	234718	1460	40	-26.2	1296-1410	1350	1350	T2
BE-14	wood	USGS	WW6095	1714	33	-25	1546-1702	1622	1610	T2
BE-08	plant material	USGS	WW6419	2030	30	-25	1898-1914 1918-2062 2086-2105	1980	1980	T2
BE-03	plant material	USGS	WW6420	2215	30	-25	2151-2326	2232	2230	T2
BE-09	charcoal	Beta	234714	4760	40	-22.8	5329-5378 5449-5589	5513	5540	T2
BE-05	charcoal	Beta	234715	5160	40	-22	5756-5823 5881-5994	5921	5920	T2
BE-02	seed	Beta	252116	6790	40	-24.1	7579-7682	7634	7630	T4
AUG-07	charcoal	USGS	WW5421	10075	35	-25	11398-11819	11640	11640	T4
N. Fork Sprague	wood	Beta	234716	3890	40	-25	4259-4263 4269-4270 4288-4411	4327	4330	na

* δ13C values of -25 are assumed in calibration unless otherwise listed. All 14C dates are calibrated using the program CALIB REV5.0.2 (http://calib.qub.ac.uk/calib/calib.html).

** Adopted Age (cal *yr* BP) is derived by selecting the age of highest probability nearest the reported mean as depicted on the probability curves created in the calibration process. Adopted Age is rounded to the nearest 10th.

*** Sample discarded due to incongruence of calibrated age range to related stratigraphy and the high likelihood of bioturbation emplacement of the sample by burrowing animals.

Table 3-1. Calibrated and adopted age of carbon samples and the related stratigraphic site and geomorphic unit.

The adopted age is rounded to the nearest decade. Descriptions of chronology and events within this paper refer to the adopted age. The probability curves for the samples are available in Appendix C.

Organic samples from all the Holocene floodplain units, except the Sycan Outburst Flood Terrace (T_3), were collected and radiocarbon dated for this research. No organic material adequate for radiocarbon dating was found within the T_3 flood deposit sequence. A conservative maximum age of the flood event is extrapolated from radiocarbon dated seeds buried directly below the deposits.

The date listed in this thesis for the pyroclastic eruptions of Mount Mazama is a mean age derived from separately published dates. I recalculated the mean age of the eruption by recalibrating the published ^{14}C dates of GSC (1971), Bacon (1983), Hallett et al. (1997), Zdanowicz et al. (1999), and Bacon and Lanphere (2006). An adopted age of 7660 cal *yr* BP was calculated, very similar to the calibrated age reported by Hallet et al. (1997).

Geomorphology of the Lower Sycan River

Channel Slope

Channel slope of the Sycan River from the mouth of Sycan Marsh to its confluence with the Sprague River was calculated using elevation data from contour lines of U.S. Geological Survey (USGS) digital topographic 7.5 minute maps and then recalculated in the lower Sycan River with LiDAR elevation data to get greater precision. From the lower Sycan Canyon to the confluence with the Sprague River channel elevation and river length were extracted at 200 m intervals along the river centerline. Where LiDAR data were not available from the channel's water surface due to the reflective properties of water, either slope was not calculated for that interval, or the lowest elevation of a low land surface next to the channel was used. The calculated slope using the 7.5 minute USGS topographic maps is 0.000270 and the slope is 0.000238 using the high resolution LiDAR data. This acceptably low difference (0.000032) between the calculated slopes validated the methodology of using topographic maps to calculate channel slope through Sycan Canyon where LiDAR data is not currently available. Figure 2-2 is a longitudinal profile showing channel slopes of sections of the Sycan River from the mouth of Sycan Marsh to its terminus.

Floodplain Inundation

To determine the frequency of a flood event that would inundate the active floodplain of the lower Sycan River, a recurrence interval analysis was done (Knighton 1998). Peak discharge data (1974-2007) from the lower Sycan River at gage 1499100 located below Snake Creek near Beatty, Oregon were ranked. The recorded discharge from spring of 2006 was used to determine the frequency of inundation because we observed inundation during that season's high-water flow. Lower flows than the 2006 spring discharge likely inundate the active floodplain but no observations were done to confirm this assumption.

Geomorphic Map

A geomorphic map of the floodplain of the Sycan Valley was created to display relationships among geomorphic units and the river. The geomorphic map units are based on stratigraphic descriptions, auger probes, field morphologic observations, USDA soils classifications, aerial imagery, and digital elevation analysis of high resolution LiDAR. The map is segmented into five plates of a finer scale to illustrate the detailed relationship of the geomorphic units. Geomorphology map plates 1-5 are in Appendix D.

Use of stratigraphic data in combination with imagery and surface topography is recommended for accurate geomorphic mapping (Brakenridge 1988; Knighton 1998). In the Sycan Valley, it was not possible to examine the stratigraphy of every floodplain surface due to the size of the study area and the complexity of the features. In areas without stratigraphic descriptions boundaries between floodplain units were extrapolated based on field observations, surface morphology, NRCS soils data, and relative elevations generated from the 2004 LiDAR. Where map scale, site distribution, and field checking allowed, the burial of Sycan Outburst Flood Terrace (T_3) units by another unit is mapped, but other floodplain unit burials are not mapped.

Characteristics of the Sycan Outburst Flood

Volume

The volume of sediment deposited and an estimated minimum discharge of the Sycan Outburst Flood were calculated from field and GIS generated data. Volumetric estimates of the flood deposits were calculated from measured depths and mapped widths of the remnant flood deposits in the Sycan Valley. Flood deposits are used to establish minimum flood stage when evidence of maximum flood stage such as strand lines or wave cuts is not visible (Williams and Costa 1988; O'Connor and Baker 1992; Enzel et al. 1994; Cornwell 1998). As described by O'Connor and Baker (1992), a deposit-based estimate reflects only the minimal values of flood stage because depth of water above the feature is unknown.

To account for the gradual downstream decreasing thickness of deposits the boundary of the flood lobe was divided into three segments prior to calculation. Average thickness, assumed to be equivalent to minimum flood depth, for each segment was derived from field measurements at stratigraphic description sites. Flood deposit segmentation and area calculations for each were combined to get total volume of deposits in the lower Sycan Valley (Figure 3-2).

Flood water volume estimates were calculated to determine the locations within the watershed capable of storing the water necessary to create the Sycan Outburst Flood. Water to flood deposit concentrations of 50% and 80% were used to establish a probable range of flood volume. These percent volumes were used because the Sycan Outburst Flood is considered a hyper-concentrated flood, for reasons discussed in Chapter IV.

The storage capacity of potential reservoir sites was determined in ArcGIS using a 10 m digital elevation model (DEM). The DEM was created by the US Geological Survey, and made available by the Oregon State Service Center for GIS through Oregon

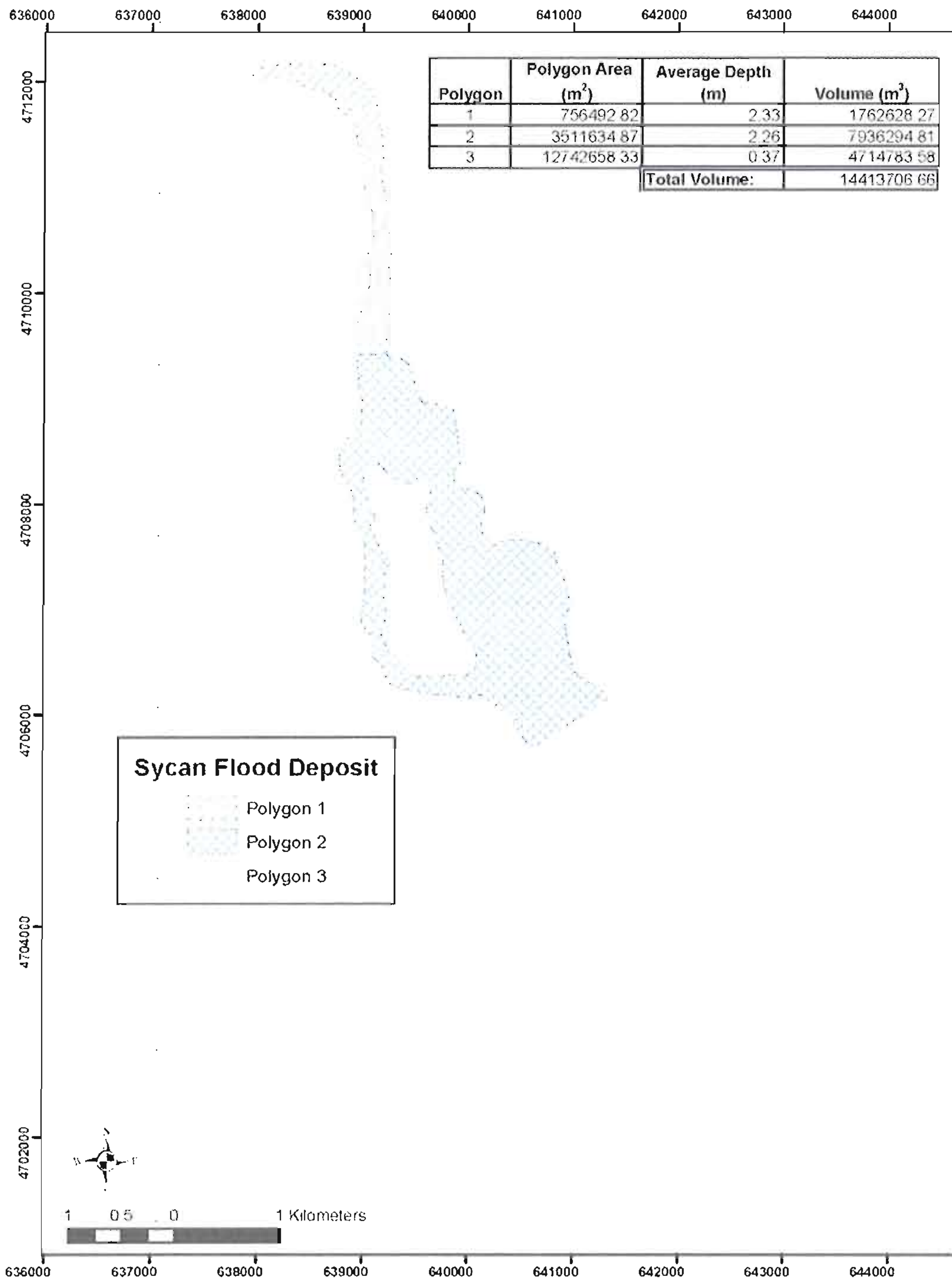

Polygon	Polygon Area (m^2)	Average Depth (m)	Volume (m^3)
1	756492.82	2.33	1762628.27
2	3511634.87	2.26	7936294.81
3	12742658.33	0.37	4714783.58
		Total Volume:	14413706.66

Figure 3-2. Area and volume estimates of the Sycan Outburst Flood deposits.

Geospatial Enterprise Office, (http://www.oregon.gov/DAS/EISPD/GEO/data/dems.shtml).

Calculating minimum flood volume from flood deposit geometry is an uncommon technique because sediment concentration is assumed. In the Sycan, additional limiting factors need to be recognized. It was assumed that the flood deposit lobe covered a horizontal valley floor unscoured by flood waters or other pre-flood processes. A channel likely existed on the valley floor prior to the flood but its depth and complexity are not known. Stratigraphic observations suggest that the pre-flood floodplain surface was marshy and the channel unincised. An additional limitation of the calculation is that deposit depths at the distal end were limited to truncated sections that display an eroded upper boundary and thus may reflect a smaller volume of sediment than was originally deposited.

Discharge

Flood discharge estimates were calculated from field and GIS (LiDAR) generated data at cross section “A” at river kilometer 15.8 near the head of Sycan Valley (Figure 3-3). This cross section location was selected because of the presence of flood deposited boulders located at the distal end of an elongate boulder bar, available stratigraphic information of the floodplain, available LiDAR data, the depth of the modern channel is easy to collect because it is a riffle, and there is minimal modern floodplain deposition within the active floodplain boundary.

Flood discharge was calculated using the basic discharge equation

$$Q=V*A$$

where Q (discharge) is equal to the V (velocity) of flow moving through a cross section of the river multiplied by the A (area) of the cross section.

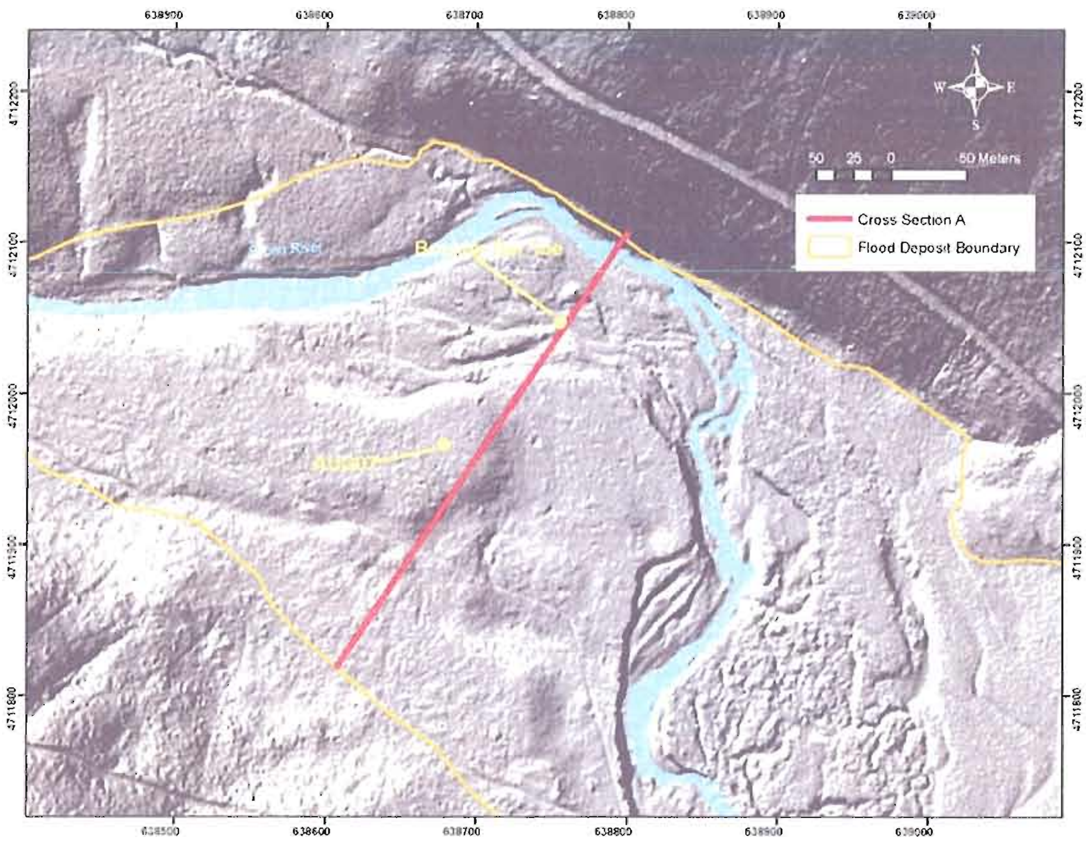

Figure 3-3. Map - cross section "A" on the Sycan River at 15.8 river km.

Velocity of flood flow was derived using O'Connor's (1993) flow competency equation:

$$V = 0.29D_i^{0.06}$$

where Di (intermediate boulder diameter) is used to determining the competency of the flow to transport boulder-sized material. Conaway (2000) used maximum boulder diameter (D_{max}) in the competency equation to estimate the discharge of the Williamson River breakout flood. For the Sycan Outburst Flood event a set of boulders with a D_{max} of approximately 100 cm located at the downstream end of an elongate boulder bar were used (Figure 3-4). These boulders are considered flood deposit boulders because they are rounded, associated with the relatively large-scale boulder bar, and larger than any of the cobbles and gravels of the modern channel by a factor of at least ten.

Area (width x depth) of the floodwater cross section was calculated from data generated digitally from the high resolution LiDAR elevation data combined with augered Outburst Sycan Flood deposit thickness (AUG-07). The width of the cross section was derived from the confining walls of the valley at the cross section. The flood depth was calculated as the difference between the highest remnant flood deposits and the pre-flood paleosol surface. The surface of the buried paleosol is assumed to be horizontal across the floodplain. Surface elevation of the paleosol is derived at AUG-07, only 17.50 m from cross section "A" (Figure 3-5).

Figure 3-4. Boulder bar toe at cross section "A" (15.8 river km).

The duration of the flood event was estimated by assuming a triangular hydograph. Using the peak discharge and flood water volume estimates the time necessary to release the quantity of water in a single flood event was calculated by dividing the discharge (m^3/sec) by the volume (m^3).

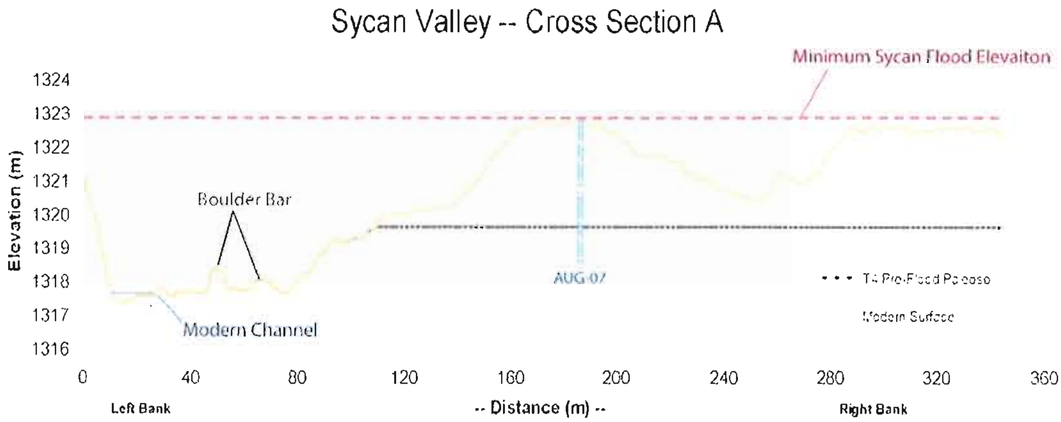

Figure 3-5. Cross section "A" on the Sycan River at 15.8 river km.

Modern discharge data collected by the U.S. Geological Survey and Oregon Department of Water Resources were used to illustrate the unprecedented discharge magnitude of the Sycan Outburst Flood compared to floods of record. The largest peak discharge on record in the Sprague River watershed occurred in mid-December of 1964 following a rain on snow precipitation event. Discharge data were not recorded on the lower Sycan River during that time period. To estimate the peak discharge of the lower Sycan River during the 1964 event a regression analysis was done correlating peak discharge events of the Sprague (gage 11501000) and Sycan Rivers (gage 1499100) from 1974 to 2007 (Figure 3-6).

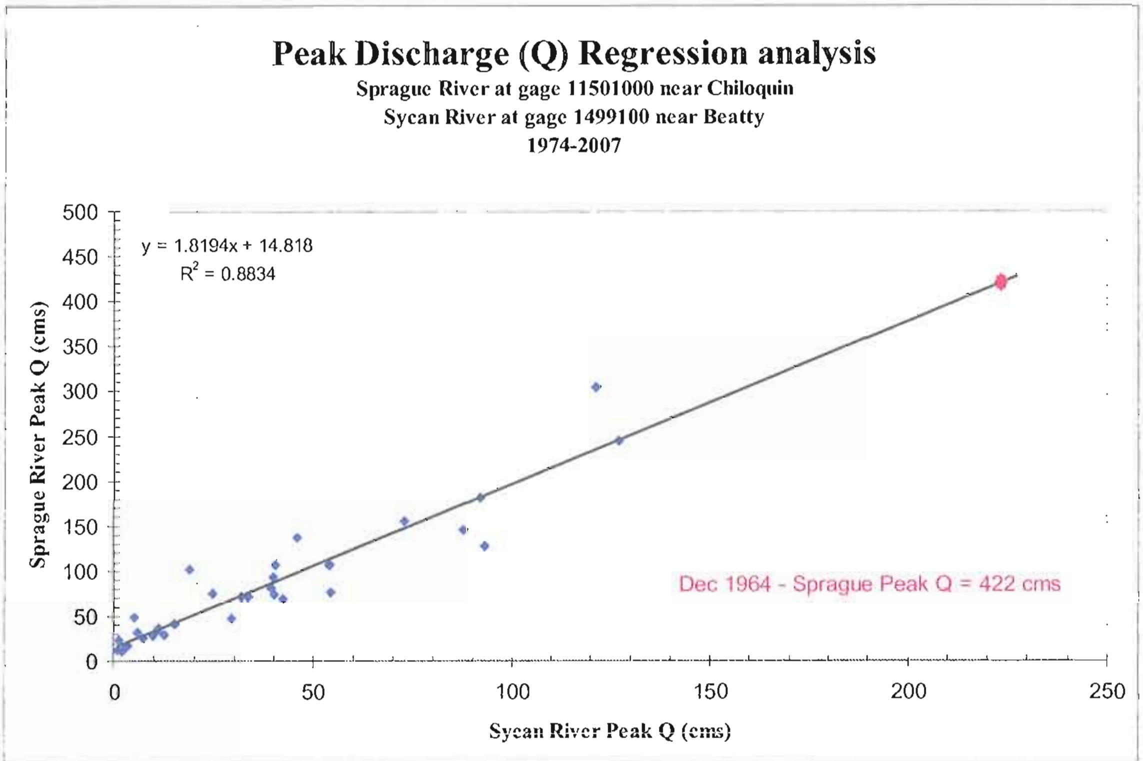

Figure 3-6. Peak discharge regression analysis of the Sprague and Sycan Rivers.

CHAPTER IV

RESULTS

Introduction

Surface morphology, stratigraphy and radiocarbon dating of floodplain features of the lower Sycan River revealed five distinct floodplain units representing specific episodes of fluvial deposition during the Holocene in the Sycan Valley. A floodplain unit is defined here as a sequence of floodplain strata, with specific characteristics, related to a depositional environment that correlates to an interval of time in the channel's history. Interpretation of the geomorphic processes related to the floodplain strata has been used to construct a model of channel and floodplain development for the lower Sycan River and Sycan Valley from 11 ka to present. The model includes seven primary periods of evolution defined by the dominant geomorphic processes related to the floodplain stratigraphy. Characterization of the floodplain units, findings related to the landscape altering Sycan Outburst Flood deposits, the channel and floodplain development evolutionary model, and a description of the modern lower Sycan River are presented in this chapter.

Major Floodplain Units of the Sycan Valley

The floodplain units of the Sycan Valley have been defined by both stratigraphic composition and surface elevations. The complexity of distribution of floodplain units is displayed in the geomorphic surface map (Figure 4-1 and Appendix D as small scale plate maps). The floodplain units shown in the geomorphic surface map of the Sycan Valley do not show all the underlying units. For example, paleosols from the early Holocene are often buried below the more modern floodplain or channel and are thus not displayed on the geomorphic surface map. Appendix B contains the stratigraphic diagrams for each primary site. The common alpha-symbol "T" is used in this paper to represent a floodplain or terrace unit with additional numeric and alpha-numeric symbols to classify the specific depositional sequence (i.e., T_{3c}).

Formation of inset terraces is a result of complex channel change over time, where variations in sediment load and stream energy result in episodic aggradation and degradation (Schumm 1979; Schumm 1985; Nanson and Croke 1992; Simon and Rinaldi 2006), usually involving lateral channel shifts during incision (Richards 1982; Brierley and Fryirs 2005). Correlation of the floodplain units is therefore resolved through stratigraphy and radiocarbon dating, not relative elevation alone (Gerrard 1992). The

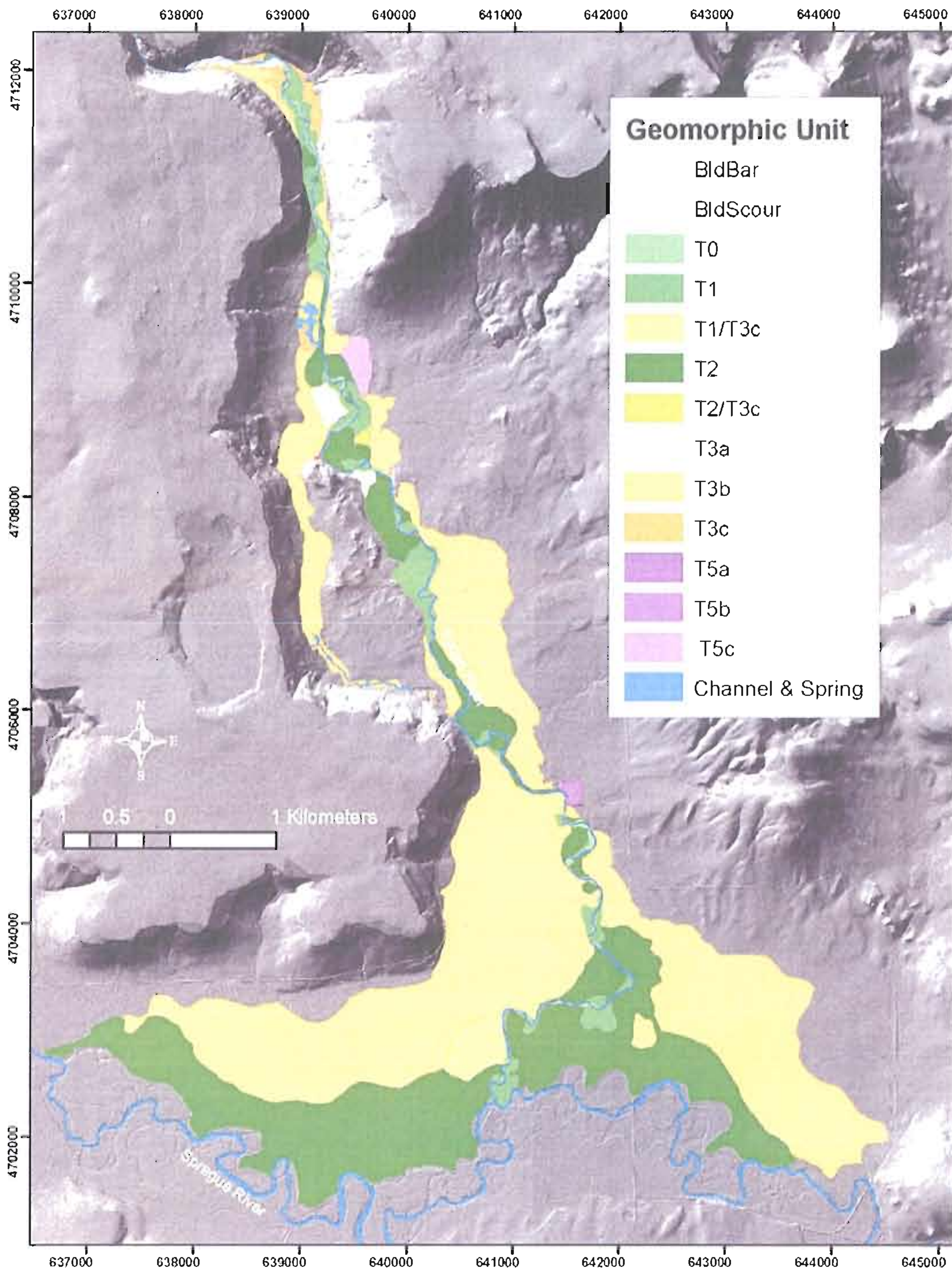

Figure 4-1. Geomorphic unit map of the lower Sycan Valley. See Appendix D for map plates (1-5).

map of sites where stratigraphic descriptions were made is provided as Figure 3-1 in Chapter III. Table 4-1 lists the stratigraphic sites where the floodplain unit types are observed.

Floodplain Unit	Stratigraphic Site Number		
	Bank Exposure (BE)	Auger Hole (AUG)	Soil Pit (PIT)
T_{5a}	07	na	na
T_4	02, 03, 05, 08, 09, 10, 12, 15, 16	02, 03, 07	01
T_3	02, 05, 09, 11, 12,15, 16	02, 03, 04, 05, 06, 07	01, 02
T_{3a}	11,12,15	na	na
T_{3b}	na	03, 04, 05, 07	01, 02
T_{3c}	02, 05, 09, 16	02, 06	na
T_2	03, 05, 06, 08, 09, 10, 14, 17, 19	01, 04	na
T_1	01, 02, 04, 13, 18, 19	02	na

Table 4-1. Floodplain unit types found at stratigraphic sites of the Sycan River.

Each floodplain unit represents a period of aggradation related to changes in behavior of the fluvial system (Womack and Schumm 1977; Gerrard 1992). In chronologic order, from modern to historic, the main floodplain units of the lower Sycan River are: Active Channel and Bars (T_0); Modern Floodplain (T_1); Late Holocene Floodplain (T_2); Sycan Outburst Flood Terrace (T_3); Early Holocene Floodplain (T_4); and Pre-Holocene Terrace (T_5). Each unit will be discussed in detail later in this chapter. The Sycan Outburst Flood Terrace (T_3) has been separated into three sub-units that are delineated where data allow. Likewise, the Pre-Holocene Terrace (T_5) has been separated into three sub-units that represent compositionally distinct paleo-terraces found on the valley floor; (T_{5a}) Walker Terrace, (T_{5b}) Wetland Terrace, and (T_{5c}) Red Rock Terrace. The T_5 units were created during pre-Holocene deposition periods that are not included in the Holocene floodplain and channel development model presented in this research, although basic descriptions are provided in Table 4-2. Also, T_5 units are included in the geomorphic surface map (Figure 4-1 and Appendix D; plates 2 and 4) because they are important landscape features on the floor of Sycan Valley.

Floodplain Unit	Pre-Holocene Terrace Unit Name	Stratigraphic Sediment Summary	Location (river km)
T5a	Walker Terrace	Gravels to silt alluvium (fines upward); 492+ cm thick; surface elevation is 2 m higher than local T_3 surface	5.2 - 5.4
T5b	Wetland Terrace	Clay dominant; weathered and blocky; surface elevation is approximately the same as local T_3 surface	10.8
T5c	Red Rock Terrace	Rounded river gravels above mudstone; duripan unit observed in one location at gravel/mudstone contact; rounded clasts of obsidian at 3cm diameter; surface elevation of terrace scarp is 6 m higher than local T_3 surface	11.7 - 12.4

Table 4-2. Summary descriptions of T_5 Pre-Holocene Terrace units.

Relative elevation of the surfaces of the primary floodplain and terrace units is not parallel across the system (Figure 4-2). The elevation difference between surfaces is greatest in the upstream end of Sycan Valley and least at the downstream end. As expected, Sycan Outburst Flood deposits are deepest at the top of the valley and related flood-trench scour was greatest here. As a result, the degree of channel adjustment (degradation and aggradation) through the processes of complex response was likely greatest initially following the flood event. Initial response to the overload of sediment was dominated by degradation (incision) in the upstream section, where aggradation was

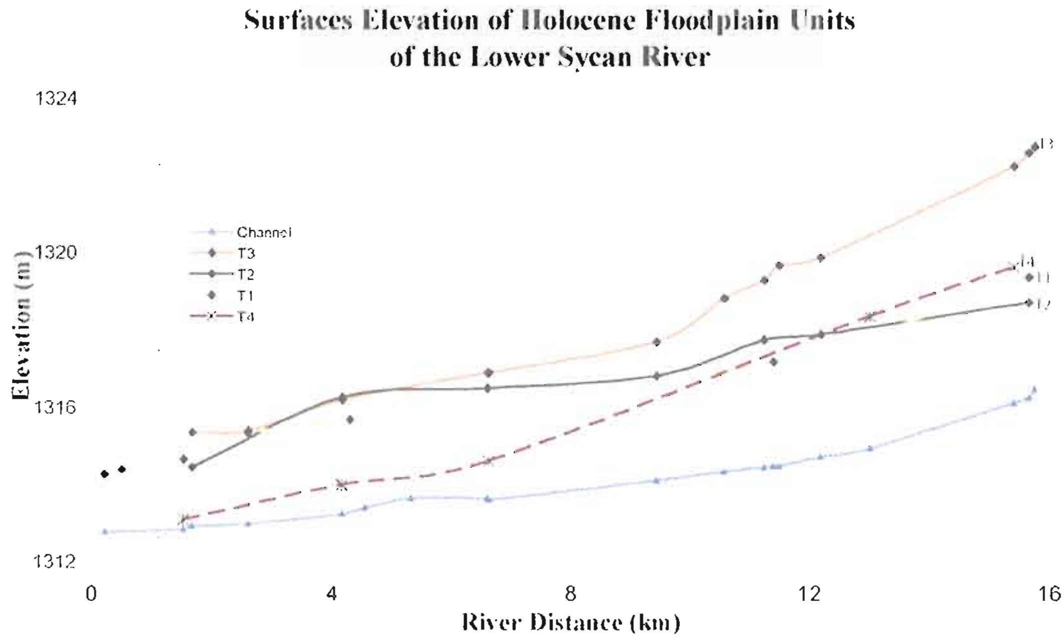

Figure 4-2. Longitudinal profile of the elevation of the modern channel during summer low-flow and Holocene floodplain and terrace surfaces of the lower Sycan River (T_1 – Modern Floodplain; T_2 – Late Holocene Floodplain; $T_{3b\&a}$ - Sycan Outburst Flood Terrace; T_4 – Early Holocene Floodplain).

the dominant process at the downstream end. This is depicted by the truncated T_3 flood deposits being overtopped with modern floodplain deposits along the lower portion of the channel. Figure 4-3 is a photo taken at river kilometer 11.46 (upstream of mid-valley) showing the surface elevation differences of floodplain units T_4, T_3, T_1, and T_0. Predominant on the floor of the Sycan Valley, the Sycan Outburst Flood Terrace unit (T_3) reveals that a fluvial disturbance occurred after the eruption of Mount Mazama (at ~ 7660 cal *yr* BP) that buried the valley floor with pumice rich sands. According to radiocarbon dating and stratigraphy, the event occurred prior to the mid-Holocene. This event influenced the channel and floodplain evolution of the lower Sycan River. To reconstruct some of the geomorphic processes responsible for the development of the pumice-rich

Figure 4-3. Photo of Holocene floodplain and terrace surfaces on the Sycan River at 11.46 river km (T_0 - Active Channel and Bars; T_1 – Modern Floodplain; T_3 – Sycan Outburst Flood Terrace; T_4 – Early Holocene Floodplain).

material that composes the Sycan Outburst Flood Terrace units, sediment composition, volume, and related landforms throughout the Sycan River watershed were examined. Findings and interpretations on the Sycan Outburst Flood are discussed below.

Sycan Outburst Flood

Flood Deposit Distribution

The Sycan Outburst Flood covered the Sycan Valley floor with a layer of pumice-rich sands. Today this deposit forms terraces from the outlet of Sycan Canyon southward for approximately twelve kilometers towards the confluence of the Sycan and Sprague Rivers. As the valley widens southward from the mouth of Sycan Canyon the flood deposits gradually decrease in thickness, from 3.35m at the head of the valley at AUG-07 to what appears to be a truncated 0.45 m at the most distal remnant, located 650 m northwest of the modern confluence of the Sycan and Sprague Rivers (BE-02) (Figure 3-1). No distinct flood deposit sequences were found further southward. This is probably due to a combination of distal thinning of the deposit and erosive processes at the confluence of the Sprague and Sycan Rivers. The thicknesses of the existing deposits suggest that outburst flood deposits may have extended an additional one thousand meters across the Sprague River to the southern edge of the valley. Figure 4-4 shows the Sycan Outburst Flood Terrace unit and the estimated boundary extent of the original deposits.

The terraces of the Sycan Outburst Flood lack evidence of post-depositional inundation. Topographically the surface of this unit is horizontal and unscarred by post-flood event fluvial activity. The only exception is at the distal flood deposits near the confluence with the Sprague River, where flow has truncated flood deposits and topped them with modern floodplain deposits. This indicates that a flood event of equivalent or greater magnitude has not occurred in this watershed since the Sycan Outburst Flood.

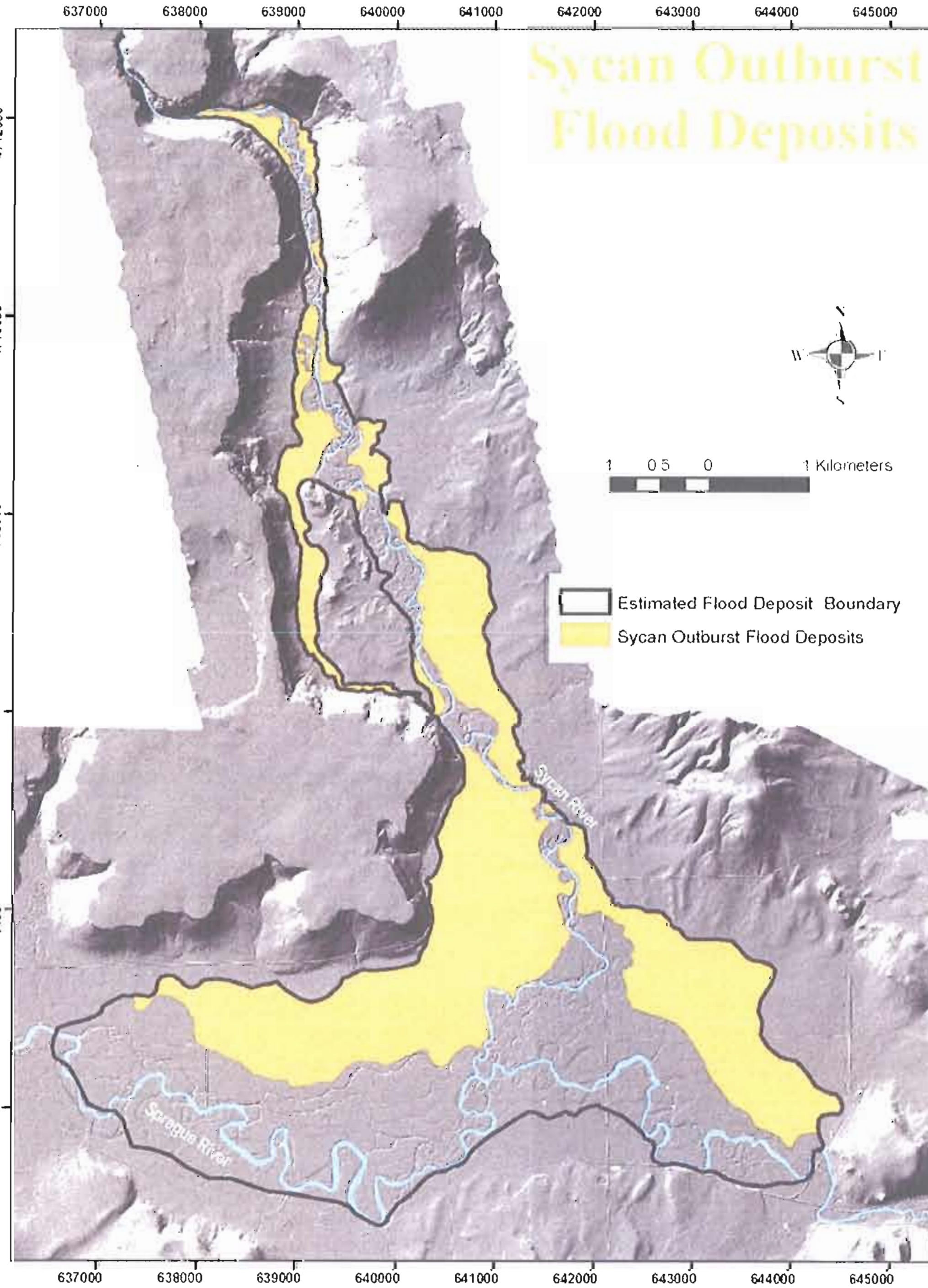

Figure 4-4. Sycan Outburst Flood deposit and estimated boundary extent.

Event Age

A maximum depositional event age-range has been established for the Sycan Outburst Flood terrace by calibrating radiocarbon dates of seeds (*Polygonum*) extracted from the buried paleosol directly below the flood deposit (BE-02). The seeds were extracted from the upper three centimeters of the paleosol. The stratigraphy sequence indicates that the flood event probably closely post-dates the age of the seeds. An age range of 7579-7682 (+/-40) cal *yr* BP is calibrated for the seeds (Beta-252116). The younger age of 7579 cal *yr* BP (7580 cal *yr* BP, adopted age) is considered the conservative maximum event age because the flood occurred after the seeds were distributed on the paleosol. And, although the seeds were collected near the distal end of the flood lobe where erosive flood processes are expected to be minimal, the erosive processes at the collection site are unknown.

Estimated Flood Discharge

A minimum discharge estimate for the outburst flood of was calculated using values of area and velocity generated at cross section “A” (Figure 3-3). O’Connor’s (1993) flow competency equation estimates the minimum velocity necessary to transport the average maximum diameter boulders present at the cross section as 4.60 m/s. Area inundated by the minimum flood stage is 1255.18 m^2. These values generate a minimum discharge for the Sycan Outburst Flood of 5773.83 m^3/s (cms).

For comparison with meteorologically generated floods on the Sycan River I examined discharge data from U.S. Geological Survey gages. The largest peak flow recorded on the lower Sycan River (U.S. Geological Survey gage 1499100) was 127.44 m^3/s in February of 1982. The largest discharge recorded in the last one hundred years for the Sprague River at USGS gage 11501000 located near the town of Chiloquin (116 km downstream from the confluence) was a rain-on-snow event in mid-December of 1964. Discharge data were not recorded on the lower Sycan River in 1964. A regression analysis correlating peak discharge events of the Sprague (gage 11501000) and Sycan Rivers (gage 1499100) from 1974 to 2007 produced an estimated discharge of 223 cms for the Sycan River during the 1964 flood event (Figure 3-6). Table 4-3 compares the estimated discharge magnitudes of these flood event data.

Flood Event	Event Date	Discharge (cms)
Sycan Outburst Flood	7580 cal yr BP	5800
Rain on Snow	December, 1964	223
Rain on Snow	February, 1982	127.44

Table 4-3. Flood event discharge comparisons on the Sycan River.

Inferred Flood Mechanics from Sediment Stratigraphy

Large-scale outburst floods imprint themselves on the landscape they impact (Baker 2002; O'Connor and Beebee in press), leaving behind evidence that allows geomorphologists to reconstruct pieces of the event. This paper limits reconstruction of the mechanics of the Sycan Outburst Flood to primary characteristics related to the landscape alterations and floodplain evolution of the Sycan Valley. The reconstruction relies on the common practice of analyzing and interpreting stratigraphy of flood deposits to identify an outburst flood and its varied depositional characteristics (Smith 1993; Enzel et al. 1994; Mack et al. 1996; Cornwell 1998; Conaway 2000; Blair 2001).

The stratigraphy of the flood deposit displays a fining-up sequence, typical of fluvial environments. No soil development or other evidence of depositional hiatus (mud cracks, organics accumulation, etc.) was found within the Sycan Outburst Flood unit. This indicates that the sediment was deposited over a short period of time and likely as a single event that probably lasted a matter of hours or days. Detailed stratigraphic descriptions of flood deposits are available in Appendix B.

Flood terrace stratigraphy reveals discharge oscillations within the flood event hydrograph. Flow oscillations often result in variations in grain size and sorting within the stratigraphic sequence (Smith 1993; Baker 2002). Such variations can be the result of surges or pulses in discharge caused by dam failure mechanisms or stages of dam collapse/breach (Costa and Schuster 1998; O'Connor and Baker 1992; O'Connor et al. 2002) as well as transmission effects within the drainage network. Another example of hydrodynamics is ponding caused by downstream obstructions or valley confinement. Ponding backs up flood waters, resulting in a period of low energy deposition (Smith 1993). However, no evidence of downstream obstructions or flow constrictions of the Sycan Valley was observed.

Evidence of flow oscillations is most visible in the stratigraphic descriptions done at the edges of the deposit near the valley walls (PIT-01, AUG-03). Here low-energy flows were most likely to have occurred, away from the main current in the middle of the valley. The exact cause of the flow oscillations in the Sycan Outburst Flood is unclear with the available data. However, the most likely explanation is surges or transmission effects resulting from dam failure.

Grain size and sediment composition variations at PIT-01 and AUG-03 suggest that the outburst flood included phases of flow oscillations. The phases include at least two episodes of low-energy deposition prior to a second discharge surge along the western margin of the valley. From the base of PIT-01 at 216 cm to 165 cm, very coarse pure pumice sand and gravel (1cm diameter) fines upward gradually to a fine to coarse pumice-rich sand of mixed lithologies. At 165 cm, composition of the deposit returns to pure pumice of medium to very coarse poorly-sorted sand. This indicates a surge in discharge that overtopped the basal 51 cm of the flood deposit. The second phase of deposits fines upward gradually over 100 cm. Figure 4-5 is a photograph at PIT-01 showing stratigraphy from approximately 210 – 10 cm depth.

Also observed in many of the outburst flood deposits are horizontal layers of very fine pumice silt only 1 to 2 cm thick. These very well-sorted laminar layers are interpreted as representing episodes of suspended sediment settling during a lower energy depositional phase of the flood. Manville et al. (2005) described similar flood surge bedding in pumice at the 1800 Taupo, New Zealand, volcano outburst flood. Pumice silt layers have been interpreted as slack-water flood deposits by Manville et al. (2002; 2005) at Taupo and by Hodgson and Nairn (2005) at Lake Tarawera (New Zealand).

One to three silt layers within the Sycan Outburst Flood deposit, similar to the layers described above at soil PIT-01, were present at many observed exposures. Specifically the layers are observed at stratigraphy sites PIT-02; BE-05; BE-16; AUG-03;

and AUG-07. These layers typically consist of well-sorted silt of salmon-pink or soft gray coloration. The coloration is clearly visible next to the cream-colored pumice sand prevalent in flood deposits. It is believed that the pumice silts and sands both originated as pyroclastic eruption material from Mount Mazama. Conaway (2000) mentions

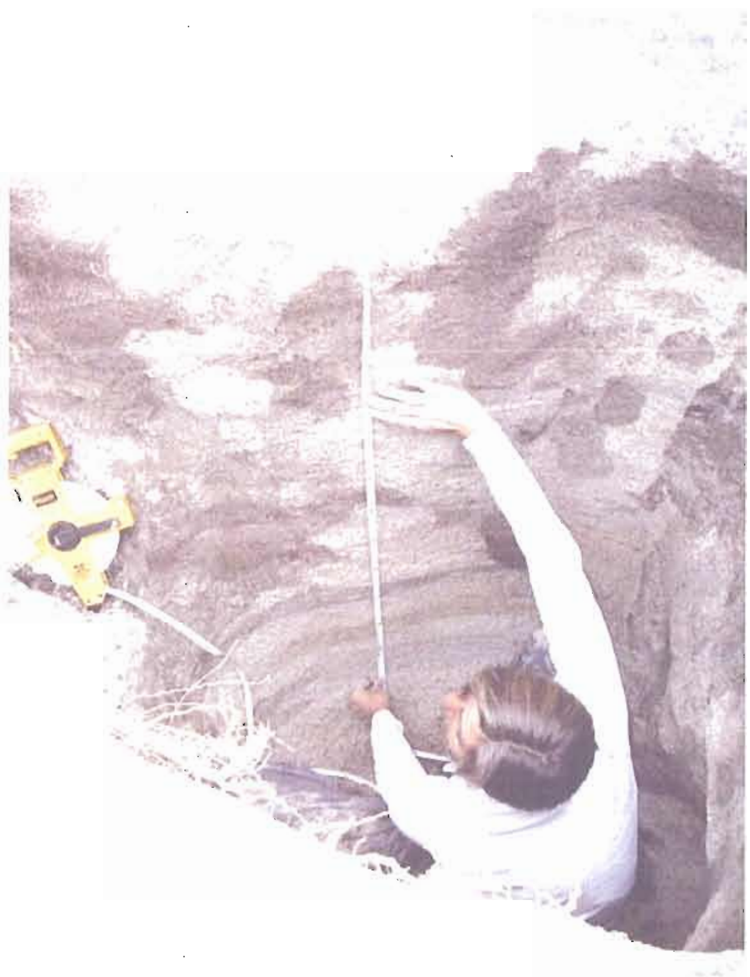

Figure 4-5. Photo of stratigraphy at PIT-01.

both "pink" and "buff" colored pumice when describing different pyroclastic Mount Mazama pumice deposits at Klamath Marsh.

The composition of the deposits above and below the silt layers in the Sycan Outburst Flood deposits is similar. This is interpreted as indicating that the low-energy depositional episodes were probably relatively brief and that flood waters likely did not completely abandon the depositional surfaces. The prevalence of the silt layer in the flood terrace units suggest that low-energy episodes during the flood were experienced throughout much of the Sycan Valley.

Evidence of flood discharge oscillation is not observed in the flood terrace deposits examined along the center of the valley (T_{3a}). It is assumed that this is due to the fluvial hydraulics of the flood flow. The proximity of mid-valley to what was likely the thalweg, where higher energy and possibly more consistent flow occurred, did not preserve the variation in deposits observed from flow oscillations described at the valley margin. Further field observations are required to confirm this hypothesis.

The mid-valley flood terrace units (T_{3a}) have a simple stratigraphy of loose pumice grains fining upward from very coarse to fine loamy sand. The surface of the mid-valley flood terrace unit is horizontal across the valley and graded to valley-margin flood terrace units (T_{3b}). Thicknesses of T_{3a} appear to be related to the elevation of the surface it is overlain onto and the relative location along the longitudinal axis of the valley. For example, T_{3a} deposited on a bedrock surface at BE-11 is 163 cm thick, but upstream at BE-12, where T_{3a} buried the pre-flood floodplain (T_4), it is 223 cm thick. Further upstream at BE-15, where deposit thickness would be expected to increase, T_{3a}

overlies a higher elevation paleosol surface and is only 130cm thick. The terrace units T_{3a} and T_{3b} thin only slightly from mid-valley out towards the valley margins. The slight thinning reflects pre-flood valley shape and perhaps some mid-valley scour related to flood hydraulics. Post-flood channel development appears to be confined to what was likely the flood-scoured trench and mid-valley thalweg of the flood. As a result, only a limited number of preserved deposits of T_{3a} as bank exposures exist.

Detailed examination of the mechanics of the Sycan Outburst Flood is beyond the scope of this paper but it is worth speculating on the hydromechanics that distributed the flood deposits across the Sycan Valley. A hyperconcentrated flood suspension (40-80% weight of flood) is probable as hyperconcentration is attainable with easily-mobilized pumice (Hodgson and Nairn 2005) and transport of pumice can be sustained considerable distances over low gradients (Mack et al. 1996). It is the buoyancy of sediment and the hydromechanics of hyperconcentrated flows that interact to support sediment suspension and transportation (Benvenuti and Martini 2002).

The concentration of sediment to water discharged during the Sycan Outburst Flood is not known. However, flood deposit characteristics and geomorphic interpretation of the watershed's geography give insight into some probable hydromechanical scenarios. For example, it is probable that during the Sycan Outburst Flood sediment bulking of flood waters occurred from the accumulated sediment from within Sycan Canyon. Also, flood velocity would have decelerated as it spread across the widening floodplain (Blair 1987) of the Sycan Valley, allowing for deposition of suspended load. The buoyancy of the pumice-dominated flood load likely influenced the quantity and percent weight of sediment transported. Manville et al. (2005) recognized that environments overloaded with easily mobilized, partially saturated pumice optimize laminar deposits in high-energy sheet floods. Considering these points, the Sycan Outburst Flood was a likely a hyperconcentrated (40-80% sediment discharge) sheet-flood that spread across the floor of the Sycan Valley.

Flood Volume

Water volume estimates of the outburst flood are restricted to the volumetric sediment deposit estimates measured in the Sycan Valley because no other evidence of flood water elevation was observed. The volume of sediment deposited in the Sycan Valley by the outburst flood is estimated to be a minimum of 14 x 10^6 m^3 (Figure 3-2). If we assume that sediment discharge and water discharge are equal ($Q_s = Q_W$) then minimum flood volume is equivalent to the deposited sediment volume (50% concentration). However, if sediment discharge was less than water discharge ($Q_s < Q_w$), then flood volume is greater than the deposited sediment volume estimates, and vice versa (Benvenuti and Martini 2002).

Assuming water was stored behind a dam, analysis of different water and sediment discharge concentrations for the Sycan Outburst Flood identified the probable location for a reservoir capable of containing a range of volumetric storage needs. The maximum storage capacity needs of a reservoir were identified assuming a concentration of 80% water to sediment volume. Minimum water volume requirements were assumed at 50% of sediment volume (Table 4-4). At 50% the water volume would be equivalent

Deposited Sediment Volume Estimate (m^3)	Flood Discharge Estimate -minimum- (m^3/s)	Sediment Concentration	Water Concentration	Calculated Water Volume (m^3)	Flood Duration*
14 x 10^6	5800	50%	50%	14 x 10^6	40 min
		20%	80%	58 x 10^6	2 hrs 50 min

Table 4-4. Water to sediment concentration calculations and event duration of the Sycan Outburst Flood.

to the sediment volume. The only area identified in the Sycan River watershed capable of containing both the estimated minimum and maximum volumes of flood water is the Sycan Marsh. Figure 4-6 is a map of the reservoir area in Sycan Marsh and the upper one kilometer of Sycan Canyon necessary to store a volume of water 14 x 10^6 to 58 x 10^6 m^3.

Upstream Evidence of an Outburst Flood

Supporting evidence of an outburst flood exists in Sycan Canyon. Large subrounded boulders with diameters of up to 2 m and boulder bars located throughout the upper reaches of Sycan Canyon indicate that a large-scale flood mobilized and fluvially redistributed boulders. Terrace-like boulder bars in several places constrain the modern pathway of the river throughout the canyon. Additionally, a single slack-water flood terrace deposit was discovered and excavated at PIT-02 in upper Sycan Canyon at 1 km downstream from Sycan Marsh. The terrace stratigraphy is 80 cm thick with a surface 220 cm above the modern floodplain. It is composed of medium to coarse pumice-rich

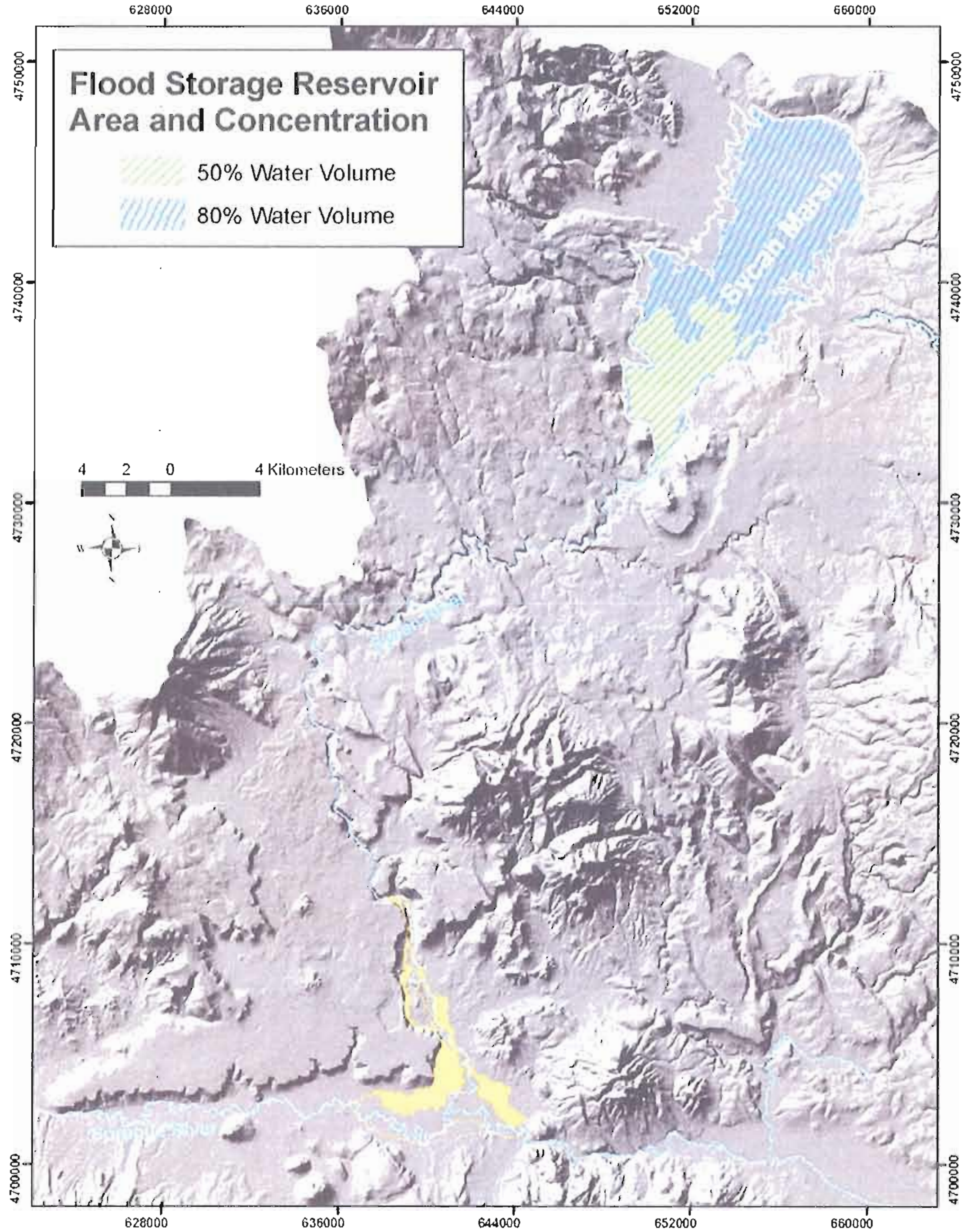

Figure 4-6. Potential water storage areas in the Sycan Marsh and upper Sycan Canyon for the Sycan Outburst Flood – at water to deposited sediment concentrations of 50% (14×10^6 m^3) and 80% (58×10^6 m^3).

sands that fine upward. A 1.5 cm thick horizontal layer of pumice silt, similar to the low-energy deposits described in the valley deposits, was observed near the base of the flood deposit. Beneath the flood deposit sequence is a silt dominated paleosol and canyon talus boulders.

At the downstream-most end of Sycan Canyon boulders up to 3.0 m in diameter are fluvially re-distributed downstream. Sourced from an upstream rockslide, the boulders now form elongate boulder bars that stretch 910 m from the mouth of Sycan Canyon (Appendix D, Plate 1). Relative boulder size decreases downstream consistently through the boulder bars to a maximum boulder diameter of 1.0 m at the toe end of the most downstream bar (at Cross Section "A", Figure 3-4). Burial depth of the boulder bars by outburst flood deposits increases downstream.

The features described above indicate that effects of the Sycan Outburst Flood event took place throughout Sycan Canyon. This evidence supports the proposal that the Sycan Outburst Flood dam was most likely located in the upstream portion of Sycan Canyon.

Other Evidence of an Outburst Flood

The magnitude of the Sycan Outburst Flood suggests that impacts would have continued downstream through the Sprague River. In fact, a pumice deposit $\geq$ 50 cm thick were found and described in Medicine Rock Cave along the Sprague River by Ira Allison in 1948 (Cressman et al. 1956). Medicine Rock Cave is located 101 river kilometers downstream from the Sycan River. The pumice layers in Medicine Rock

Cave were interpreted by Allison (1948) as fluvial deposits from large floods (Cressman et al. 1956). Based on the described composition and thickness, I think it is possible that the 50 cm pumice layer in the cave is from the Sycan Outburst Flood. This suggests that the outburst flood was extensive and may have had geomorphic effects far downstream.

Additional evidence of a massive flood exists in Upper Klamath Lake. A notable peak of reworked Pliocene diatoms deposited in Upper Klamath Lake shortly after the eruption of Mount Mazama is attributed to "seasonally strong precipitation and flashy runoff" from the Sprague River drainage, by Bradbury et al. (2004). However, a hydrologic explanation for the flush of Pliocene diatoms does not correspond to the reconstructed climate at that time (low effective moisture). Bradbury et al. state that the Pliocene diatoms are from the geologic formation known as Yonna (classified as Tcs, continental sedimentary rocks of the Pliocene and Miocene in Sherrod and Pickthorn 1992). The Tcs is mapped extensively along the Sprague River and at the edges of Sycan Valley. With the advantage of the data presented in this research, I propose an alternate cause for the increased quantity of Yonna diatoms into Upper Klamath Lake -- erosion into the Yonna Formation by the Sycan Outburst Flood. The flood would have created a pulse of diatoms into the lake. Post-flood fluvial processes across the freshly exposed Yonna Formation may have provided additional diatom inputs to the lake. Bradbury et al. Figure 7b indicates that the Pliocene diatom pulse was at approximately 7.3 - 7.5 cal *yr* BP. These calibrated dates are only slightly younger than the conservative maximum age recorded with radiocarbon dating for the Sycan Outburst Flood at 7580 cal *yr* BP (Beta-252116).

Damming Mechanism of the Sycan Outburst Flood

Meteorologically generated floods - even rain-on-snow events - are unable to create the very large discharge often observed from outburst floods (Costa 1988; Blair 2001; Blair 2002; O'Connor et al. 2002). In the case of the Sycan Outburst Flood, water and sediment accumulation facilitated by the presence of a temporary dam is hypothesized by this research. Mechanisms of damming and probable locations of the dam are discussed below.

Field investigation and aerial photo analysis of upper Sycan Canyon did not reveal evidence of canyon blockage from a landslide or rock fall capable of impounding the Sycan Outburst Flood. A large rock fall is present in the most downstream end of the Sycan Canyon (known as Coyote Bucket). At this rock fall are concave scarps on the left canyon wall and a mass of bouldery debris rising more than 15 m above the current channel against the right canyon wall. This indicates that this rock slide buried the channel in the past, and could have dammed the river. However, the narrow basalt-walled canyon upstream from the rock slide does not have adequate water storage to generate the Sycan Outburst Flood.

Based on the evidence presented in this research the most likely dam sites are at the outlet of Sycan Marsh and the uppermost Sycan Canyon. A wide basin, such as Sycan Marsh, located upstream from a confining landscape feature makes for an ideal location to impound water and sediment behind a natural dam (Costa and Schuster 1988; Blair 2001).

Aeolian redistribution of Mount Mazama pumice is considered a possible damming mechanisms by the development of a large aeolian dune(s) at the mouth of Sycan Marsh or by in-filling of upper Sycan Canyon by mobile dunes coming from the surrounding plateau. The large stabilized (vegetated) tephra dunes present in the uplands today are transverse out of the northwest (Sherrod and Pickthorn 1992). When they were actively migrating across the plateau top, these dunes would have spilled into the canyon, potentially filling it. Small areas of falling pumice sand from the top of canyon walls and local accumulations on the canyon floor are present today. An issue with these explanations is whether sufficient sand could have accumulated in the canyon without being washed downstream by fluvial action.

Today the upper 17 km of Sycan Canyon carries only seasonal channel flow from precipitation or overflow from Sycan Marsh. Torrent Springs, at 17 km downstream from Sycan Marsh is perennial. If functional at the time of the Sycan Outburst Flood, Torrent Springs would have inhibited gradual accumulation of pumice downstream from the spring. Under present conditions it is common for the channel to be basically dry by late summer between Sycan Marsh and Torrent Springs (USGS 2007). If precipitation conditions were drier than present, as suggested by the climate record, it is possible that a pumice dam could have accumulated in the upper canyon during a dry period or season.

Historic climate reconstructions from lake cores and middens during or directly following the eruption of Mount Mazama across the region show a period of warmer and drier conditions than today. In many examples this was the driest period of the Holocene. In Upper Klamath Lake the lowest lake levels of the Holocene occurred during 7.5 – 5 ka due to reduced hydrologic discharge inputs coupled with increased sediment inputs directly related to influences from the eruption of Mount Mazama (Bradbury et al. 2004). Evidence for a drought period following the eruption of Mount Mazama was also seen as far north as Flathead Lake in northwestern Montana where the lake dropped approximately 15 m below modern levels for about 150 years immediately after the massive eruptions (Hofman 2005). Maximum aridity during the Holocene in Long Valley, Idaho has also been correlated to the deposition of Mazama airfall that was followed by a decrease in effective moisture, resulting in the disappearance of wetlands (Doerner and Carrara 2001). This hot and dry period of the northwestern Great Basin began at 7 ka (Wigand and Rhodes 2002) to 7.5 ka (Grayson 1993). During this time lakes just east of the Sycan basin in Harney County were reduced or eliminated as part of severe regional droughts that led to aeolian activities. A period of drought following the deposition of Mount Mazama pumice increases the probability of aeolian blockage as a damming mechanism. Loose pumice tephra across the basalts of upper Sycan watershed would likely leave the landscape with minimal vegetation cover or soil development.

This proposal for dune damming as a mechanism for an outburst flood is unique. Of the numerous examples of outburst floods in the literature (Baker and Bunker 1985; Donnelly-Nolan and Nolan 1986; Blair 1987; O'Connor and Baker 1992; Smith 1993; Enzel et al. 1994; Mack et al. 1996; Cornwell 1998; Costa 1988; Blair 2001; Knudsen et al. 2002; O'Connor et al. 2002; Beebee 2003; Hodgson and Nairn 2005; O'Connor and Beebee in press) most refer to glacial, volcanic, or landslide damming mechanisms. Dunes have been known to create coastal lakes by blocking or altering channel pathways.

But only two references were found in the literature suggesting aeolian dunes as a damming mechanism for outburst floods, at Moses Lake, Washington (referenced in Costa and Schuster 1988) and Smith Canyon dune field, Washington (Gaylord et al. 2001).

Pumice is unusual damming material due to its neutral or negative buoyancy (depending on saturation) in water (Manville et al. 2005; Manville et al. 2002; Mack et al. 1996). Damming of large quantities of water behind a pumice dam would require a massive quantity of pumice compared to channel discharge. A relevant example of pumice as a damming mechanism has been reported on the Williamson River (Conaway 2000), the single drainage system between the Sycan River and Mount Mazama. Conaway (2000) concluded that pyroclastic pumice-rich flow off the eastern flank of Mount Mazama blocked the Williamson River Canyon. Water, laden with rafting pumice, backed up behind the dam in the Klamath Marsh to a depth 22 m above current water levels prior to dam failure and rapid drainage of the marsh. Conaway's research confirms that Mazama pumice-rich material is capable of damming and storing large quantities of water under the right conditions. However, at the Williamson River the material is pyroclastic flow mixed with airfall deposits. In the Sycan pumice deposits are limited to less-dense airfall tephra.

Very few examples of pumice dominated lithofacies in low gradient, non-volcanic settings like that of the Sycan Valley are available. Flood events with entrained pumice usually occur in close proximity to the volcanic source in highly active environments. Flood deposits on the low gradient Rio Grande offer one example where flood loads of pumice were rapidly transported over 400 km from its source due to the buoyancy of the sediment (Mack et al. 1996). Hodgson and Nairn (2005) describe the sediment distribution from outburst flood waters from Lake Tarawera as maintaining pumice loads after denser bed load was deposited. This supports the findings of Manville et al. (2002) that pumice is entrained easier and settles out after other grains of the same size due to its buoyancy.

In summary, the Sycan Outburst Flood of approximately 7580 cal *yr* BP (Beta-252116) altered the landscape of the Sycan Valley. This research concludes that the flood waters were generated by accumulation behind a temporary dam located in the upper section of Sycan Canyon or the mouth of Sycan Marsh. Considering the region's geology, lack of evidence for other damming mechanisms, and the climate record that indicates a relatively dry period during the time of the eruption of Mount Mazama - dune development or canyon infilling of pumice from aeolian processes is presented here as a potential damming mechanism. The eventual failure of the dam released a pumice-laden flood with a minimum discharge of ~ 5800 m^3/s and an estimated water volume range of approximately 14 x 10^6 m^3 to 58 x 10^6 m^3. The estimated minimum discharge is twenty-five times larger than any flood on record in the last one hundred years. The stratigraphy of the flood deposit sediment indicates that discharge oscillations in the flood hydrograph did occur during the short-lived event. Assuming that the flood occurred as a single event its duration may be a short as one to three hours long. Further investigation of the mechanics of the Sycan Outburst Flood, specifically at the area of dam breach, the mouth of Sycan Marsh, throughout the confining walls of Sycan Canyon, and its effect on the Sprague River, should be undertaken.

Channel and Floodplain Development of the Lower Sycan River
(Early Holocene – present)

Introduction

The channel and floodplain development model presented here for the lower Sycan River is based primarily on valley morphology and stratigraphic analysis of alluvial deposits. No channel or floodplain development model existed prior to this research for low gradient systems altered by outburst floods of non-cohesive pumice sands. The evolutionary processes of the Sycan River model rely on concepts of complex channel response related to geomorphic threshold and non-linear system recovery where channel change is more rapid at first then decreases over time.

Decade-scale aspects of this model are based on Simon's (USGS 1999) evolution model created for the Toutle River, WA and Simon and Thomas' (2002) channel evolution model for the Yalobusha River, MS. Like the Toutle River's response to the eruption of Mount Saint Helens in 1980, after the Sycan Outburst Flood the lower Sycan River was forced to redefine its channel through non-cohesive tephra. But unlike the Toutle River the lower Sycan River is a low gradient system. Here fluvial processes occur primarily during seasonal high-flows similar to the Yalobusha River.

The periods of channel and floodplain development of the lower Sycan River represent temporally distinct episodes of aggradation and degradation. Changes in stream gradient and channel geometry are assumed to be related to variations in sediment load and stream power. The oscillating bed level changes (aggradation and degradation) are correlated to upstream migrating knick-zones, similar to other channel evolution models (Schumm 1979; Simon and Hupp 1986; Richards 1982; Schumm et al. 1987; Simon 1989; Simon 1992; USGS 1999; Simon and Darby 1999 Simon and Thomas 2002; Simon and Rinaldi 2006). The zone where channel bed change is most prominent is referred to as the area of maximum disturbance (AMD) (Simon and Hupp 1986). In the sand dominated lower Sycan River the AMD is called a knick-zone. In sand dominated systems the knick-zone is usually a broad channel section that is locally steeper (Schumm 2005; Simon and Rinaldi 2006).

For each period of the channel and floodplain development model, the dominant geomorphic process is identified. Seven major periods of channel and floodplain development during the Holocene are identified for the lower Sycan River: I. Early Holocene Dynamic Equilibrium; II. Sycan Outburst Flood; III. Initial Channel Formation; IV. Degradation and Widening; V. Aggradation and Lateral Migration; VI. (Secondary) Degradation and Widening; VII. Modern Dynamic Equilibrium. The association between each geomorphic period and floodplain unit characteristics is shown in Table 4-4.

A natural system experiences a complex set of intrinsically and extrinsically generated environmental variables that influence its geomorphic response (Schumm 1979). During the Holocene the Sycan River system has experienced both. Possible

Period	Adopted Age Range cal yr BP	Floodplain Unit	Stratigraphic Sediment Summary	Dominant Geomorphic Process	Interpreted Channel Form
I	1164 - 7580	T4	organic rich, clay and slit dominated	quasi dynamic-equilibrium: low-energy seasonal overbank deposition	single-thread or anastomosing: laterally stable with vertical banks, moderately sinuous
II	7580	T3	pumice-rich sands that fine upward from very coarse pure pumice to a sandy loam	Sycan Outburst Flood deposition	splay of shifting braids atop the flood deposits
III	7580 for (1-150 yrs)	---	EROSIONAL - no preserved depositional record	incision	braided
IV	7600 - 5920	---	EROSIONAL - no preserved depositional record	incision and widening	shifting locally between briaded and single-thread: low sinuosity
V	5920 - 1350	T2	pumice-rich sands that fine upward from course sand up to a silty or sandy loam	aggradation and lateral migration	shifting locally between single-thread and braided, enlarged depositional bedforms and bars, cut-off chutes; moderate sinuosity
VI	1350 - 590	---	EROSIONAL - no preserved depositional record	incision and widening	single-thread; reduced sinuosity
VII	590 - present	T1	pumice-rich sands that fine upward from coarse-medium sands to a silty or clay loam	incision, aggradation and lateral migration	single-thread with cut-off chutes; moderate sinuosity
		T0	sands and pebbles/gravels	depositionally active bars or scoured surfaces	

Table 4-5. Geomorphic periods of channel and floodplain development of the lower Sycan River and summarized floodplain unit characteristics.

environmental variables are presented for each evolutionary period of the model. Because of the inherent complexity of natural systems both intrinsic variables, such as the evolution of channel geometry, and extrinsic influences, such as shifts in climate trends, are considered when possible.

A schematic of the channel and floodplain evolution model for the lower Sycan River is presented in Figure 4-7, at a cross section representative of the lower Sycan River slightly upstream from mid-valley. A mid-valley location is chosen for model depiction because the evolutionary adjustments are easily recognized on the landscape here. Similar channel adjustments are expected throughout the lower Sycan River with

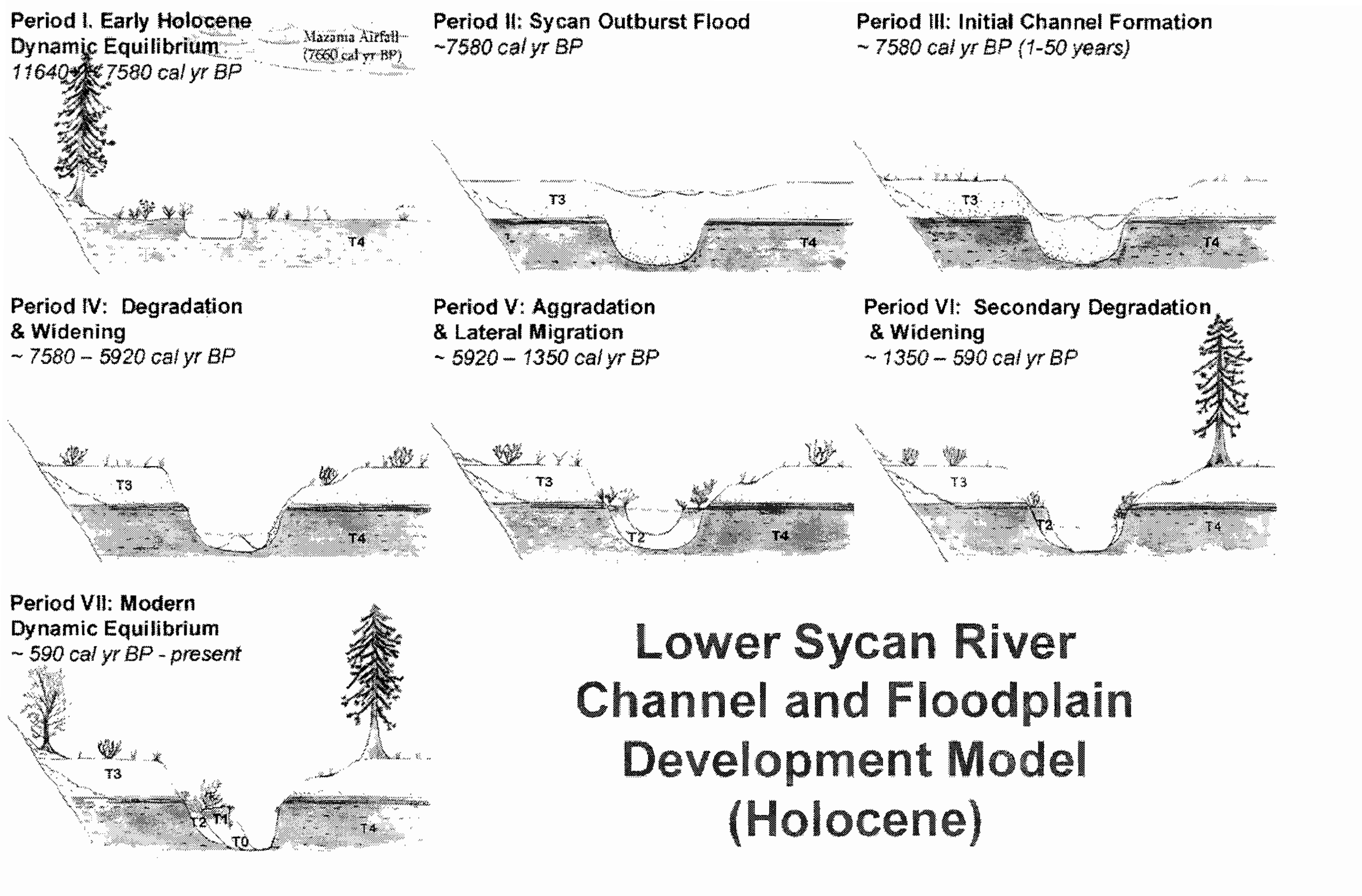

Figure 4-7. Holocene channel and floodplain development model.

more exaggeration of adjustments upstream and less downstream. The graphics of the model are drawn to show the area of maximum disturbance (AMD) occurring at the cross section during maximum channel adjustment of each period. Channel elevation is drawn in the model to represent bank full flow. The vegetation included in the model drawings is simple artistic renditions of probable vegetation cover. There is limited evidence for the actual type and density of vegetation cover on the floodplain during each period.

Channel and Floodplain Development Model Description

The list of stratigraphic sites where data were recorded on the composition and thickness of the floodplain units used in this model is provided in Table 4-1 and a map of the stratigraphic site locations is provided in Figure 3-1 for a visual reference.

Period I. Early Holocene Dynamic Equilibrium – *11640 ~ 7580 cal yr BP*

The Early Holocene Floodplain unit T_4 is interpreted as forming during a period of dynamic equilibrium where the system was gradually aggrading during a state of relative stability, over time.

Stratigraphy. The Early Holocene Floodplain unit T_4 is dominantly composed of dark, organic-rich clay and silt. Observed T_4 unit thicknesses decrease down valley from over 210 cm at AUG-07 at the upstream end of the valley to 64 cm at BE-02 near the mouth of the Sycan River. Clay content increases downward within the soil profile. The paleosol is very dark brown to black when moist (gray and hard when dry) and has some evidence of mottling. The T_4 unit is buried below the Sycan Outburst Flood T_3

floodplain units, and locally below floodplain units T_2, T_1, and T_0. The T_4 unit does not outcrop at the surface anywhere but is visible in bank exposures along the channel. Observations suggest that this unit extended across much of the valley floor. The photo in Figure 4-8 shows the horizontality of the surface of this unit buried below the T_3 deposits.

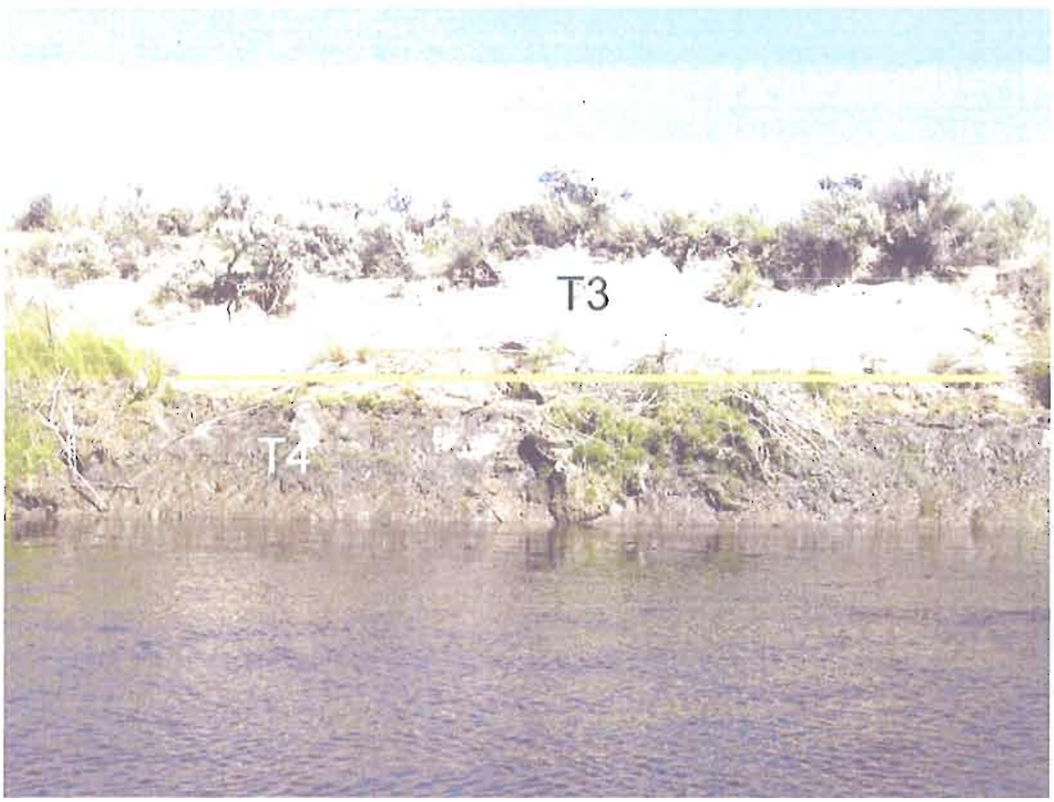

Figure 4-8. Horizontal contact boundary between T_3 (Sycan Outburst Flood Terrace) and T_4 (Early Holocene Floodplain) at 8.4 river km.

The top 5 to 10 cm of floodplain unit T_4 contain well-sorted angular pumice grains ~ 2.5 mm in diameter. Stratigraphically, the pumice grains occur either as a distinct horizontal layer approximately 5 cm thick or as dispersed grains within the top 10 cm of the clay loam matrix. Where the airfall tephra is a distinct horizontal layer it is usually topped by an additional 3-5 cm of organic-rich clay loam that is slightly higher in sand content but otherwise similar to the clay and silt dominated soils below the pumice airfall layer (Figure 4-9). Where stratigraphic analysis continued below the clay-silt paleosols of floodplain unit T_4, fine to medium sands and gravels are observed. The boundary between the clay paleosol and the buried sands and gravels is distinct yet gradational over a few centimeters. Commonly the fine to medium sands and gravels are composed of mixed lithologies with blue-gray color.

Floodplain Development. The characteristics of the Early Holocene Floodplain unit T_4 indicate that throughout Period I (Early Holocene Dynamic Equilibrium) the lower Sycan River was geomorphically a low-energy system. Seasonal overbank flow probably frequently inundated the valley floor, depositing fines across the floodplain. The dark brown to black coloration throughout the unit, plentiful organics (in situ seeds and plant fragments) found in the top few centimeters, and evidence of mottling indicate a well vegetated surface, presumably experiencing gradual vertical accretion of fine grained deposits.

Seeds extracted from the top 3 cm of unit T_4 at BE-02 were identified as *Polygonum* (Martin and Barkley 1961; NPSO 2007), which is a riparian or wetland forbs. This plant type, combined with T_4 soil characteristics, suggests that much or parts of the floor of the Sycan Valley during the early Holocene was a moist floodplain environment. Today several generous perennial springs located on or near the valley floor (USGS

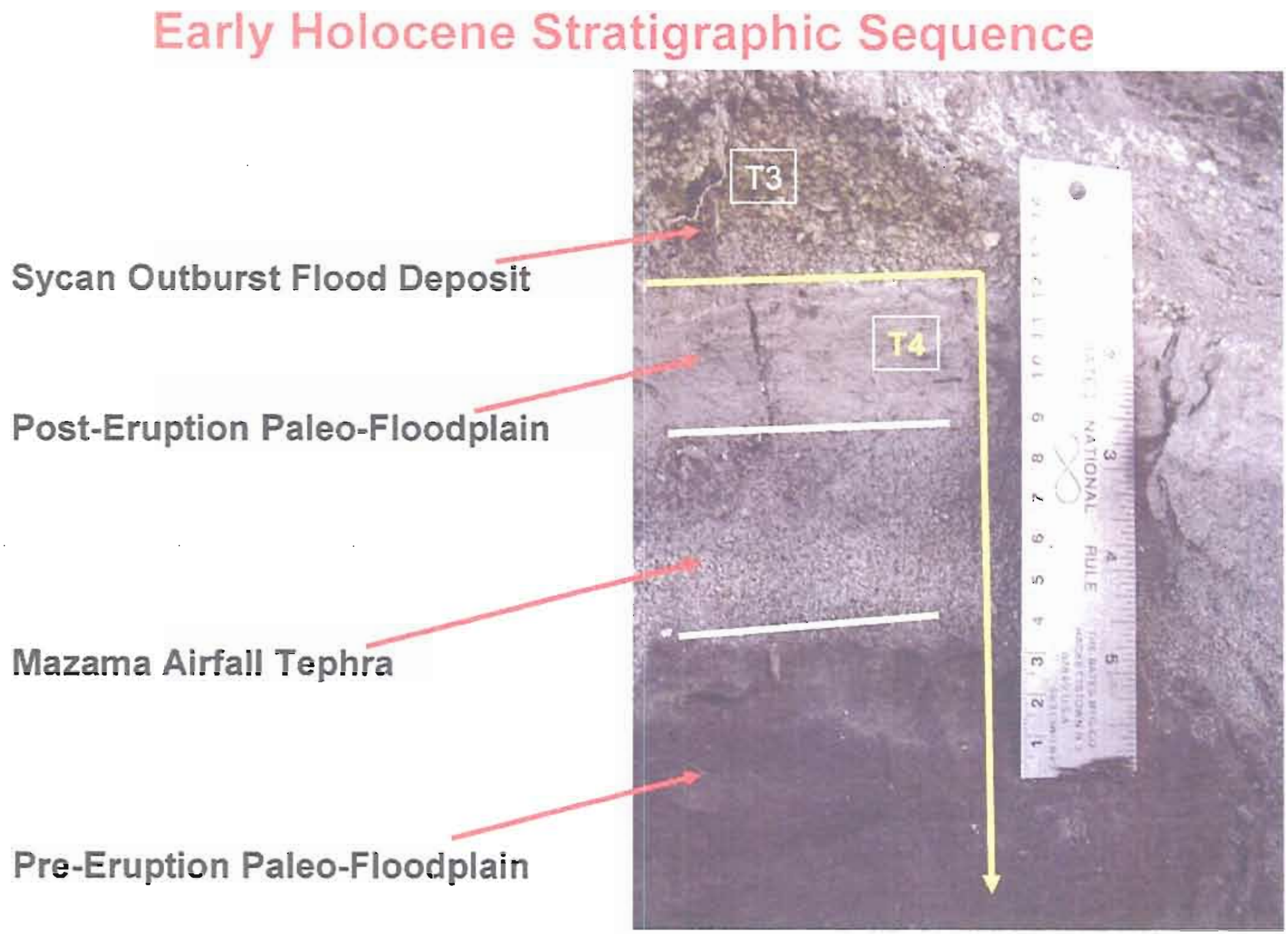

Figure 4-9. Photo of floodplain stratigraphy at BE-02
-- depicts sequence of deposition during the early Holocene on the lower Sycan River.

2007) contribute to groundwater that maintains high soil moisture levels (at or near saturation) at most observed sites of floodplain unit T_4.

Compositionally, the clays of unit T_4 are presumably the weathering product of the basalts and other volcanic rocks within the watershed. The well-sorted pumice grains in the top 5-10 cm are interpreted as Mount Mazama tephra aerially deposited onto the floodplain surface. Where the Mazama airfall pumice is not a distinct sedimentary layer but rather dispersed within the top 10 cm, this is interpreted as a reworking of the pumice airfall deposits by low-energy overbank flow and/or bioturbation.

The sands and gravels observed at some locations in the lower one-third of the Sycan Valley as a layer near or at the base of the clay-silt dominated paleosol suggests that localized sandy gravel channel beds may have existed there during this period of the Holocene. In the upper third of the Sycan Valley buried sands and gravels were rare. Excavation beyond the base of unit T_4 did not occur at all sites, usually due to the increased thickness in the upper valley. Therefore it is not possible to definitively describe the range and distribution of materials at the base of this unit. Incision has exposed sands and gravels at the base of T_4 units in the downstream portions of the channel to contemporary river processes in the lower Sycan Valley.

At auger site AUG-07 recovery of a charcoal fragment at 90 cm depth below the top of unit T_4 generated an adjusted date of 11,640 cal *yr* BP (USGS-WW5421). The charcoal sample was retrieved from the clay soils of unit T_4 at approximately mid-unit depth. This date confirms that the early Holocene period of low-energy floodplain development maintained a state of relative dynamic equilibrium for over 4 ka years prior to the Sycan Outburst Flood that buried the T_4 unit.

Channel Characteristics. Prior to the Sycan Outburst Flood the lower Sycan River flowed through a wide, clay-silt floodplain. Based on sediment characteristics and gradient, the channel was probably a single-thread or anabranching channel of moderate to high sinuosity (Schumm 1985; Graf 1988b; Brierley and Fryirs 2005; Schumm 2005). The clay and silt dominated low gradient floodplain displays characteristics similar to Nanson and Croke's (1992) laterally stable single-channel or an anastomosing-river of a low-energy cohesive floodplain. It is likely that the laterally stable banks were fairly vertical and that point bar development was minimal (Nanson and Croke 1992; Schumm 2005). Since lateral migration rates were low the primary fluvial process was most probably overbank accretion during seasonal discharge (Graf 1985).

Lack of sands or gravels within the clay-silt dominated paleosol in the upper half of the valley implies that the bed of the channel was presumably clay-silt dominated here. In the lower portion of the valley the channel may have had sand and gravel beds derived from localized bedrock or interaction with the Sprague River near the confluence. Within this type of low gradient system a network of shallow distributary and tributary channels probably twisted across the floor (Graf 1988a; Nanson and Croke 1992) of Sycan Valley, with many originating at springs along the margins of the valley.

Geomorphic Thresholds. From the data provided, Period I appears to have been relatively stable. The stratigraphy of floodplain unit T_4 does not offer any evidence of episodic complex channel response during this period. Even airfall pumice from the eruption of Mount Mazama (7660 cal *yr* BP) did not appear to significantly alter the channel and floodplain development processes in the Sycan Valley. In other words, though the system's sand content was increased by the aerial deposits of Mazama pumice, no major geomorphic threshold was exceed. After aerial deposition, low-energy vertical accretion continued on the floodplain.

Though the specific hydrologic history of the lower Sycan River through the Holocene is unknown, the climate of the early Holocene generated ground and surface water enough to support a wetted floodplain environment on the valley floor. Bradbury et al. (2004) suggest that there was reduced hydrologic input (surface water discharge) from upstream during the early Holocene in to the Upper Klamath Basin due to a drying trend. However, increased summer monsoons during this dry period were inferred by Minckley et al. (2007) from sediment and pollen data collected from lakes in the area. Climate records from lakes in the Siskyou Mountains, west of the Klamath Basin, suggest an increase in precipitation in winters (Briles et al. 2005).

Termination of Period I. Period I (Early Holocene Dynamic Equilibrium) abruptly ended with the landscape altering Sycan Outburst Flood at approximately 7580 cal *yr* BP. At this point the evolutionary period of channel and floodplain development in the Sycan Valley rapidly shifted from clay and silt dominated to a system dominated by pumice-rich sand. The outburst flood buried the preexisting T_4 floodplain, scoured a trench into T_4 -- altering the gradient of the floodplain and probably also the channel bed.

Period II. Sycan Outburst Flood ***~7580 cal yr BP***

The Sycan Outburst Flood was a cataclysmic event that buried the preexisting T_4 floodplain, low terraces, and colluvium on the floor of Sycan Valley. A landscape transforming event such as this is referred to by Schumm (1969; 2005) as a river metamorphosis. It appears that the floodwaters scoured a trench into T_4 to accommodate flood discharge. The sediment deposited as a result of the Sycan Outburst Flood altered the gradient of the floodplain and probably also the channel bed. The resulting flood deposits (Sycan Outburst Flood Terrace Unit T_3) form a distinct geomorphic surface that is visible today as horizontal terraces that flank the inset Sycan River and floodplain.

Stratigraphy. The Sycan Outburst Flood Terrace T_3 units of the Sycan Valley are dominantly pumice-rich sands that generally fine upward from very coarse pure pumice ($\leq$ 1.5 cm diameter grain size) to a pumice-rich sandy loam. The stratigraphy within the terrace unit is horizontal with no evidence of depositional hiatus. Remnant thicknesses range from 350 cm at the head of Sycan Valley (AUG-07) to a truncated 45 cm near the mouth of the river at the southern end of the valley (BE-02). Figure 4-10 is a stratigraphic diagram of T_3 at PIT-01.

Sycan Outburst Flood Terrace floodplain unit T_3 has been divided into three subunits (T_{3a}, T_{3b}, and T_{3c}).

T_{3a} (Mid-Terrace floodplain unit) is observed longitudinally along the middle of the valley where high-energy thalweg flood mechanics likely occurred. T_{3a} is predominately composed of loose pure pumice with slight grain size variations expressed

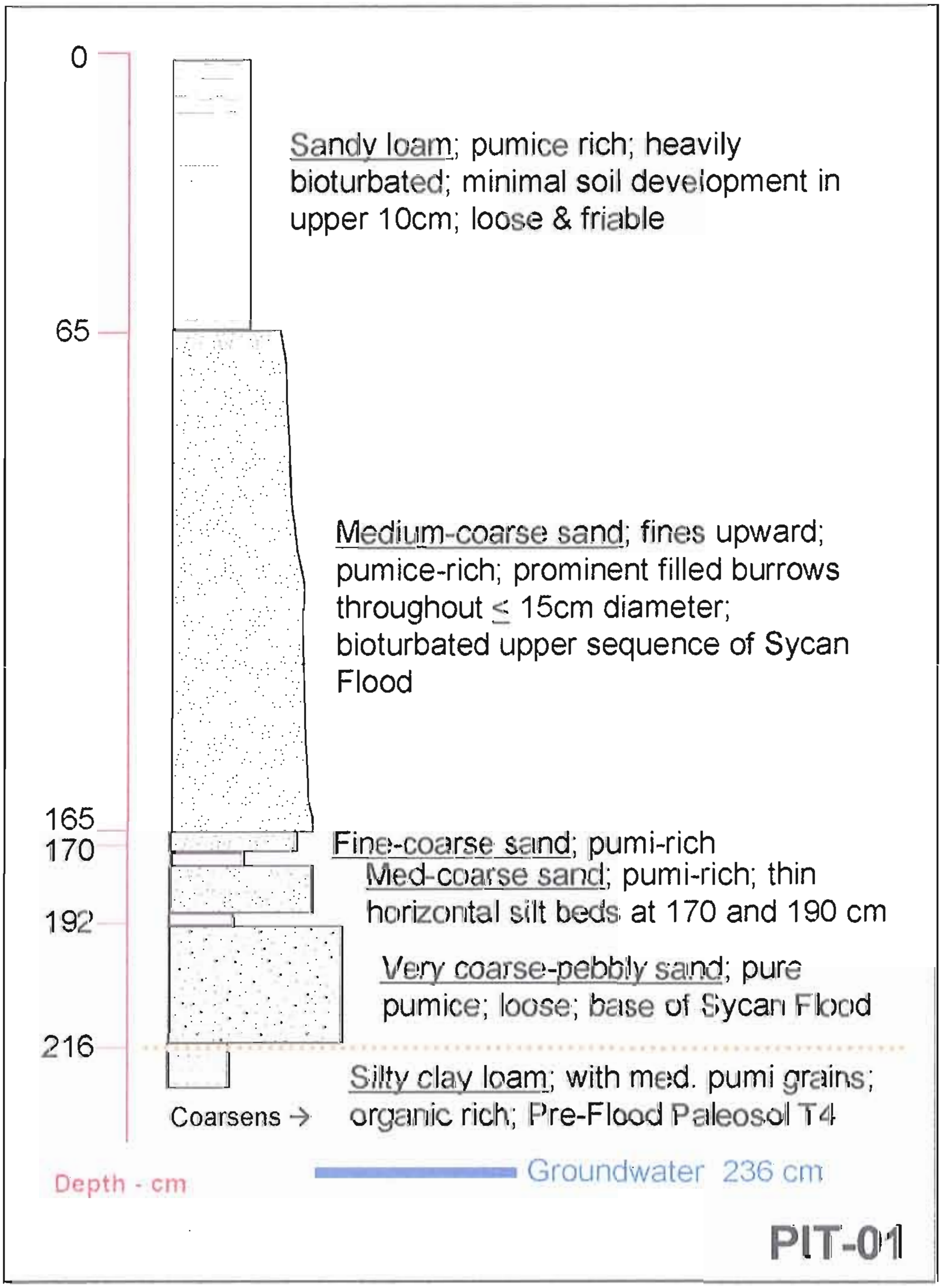

Figure 4-10. Summarized soil stratigraphy (T_{3b}) at PIT-01.

horizontally throughout the unit from gravels and coarse sand up to fine sand. The upper ~10 to 65 cm is extensively bioturbated by roots and burrowing animals. The basal contact is usually on a pre-flood paleosol floodplain surface (T_4) or bedrock. The surface of T_{3a} is topographically horizontal and continuous with T_{3b}.

T_{3b} (Terrace-Margin floodplain unit) is observed toward the margins of the flood terraces. This unit is defined by horizontal stratigraphic layers with variations in grain size (very coarse sand and gravels to silt), lithic composition, and sorting indicative of hydrologic flood pulses. The upper ~165 cm of unit T_{3b} is extensively bioturbated by roots and burrowing animals. The basal contact is most often horizontal and rests on top of a pre-flood paleosol floodplain surface (T_4) or bedrock.

T_{3c} (Truncated floodplain terrace unit) is Sycan Outburst Flood Terrace units T_{3a} or T_{3b} with some quantity of the upper layers fluvially eroded. The extent of truncation is dependent on localized historic erosional processes resulting in varied surface elevations. The upper boundary of T_{3c} units is often an erosional contact that is usually topped with post-flood depositional sequences of reworked flood deposits and/or modern floodplain units (T_1 or T_2).

Floodplain Development. The Sycan Outburst Flood exited the mouth of the Sycan Canyon and immediately began transforming the landscape of the Sycan Valley. Transportation and then deposition of mass quantities of sediment across the floodplain probably was accompanied by erosion and enlargement of the existing channel commonly observed with outburst floods (Blair 2001; Blair 2002). Floodwaters scoured a trench through the pre-flood paleosol unit T_4 to accommodate the flood's massive discharge. Scour such as this often occurs with the first phase of hydrograph recession (Baker 1988) as flood water discharge is concentrated to a narrower pathway, increasing its energy and transport capacity. Continued waning of flood waters eventually cause infilling of the scoured trench with flood-load deposits (Baker 1988; Blair 2002). Similar to changes in the North and South Fork Toutle Rivers that resulted from lake outburst flows and lahar flows respectively (Simon 1999), the lower Sycan River likely experienced more relative trench scour upstream and greater infilling downstream.

Channel Characteristics. Immediately after the flood the channel was likely a network of shifting braids across the top of the newly laid deposits. Braiding is common in channels contending with an over-abundance of easily mobilized sediment.

Geomorphic Thresholds. Period II (Sycan Outburst Flood) is a temporally short episode of massive net deposition in the Sycan Valley. This event was an extrinsic variable to the Sycan Valley that resulted in a river metamorphosis of the lower Sycan River.

Termination of Period II. The wane of flood waters generated by the Sycan Outburst Flood ended Period II.

Period III. Initial Channel Formation / Incision ~ *7580 cal yr BP for 1-50 years*

In response to the abundance of non-cohesive, easily transported sediment, as well as an altered channel elevation and gradient, a series of channel forming processes dominated by incision was initiated after the Sycan Outburst Flood. The capacity of the system to define a channel would have been driven by the discharge regime of this period.

Floodplain Development. As a period of net erosion, no new floodplain unit was developed. During this period the Sycan Outburst Flood deposits were truncated and reworked through processes of both incision and channel widening. Truncated Sycan Outburst Flood unit T_{3c} is shown on the geomorphic map of the upper valley (Appendix D, Plates 1 and 2). The T_{3c} areas are relatively broad landforms that suggest that initial incision into the flood deposit occurred by a wide or shifting low-energy channel(s) or overbank scour processes.

Channel Characteristics. Since it was mobilizing abundant non-cohesive sediment, the newly forming lower Sycan River was most probably a braided channel (Richards 1982; Nanson and Croke 1992; Brierley and Fryirs 2005; Schumm 2005; Simon and Rinaldi, 2006). Similar to the North Fork Toutle River, Washington (USGS 1999), initial channel erosion into the non-cohesive banks would have promoted channel widening. This resulted in an increased sediment load and reduced/dissipated stream energy.

Geomorphic Thresholds. This period most likely experienced rapid channel bed oscillations generated by headward migrating knick-zones as the system adjusted internally to the over-abundance of sediment. Successive waves of headward migrating knick-zones would have incised the bed, periodically increasing localized channel slope. Such changes in slope or stream power relative to sediment load would have instigated episodic complex response cycles (Schumm 1979; Schumm et al. 1987). These response cycles would have included repeated periods of incision upstream, widening through mass-wasting at the area of maximum disturbance, and aggradation downstream. Incision increased channel depth which also increased bank height. An increased bank height would have resulted in mass wasting of the non-cohesive banks as bank shear strength was exceeded. Lateral shifts in channel location may also have occurred.

Termination of Period III. This fluvially dynamic period was probably relatively short, perhaps lasting between one peak flow and fifty years, depending on discharge. The end of Period III is marked by the eventual definition of the channel's pathway through incision processes.

Period IV. Degradation and Widening *~ 7580 - 5920 cal yr BP*

Period IV is an extension of the active incision and net erosion begun during Period III. Once a pathway for the channel was formed the available stream power would have been more concentrated than during the previous period. This likely intensified the shear stress and transport capacity of the system during high flow events.

Floodplain Development. As a period of net erosion, no new floodplain unit was developed. During Period IV full abandonment of the Sycan Outburst Flood Terrace units (T_3) occurred. Reworking and truncation of the flood deposit material would have continued within the defined channel pathway.

Channel Characteristics. Shifting channel form between single-thread meandering and braided probably occurred, as sediment inputs varied spatially (Schumm 1979; Lane and Richards 1997). At site AUG-06 a few faint, thin beds of fine sands and silts are found between slightly reworked flood deposits. This is indicative of channel abandonment and reactivation typical of systems that are braided or shifting between braided and meandering. Based on Schumm's (2005) discussion of river variability, these conditions would have resulted in low channel sinuosity.

Geomorphic Thresholds. The river continued to incise into the Sycan Outburst Flood unit. Compared to the previous period, the erosive processes were likely intensified during high flow events due to the increased stream power and shear stress of a defined channel. Channel bed degradation into the pumice-rich flood deposits would have continued to destabilize the non-cohesive banks, resulting in mass-wasting and channel widening (Simon 1989; Simon 1992; Simon and Darby 1999; Simon et al. 2000; Simon and Rinaldi 2006). This would have resulted in continued oscillations in bed elevation as knick-zones migrated upstream. The complex channel response would have increased downstream aggradation as knick-zones migrate upstream causing increased degradation and bank failure.

The reconstructed climate history of this period (Table 1-1) suggests that the northwestern Great Basin was relatively warm and dry. Wigand and Rhode (2002), and Grayson (1993) report findings that suggest droughts in the region until approximately 6 ka . If the extrinsic variable of precipitation in the Sycan River was low, then it is assumed that the system's quantity and/or frequency of available discharge were also low. A limited flow in a low-gradient, sediment-abundant system would likely slow the timing and rate of the internal channel adjustments occurring during this period.

Termination of Period IV. The dominant geomorphic process of incision (Period IV) ended when incision eventually reached the more resistant flood-scoured trench of the clay-dominated Early Holocene Floodplain unit T_4. It is expected that erosive processes would then have caused channel widening and lateral migration into the non-cohesive pumice-rich banks (Simon and Thomas 2002; Simon and Rinaldi 2006). Erosion was likely relatively minimal into the more resistant clay bed (Schumm 1979). A shift in trending climate conditions from a warm drier climate towards wet cooler conditions at this time could have changed the system's discharge regime and thus its sediment transport capacity.

Period V. Aggradation and Lateral Migration ~ *5920 – 1350 cal yr BP*

Period V is a relatively long period resulting in net deposition and the development of a meandering channel and its active floodplain. The Late Holocene floodplain unit T_2 was developed during this period through the geomorphic processes of aggradation and lateral migration that dominated channel and floodplain development during Period V.

Stratigraphy. The Late Holocene floodplain unit (T_2) is an overall fining upward sequence of very coarse sands to silt or sandy loam, typical of floodplains of meandering channels (Knighton 1998). Figure 4-11 is a stratigraphic diagram of T_2 at BE-08. The basal composition of the T_2 floodplain unit is typically very coarse pumice sand, with common pebbles or gravels and/or organic detritus (small wood pieces). Pumice-rich dominated sand beds 4 – 100 cm thick are prominent in the lower portion of the unit with

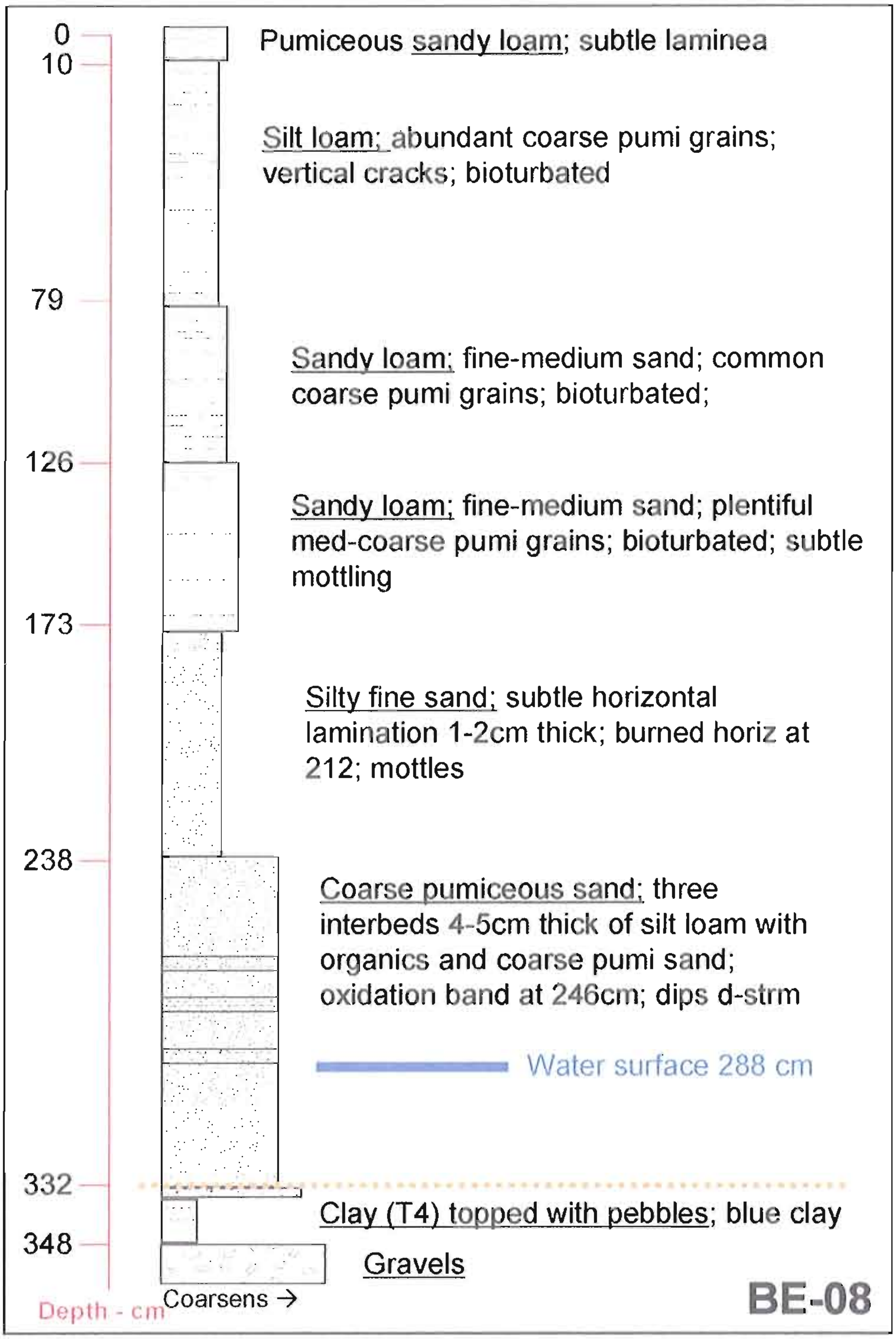

Figure 4-11. Summarized soil stratigraphy (T_2) at BE-08.

grain sizes of very coarse sands to fine sands and silts that can be rich in organics (small wood pieces). These beds sometimes dip at a downstream angle with wavy bedding and/or lenses. The base of unit T_2 usually extends to or below low flow modern channel surface elevations, except where it onlaps onto an older depositional unit (T_{3c} or T_4). Sand or silt loam is dominant in the upper ~ 10 to 80 cm of this unit. Laminae of silt or sandy loam from overbank deposits are present in the upper strata. The sandy loam portion is been bioturbated by roots and animal burrows.

Floodplain Development. The lower sand-dominated portion of unit T_2 is interpreted as bar development and bed aggradation in an active, laterally migrating channel. The upper silt loam or sandy loam portion of unit T_2 is interpreted as being created by vertical floodplain accretion. As a result, at channel bank exposures the less cohesive toe of the unit often slopes gradually and the upper accreted silts and sands usual display vertical or convex banks (Figure 4-12).

The surface of floodplain unit T_2 is inset below T_3 by up to 2.25 m in the upper valley. Depth of inset decreases gradually downstream (see Figure 4-1). Surface elevations of unit T_2 are normally higher than the modern floodplain unit T_1. In the most downstream portions of Sycan Valley or where T_2 has been vertically truncated, surface elevations have been observed as equal to T_1. However, throughout the Sycan Valley the upper portion of the Late Holocene floodplain unit T_2 is overlain by modern overbank deposits. Observed flooding in the spring of 2006 indicates that this floodplain unit remains connected to the modern channel at a flood recurrence interval of at least two years.

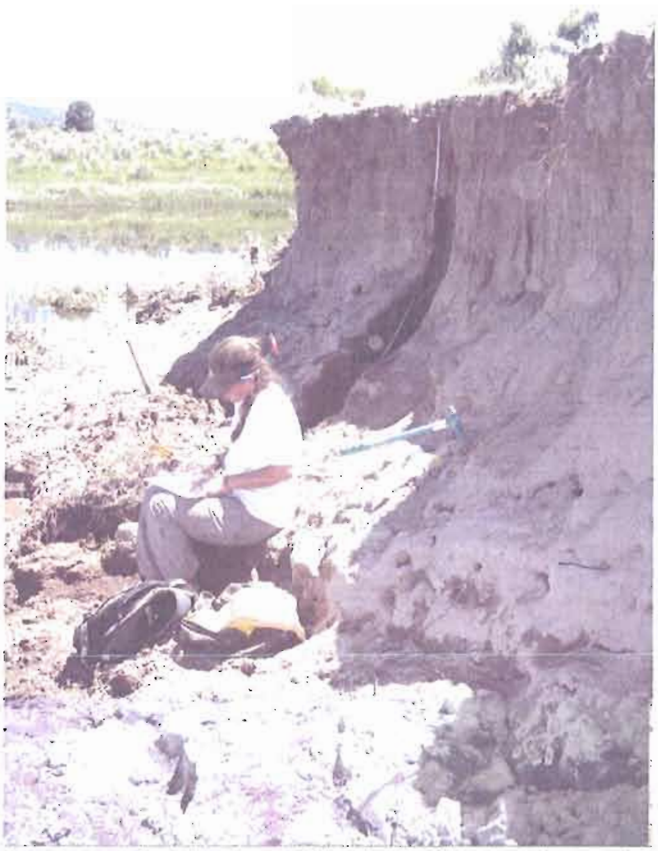

Figure 4-12. Photo at BE-10 (T_2 floodplain unit).

The surface of the Late Holocene floodplain unit T_2 has shallow swales that appear to be infilling meander scars or chutes. Relatively modern floodchannel features, formed from erosive scour during overbank discharge events (Brierley and Fryirs 2005), also mark some of the floodplain surfaces of this unit. The marks resemble shallow canal-like swales that are perched on the floodplain. Today, this unit is vegetated with dryland grasses and shrubs.

Channel Characteristics. The characteristics of the Late Holocene floodplain unit T_2 indicate that the channel during this time likely experienced periodic shifts from braiding to a sinuous single-thread meandering morphology. Cut-offs and large sandy bed forms and bars were most likely prominent. These characteristics are similar to Nanson and Croke's (1992) meandering, medium-low energy system with a non-cohesive floodplain that laterally migrates gradually or shifts with chute cut-offs resulting in scrolled floodplains.

The complex stratigraphy at a few sites supports channel location shifts as part of the overall episodic behavior of this period. For example, at site BE-08 the stratigraphy displays a cut-and-fill process recognized by an unconforming boundary and separate depositional sequence within the bank exposure.

Geomorphic Thresholds. During Period V, the Sycan River's adjustments may have been due to continued response to the disequilibrium imposed by the outburst flood (intrinsic) or to effects of climate change (extrinsic). The channel widening initiated at the termination of Period IV may have set in motion an intrinsic feedback effect involving floodplain morphology and development. Channel widening would have likely increased sediment load, dissipated or reduced stream energy, initiated lateral channel migration, and consequently led to channel aggradation, as described in other models of channel evolution by Simon (1999), Simon and Darby (1999), and Simon et al. (2000). As a result a sinuous meander belt would have evolved (Knox 2006).

On the lower Sycan River lateral migration was partially confined within the walls of the more resistant T_4 clays of the flood trench, except at the mouth of the Sycan River below the extent of the T_4 unit. The erosive processes of high-flow events and successive waves of headward migrating knick-zones probably resulted in lateral migration and shifts in channel location that generated additional sediment, promoting a complex channel response feedback effect.

Climate records indicate a shift in climate trends during Period V. An increase of effective moisture (wetter conditions) is noted throughout the region beginning between 6 to 5 ka , mostly coming as increased winter precipitation (Grayson 1993; Wigand and Rhode 2002; Bradbury et al. 2004; Briles et al. 2005; Minckley et al. 2007). Most notable is the increase in lake level at Upper Klamath Lake (Bradbury et al. 2004) beginning at 6 ka , which is attributed to increased precipitation and river flow into the lake. This implies an increased discharge regime in the river systems upstream from the lake such as the Sycan River. If this period of increased moisture included higher flood discharges, building of the T_2 unit could be attributed to an active fluvial system with abundant sediment. Available sediment sources would have included local stores from the outburst flood deposits and some upstream channel network extension (Tucker and Slingerland 1997).

Termination of Period V. One possible explanation for the shift from Period V to Period VI is internal geomorphic evolution, and a second possible explanation is some external forcing such as climate change or other disturbance events. The feedback mechanisms that developed a sinuous meander belt and the Late Holocene Floodplain unit T_2 eventually evolved past the system's geomorphic capacity to continue a period dominated by aggradation and lateral migration. Where the sinuosity of the channel increased along with a continued decrease of gradient, stream energy would have reduced such that sediment transportation capacity was limited. Additionally, the quantity of available easily-transported sediment was likely reduced by fluvial reworking and floodplain storage. The fluvial reworking process had increased the percent of silt and fine sand in the upper channel banks thus increasing bank stability. Available sediment input from the Sycan Canyon and even locally may have been reduced by an increased vegetation cover supported by the increased moisture of this period.

Alternatively, decreased available moisture (decreased precipitation) related to the Little Ice Age starting around 2,000 (Starratt et al. 2002; Wigand and Rhode 2002) may have triggered the change from Period V to VI. Depending on timing and duration, a period of reduced precipitation may have also reduced the quantity of discharge events, also reducing the system's ability to transport the available sediment. This type of extrinsic climate change could have initiated the feedback loop described above where reduced discharge resulted in decreased sediment transport capacity. The resulting reduction in channel gradient and availability of easily transported sediment eventually initiated a secondary period of degradation (Period VI) that likely began downstream as headward migrating knick-zones.

Period VI. Secondary Degradation and Widening ~ *1350 – 590 cal yr BP*

Period VI is a hiatus in the stratigraphic record, and it is inferred to be a period dominated by incision into the Late Holocene Floodplain unit T_2 banks and bed.

Floodplain Development. As a period of net erosion, no new floodplain unit was developed. The percent of fines in the bank material of Late Holocene Floodplain unit T_2 are greater than in Sycan Outburst Flood Terrace unit T_3, giving the banks more shear strength. Bank failure thus likely occurred at a greater depth and a lesser rate than during pervious post-Sycan Outburst Flood periods of incision.

Channel Characteristics. Degradation of the channel bed would have instigated channel widening once bank height from incision exceeded bank shear strength (Simon et al. 2000). It is not possible to determine the maximum width of the degrading channel during Period VI but it is hypothesized that it was narrower than during the previous degradation episodes of Period III and IV. This assumption is based on the increased fines of T_2 and how “bank material exerts an important sedimentological control on the strength and stability of channel banks, therefore on the adjustment of channel width” (Knighton 1998, 175). Incision should have reduced channel sinuosity slightly, especially at the areas of maximum disturbance. It is inferred that channel form probably remained primarily single-thread meandering.

Geomorphic Thresholds. The Sycan River's evolution during Period VI was likely due to the crossing of intrinsic geomorphic thresholds through channel evolution and/or effects of climate change. Reduced sinuosity as a result of incision would have created a positive feedback mechanism where channel slope and stream energy are increased, thus enhancing the systems capacity to remobilize and transport sediment. At areas of maximum disturbance it is likely that complex channel response occurred with headward migrating knick-zones. Eventually the channel bed incised to the more resistant flood-scoured trench of the clay-dominated Early Holocene floodplain unit T_4. Similar to the geomorphic process of channel widening hypothesized in Period V, once incision reached the more resistant materials of T_4 erosive processes would have widened into the less-cohesive sand dominated lower banks of T_2, leading to bank failure. Slight incision into floodplain unit T_4 probably occurred during high flow erosive events. It is assumed that the hypothesized channel widening dissipated stream energy while adding more local bank sediment into the system.

Climatologically, decreased available moisture (decreased precipitation) related to the Little Ice Age around 2-1 ka may have triggered the geomorphic processes of Period VI. Depending on timing and duration, a period of reduced precipitation likely reduced the size of discharge events. Mohr et al. (2000) also reported a dry period at Cedar Lake, California south of the Klamath Basin 1-2 ka . However, the general trend in climate reconstruction depicts the later Holocene as being more wet and cool than previous conditions (Mohr et al. 2000; Bradbury et al. 2004; Minckley et al. 2007). In conclusion, it is unclear how much the extrinsic variable of climate played during the channel response of Period VI.

Termination of Period VI. This model proposes that the processes of channel degradation and widening rejuvenated the sediment available for localized and downstream aggradation by reactivating sediment from the banks and bed. The dominant geomorphic process of incision likely ended when incision reached the more resistant flood-scoured trench of the clay-dominated Early Holocene floodplain unit T_4. Increased stream energy as a result of incision or increased available discharge related to climate conditions could have instigated the shift between Period VI and VII.

Period VII. Modern Dynamic Equilibrium *~ 590 cal yr BP - present*

The present Period VII appears to be one of relative equilibrium. At present, floodplain inundation frequencies and dispersed channel migration indicate that deposition and erosion are relatively balanced in the lower Sycan River. The Modern Floodplain units T_1 and Active Channel and Bars T_0 were developed and continue to be maintained through the geomorphic processes of aggradation, degradation, and lateral migration that dominate the modern channel and floodplain.

Stratigraphy. The Active Channel and Bars unit T_0 consists of active bars and scoured surfaces located at the channel margins. This unit is composed dominantly of pumice rich sands and some pebbles/gravels.

The Modern Floodplain (T_1) unit is a gradual fining upward sequence common in the floodplain of meandering channels with a stratigraphic sequence of course to medium sand that fines upward to silt or clay loam. Mottling is sometimes visible. Dispersed accumulations of charcoal are often found throughout the entire strata of floodplain unit T_1. Similar to the other depositional sequences of the lower Sycan Valley, the thickness of T_1 is greater upstream (270 cm at BE-18) than downstream (160 cm at BE-01).

The base of the T_1 floodplain unit is usually sand dominated with sand, pebbles, or gravels and/or organics (small wood detritus) in the lowermost part. The base of unit T_1 usually extends to or below modern low-flow channel surface, except in the situation where it has been overlaid on top of an older depositional unit such as T_2, T_{3c}, or T_4. In the upper portions of the basal section, horizontal and sometimes wavy bedding and/or lenses (2 to 20 cm thick) of varying grain sizes (silt or fine to medium sand) are found at some sites.

Silt or silt and clay loam is prevalent in the upper ~1.0 - 2.0 m of unit T_1. Here the channel banks are vertical and often have vertical desiccation cracks during summer. Laminae from modern overbank fine deposits are present in the upper-most strata. Bioturbation by roots and animal burrows are common. Figure 4-13 is a stratigraphic diagram of T_1 at BE-01.

Floodplain Development. These geomorphically active units are the lowest and most inset floodplain surfaces of the lower Sycan River. Bar development and maintenance often appears to be related to downstream proximity from a localized sediment source. Usually the surface of T_0 floodplain units are unvegetated or only seasonally vegetated with riparian species. Similar to the processes creating the modern Active Channel and Bars (T_0), the lower portion of the Modern floodplain unit T_1 is interpreted as aggradation related to lateral channel migration and bar development.

The upper portion of floodplain unit T_1 is interpreted as vertical floodplain accretion generated by overbank deposits. Today high-flow events with a recurrence interval of 2 years or less continue to inundate and deposit sediment on the Modern floodplain unit $T_{1,}$ as well as most of the Late Holocene (T_2) floodplain units. Active Channel and Bars (T_0) are inundated annually with seasonal high flows.

Because the lower Sycan River remains a sand-dominated system that experiences seasonal high flow events, the state of equilibrium is geomorphically active and perhaps difficult to identify in places. Lateral, vertical and oblique accretion processes develop

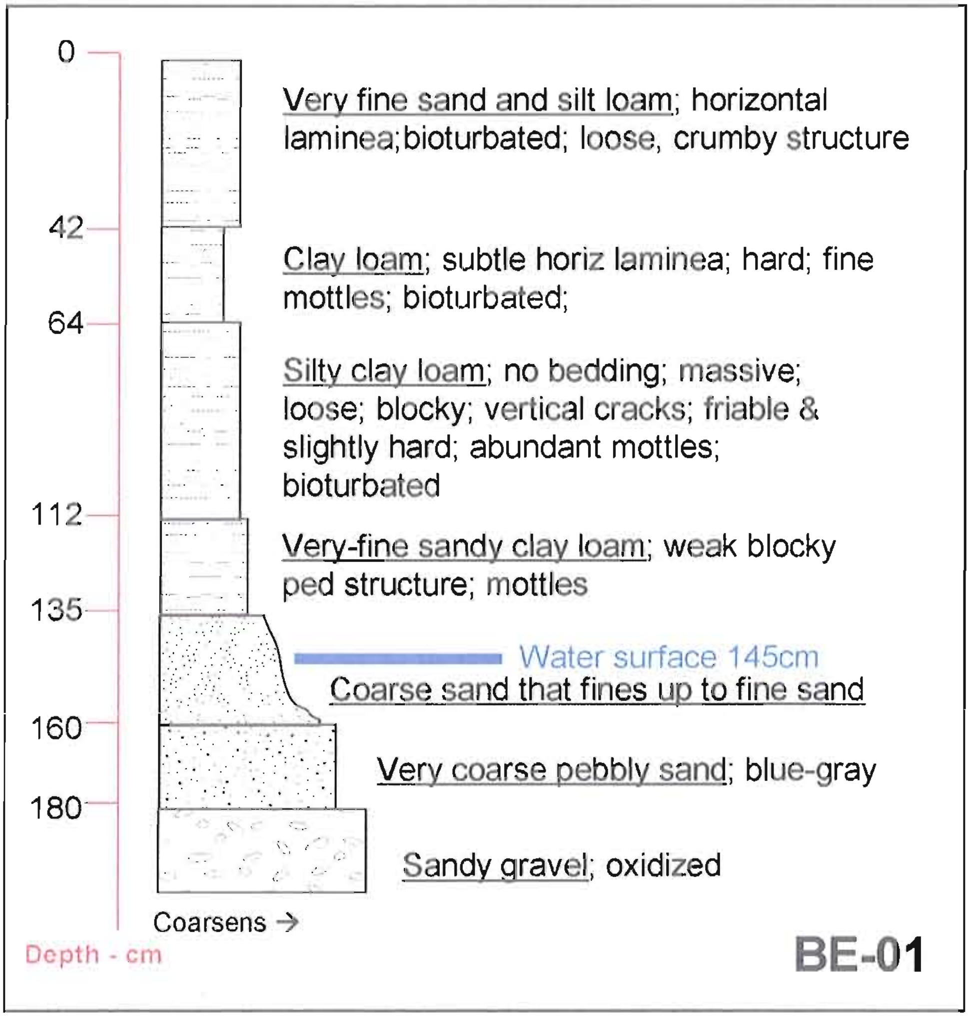

Figure 4-13. Summarized soil stratigraphy (T_1) at BE-01.

and maintain bed forms. Point bars and cut banks are found in the meandering sections of the channel but not at every meander bend. While most channel change occurs during seasonal high flows, even at low flows the non-cohesive sands on the lower banks may erode. As described by Brierley and Fryirs (2005), eventually basal erosion of less-cohesive bank toe material creates undercut banks that fail even when upper-banks are relatively cohesive. Bank failure remains an important aspect of the modern channel's process of lateral migration into the T_1 and T_2 floodplain units and sediment reactivation into the system.

The surface of floodplain unit T_1 is lower than the surface of T_{3a} by up to 3.30 m at mid-valley. The surface of T_1 is also often lower in elevation than T_2 in the upper valley by about 1.5 m, with the elevation difference decreasing to null in the lower part of the valley. The surface of the Modern Floodplain unit T_1 is scarred by scroll marks, abandoned channels, and cutoff chutes at different stages of infilling. Floodchannels caused by erosive scour of overbank discharge events are also found on the surface of this unit. The surface relief of T_1 is greater than T_2, probably due to less time infilling from overbank deposits. The surface is vegetated with a mix of grasses, shrubs, and forbs. Along oxbows or other abandoned channel indentations, populations of willow, current and/or rose are found (Massingill 2008).

Channel Characteristics. The increased percent fines of the Modern Floodplain unit T_1 make for more resistant channel banks than floodplain units T_2 or T_3. More resistant bank material allows for a channel form that is less wide than that of less-cohesive bank material. The lower Sycan River has characteristics of a channel within a floodplain most similar to Nanson and Croke's (1992) classification of medium-low energy, with partially-cohesive materials, lateral migration and a scrolled floodplain.

Geomorphic Thresholds. A combination of geomorphic evolution and climate change probably combined to instigate the shift in the dominant geomorphic process from erosive (Period VI) to a period were depositional and erosive processes were more balanced (Period VII). The channel widening processes at the close of Period VI initiated lateral migration and thus an increase in channel sinuosity in Period VII. It is assumed that lateral migration reactivated localized bank sediment that eventually led to reduced channel gradient through cycles of complex response. The resultant stream energy, channel geometry, and hydraulics have adjusted to the available sediment in the system today.

During Period VII localized incision into the walls and bed of the resistant flood-scoured trench, at relatively low rates, has occurred, except at the mouth of the Sycan River. Here incision has eroded through the T_4 paleosol into less resistant sands. Erosion of the T_4 floodplain unit probably occurs only during high-flow or flood events.

At 300 years ago Bradbury et al. (2004) reports increased lake levels in Upper Klamath Lake linked to increased precipitation. As a primary tributary to this system, it is assumed that the Sycan River also experienced an increase in precipitation.

Predicted Termination of Period VII. The state of equilibrium of Period VII is considered "dynamic" because of the nature of fluvial systems to eventually adjust or evolve to a state of instability (Schumm 1979; Lane and Richards 1997). Also, the set of complex response adjustments that shaped the modern Sycan River offer numerous variables for future change. For example, future shifts in geomorphic processes of the Sycan River could be instigated by subtle changes in climate. A change in climate can alter the system's annual hydrograph and discharge regimes as well as vegetation cover. An increase in sediment supply from upstream via reduced vegetation cover (forest fires or a change in climate to drought conditions) could lead to canyon infilling which could produce an increase in available sediment to the system. That sediment may be fluvially transported downstream into the lower Sycan River system. Or, if drought conditions are severe enough, available sediment may accumulate to create another temporary dam. Temporary damming from a rock fall or landslide dam along the steep geologically faulted Sycan Canyon should also be considered. Conversely, intrinsic variables such as the continued accretion of vertical bank development from overbank deposits, combined with a lack of upstream or locally available bed material may increase channel incision to the point of disconnecting the channel from its current floodplain. This would increase stream energy by confining high-flows to within bank area, and thus shifting the system into yet another period dominated by episodes of degradation.

Land-use practices pose another variable with possible impacts on the stability of the channel. Noted in the field are areas of reduced bank stability as a result of trampling and vegetation removal along the lower Sycan River where overgrazing was permitted within the riparian zone. If these practices continue or increase, the channel will be forced to respond.

The Modern Lower Sycan River

General Characteristics

The contemporary lower Sycan River is a low gradient meandering system that remains dominated by pumice-rich sand deposited by the Sycan Outburst Flood. Abandoned terraces of flood deposits (T_3) flank the channel and its modern floodplain. Seasonal high flows regularly overtop modern channel banks, maintaining connectivity between the channel and its active floodplain surfaces (T_2, T_1, and T_0). This connectivity results in both accumulation and supply of sediment to the system.

Modern lateral migration of the lower Sycan River appears to be driven by both avulsion and gradual cut-bank erosion processes (Figure 4-14). Digital analysis of historical aerial photos (1940 and 2000) identified sixteen obvious channel avulsions in a 60 year time period within the 16 river km of the lower Sycan River. Lateral migration rates during this time vary spatially through the system from almost nothing, where the channel is confined by bedrock or resistant T_4 banks, to a maximum of 54 m at a translational/rotational migration bend at the unconfined mouth of the channel at 0.243 river km.

The 60 year time period of lateral migration measured from the aerial photos has obviously been influenced by modern anthropogenic activities. However, paleo-channels on the inset floodplain surfaces (T_2 and T_1) are visible in high resolution LiDAR imagery (Figure 4-15). The paleo-channel patterns suggest that the lower Sycan River actively migrated laterally during floodplain development periods that created floodplain units T_2 and T_1. It is expected that lateral migration and channel avulsion rates in the mid-late Holocene were greatest during the development of floodplain unit T_2, due to the less cohesive composition of its material. Further digital analysis and floodplain reconstruction would be necessary to estimate paleo-channel migration rates.

Lateral migration of the modern lower Sycan River predominately occurs where the channel banks are composed of Modern Floodplain unit T_1. Bank failure from basal

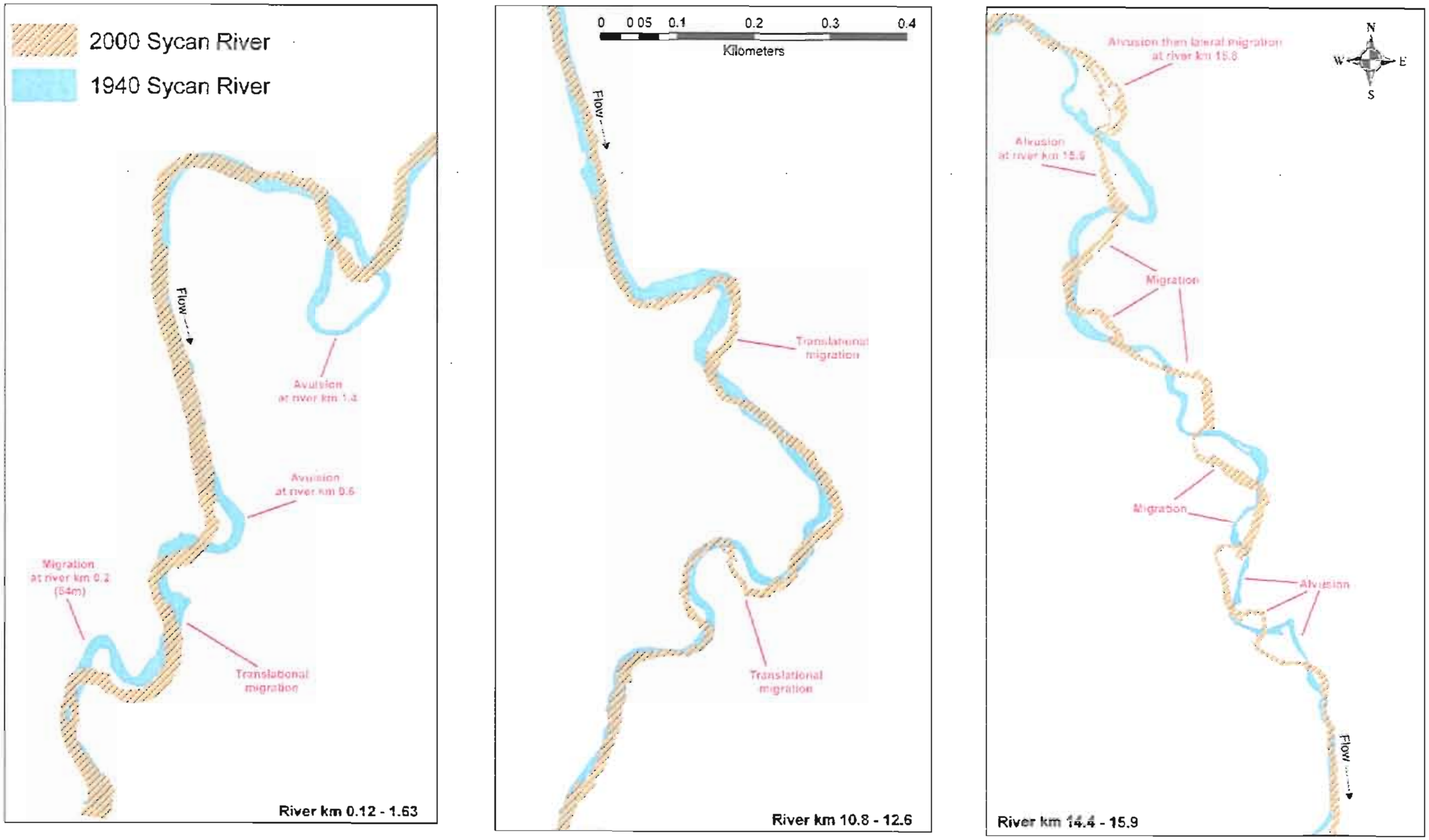

Figure 4-14. Examples of channel shift along three sections of the lower Sycan River between 1940 and 2000.

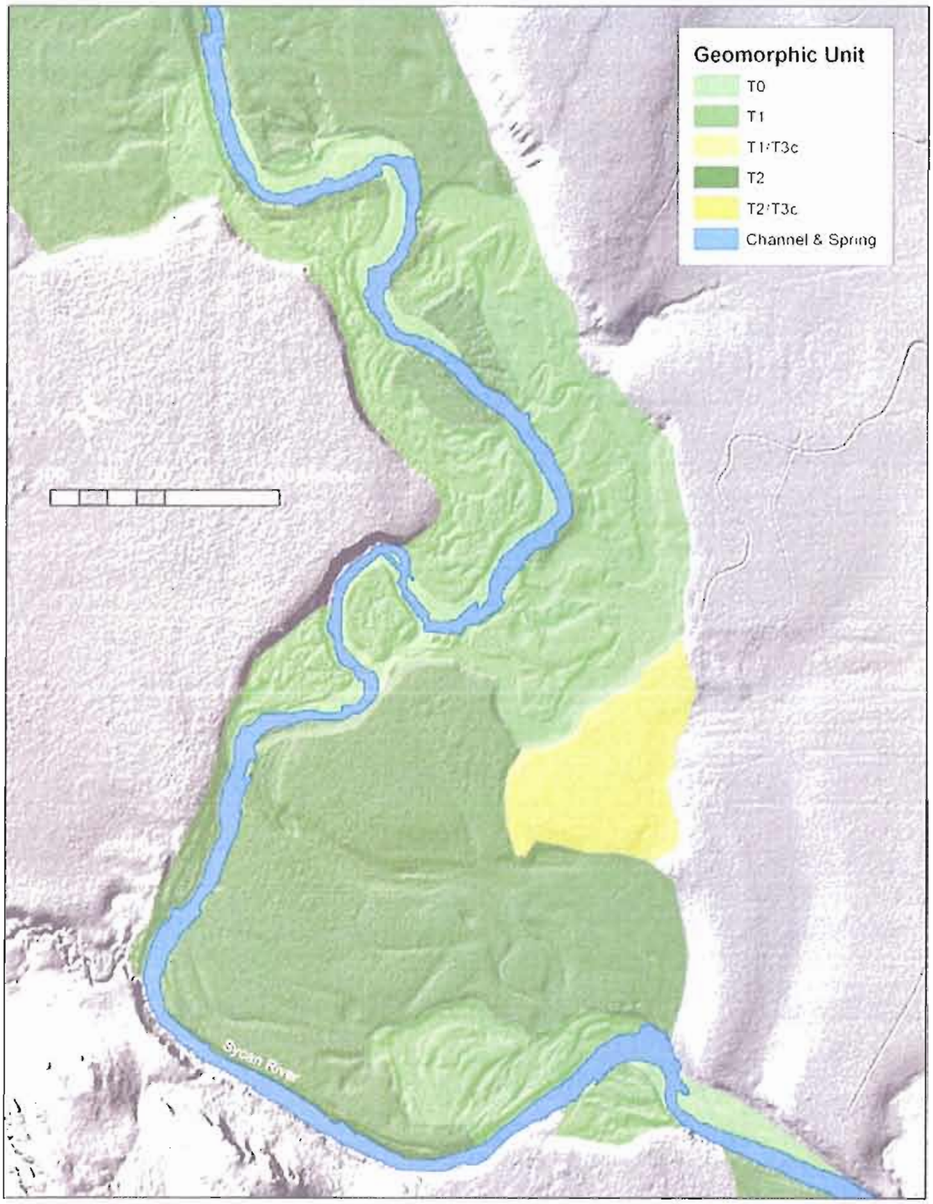

Figure 4-15. Active floodplain surfaces of the lower Sycan River (at 10 – 12.4 river km). LiDAR imagery visually displays scarred surface topography.

toe-bank erosion is an important erosive process on floodplain unit T_1, at both high and low flow regimes. Channel avulsion on the lower Sycan River is commonly initiated by overbank scour of flood channels that result in meander chute cut-offs, or reactivation of anabraching paleo-channels.

Form and composition of the lower Sycan River and its floodplain are indicators of how the system functions geomorphically. Understanding the channel's evolution and its contemporary channel and floodplain characteristics allows for prediction of future channel processes (Simon and Rinaldi 2006). The characteristics of the lower Sycan River's active floodplain and channel bed are presented below.

Active Floodplain of the Lower Sycan River

Graf (1985) and Nanson and Croke (1992) define regularly inundated surfaces as the "hydrologic or hydraulic floodplain" and "genetic floodplain" as surfaces created by present flow regimes. According to both definitions, all of the inset floodplain units (T_2, T_1, and T_0) of the lower Sycan River are both hydraulic and genetic floodplains. Floodplain unit T_0 (Active Channel and Bars) is inundated with seasonal bank-full flows, T_1 (Modern Floodplain) is inundated with seasonal overbank flows, and T_2 (Late Holocene Floodplain) is topped with modern over-bank deposits from inundation during seasonal flood events with a minimal recurrence interval of only two years. To accurately simplify terminology (hydraulic floodplain + genetic floodplain) the inset floodplain units T_0, T_1, and T_2 are hence referred to collectively as the active floodplain of the lower Sycan River.

The active floodplain of the lower Sycan River is inset within and thus confined by the Early Holocene Floodplain (T_4) and Sycan Outburst Flood Terrace (T_3). Prior to the Sycan Outburst Flood the lower Sycan River was a low energy fluvial system that spread overbank flow across the valley floor dissipating stream energy. Compared to the floodplain of the Early Holocene (Period I) the modern active floodplain acts as a "flume-like" conduit for seasonal high flows. Simon and Rinaldi (2006, 369) describe how storm flows in an incised constrained system result in the flow "having greater erosive power than when flood flows could dissipate energy by spreading across the flood plain." The morphologic alteration from an unconfined to a relatively confined floodplain creates a system with increased potential stream energy during high flows.

Width of the active floodplain varies as it crosses the Sycan Valley. A higher degree of channel sinuosity exists in areas of greater active floodplain width. Figure 4-16 shows the variations in active floodplain width and modern channel sinuosity relative to river kilometer. The width of the active floodplain is limited by confining factors such as

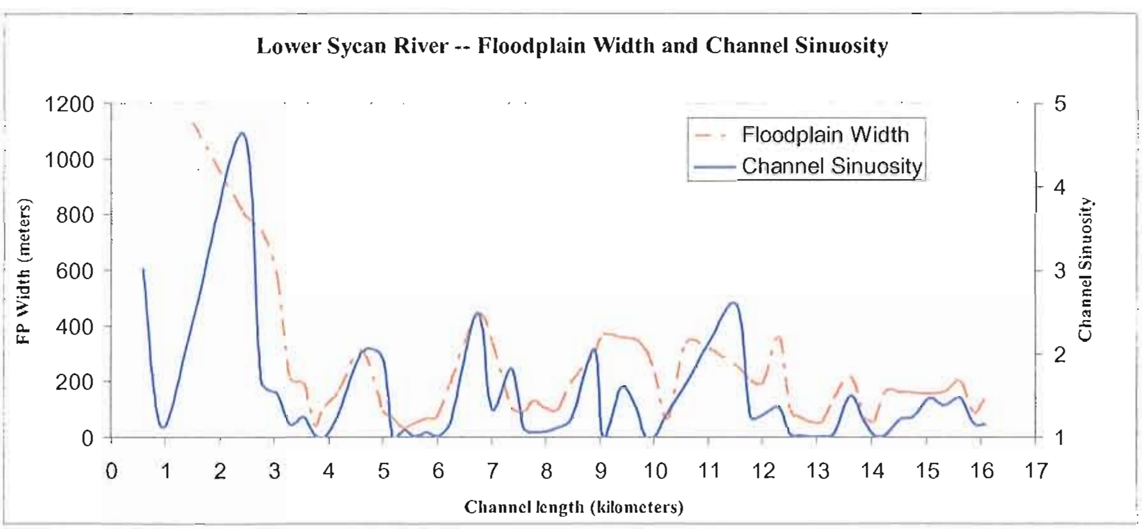

Figure 4-16. Active floodplain width and modern channel sinuosity.

hillslope bedrock, flood trench scoured banks, and paleo-terraces. Valley widening, combined with the overlapping fluvial processes of the Sprague River at the confluence, seem to have resulted in less channel confinement in the lower-most section of the Sycan River. Here, the floodplain and channel are dominated by silts and sands.

Channel Bed Morphology

The lower Sycan River is somewhat heterogeneous. However, even at low flow the surface of the water is calm and often void of surface breaks. This is likely due to the channel's overall low gradient. A detailed channel unit survey was not undertaken as part of this research, but field observations indicate that the primary channel units are glides and pools. Very few riffles are present, except at the most upstream portion of the channel. The relatively shallow riffle-like sections downstream often display a more glide-like smooth water surface, except where gravels are found.

The bed of the lower Sycan River is not consistent throughout. Cobbles and gravels with sparse boulders comprise the bed of the channel in the upper-most transition area between Sycan Canyon and Sycan Valley. At these most upstream meanders bar and bed material is gravel and pebble dominated. The gravels reduce quickly to sparse pebbles on a pitted clay bed, which is interpreted as the basal section of Early Holocene Floodplain unit T_4. The channel bed then evolves rapidly downstream to clay (T_4), silt or sands depending on localized channel morphology. Sparse gravels, often resting on pitted clay beds, are only found at sections of the channel in close proximity to bedrock sources or where the channel has incised into paleo-deposits of sandy gravel. Gravels are found in the channel at Drews Road bridge near mid-valley where the channel cuts into the sands and gravels of paleo-terrace T_{5a}. When incised, clay beds (T_4) occur as ledges that are locally exaggerated when incision reaches the easier eroded sand layers beneath the clays.

Near the mouth of the Sycan River the channel has eroded through the clay-silt paleosol (T_4) into more easily erodible sands and small gravels. Here the depth of the channel increases slightly creating what acts as a very gradual headward progressing knick-point. Approximately 1.6 km up the Sycan River from the confluence is where the knick-point into the clay paleosol occurs. Influence of this knick-point on future channel adjustments would be an important component to consider when predicting future channel evolution of the lower Sycan River.

The channel and floodplain units of the lower Sycan River are a legacy of the history of the landscape its watershed occupies. After an extended period of relative equilibrium in the early Holocene, the Sycan Valley and lower Sycan River was transformed by the Sycan Outburst Flood. After thousands of years of channel and floodplain evolution the modern channel appears to have reached a new period of relative equilibrium. Table 4-5 displays channel characteristics of the modern lower Sycan River along side the interpreted characteristics of the early Holocene equilibrium prior to the outburst flood. During the Holocene a transformation of the system has occurred.

Lower Sycan River	
Early Holocene Dynamic Equilibrium	**Modern Dynamic-Equilibrium**
CHANNEL CHARACTERISTICS	
Single-thread or anastomosing; high sinuosity	Single-thread; moderate sinuosity
Laterally stable	Meandering (irregular); lateral migration & cut-off chutes
Low-energy	Low-medium energy
Minimal or no bars; vertical banks	Sand-gravel bars; banks sloping at sandy base & vertical in upper silt-dominated portion
FLOODPLAIN CHARACTERISTICS	
Cohesive floodplain (clay and silt dominated) – T_4	Non-cohesive floodplain (sand and silt dominated) – T_2, T_1, T_0
Floodplain slope – 0.00047	Floodplain slope – 0.00032
Vertical accretion	Lateral, vertical and oblique accretion
No evidence of floodplain surface topography	Irregular and scarred floodplain surface topography
Inundated by seasonal overbank flow	Inundated by seasonal high flow events
Organic rich, wet soils	Organic poor, permiable soils
Well vegetated with wetland forbs and grasses	Surface vegetated with arid grasses and shrubs; riparian vegetation at channel margin

Table 4-6. Comparison of channel and floodplain characteristics of the early Holocene and modern periods of dynamic equilibrium.

CHAPTER V

DISCUSSION

This thesis presents new data on the floodplain composition, history, and modern geomorphic state of the lower Sycan River. Some additional implications of these findings for topics such as climatic influences, intrinsic and extrinsic geomorphic variables, channel relaxation, and landscape history are presented below.

Climatic Influences

Based on the reconstructed climate history of the area (see Table 1-1) it is evident that the Sycan River has experienced changes in climate during the Holocene. Some of the climatic changes likely altered the precipitation regime of the Sycan watershed, thus potentially influencing historic channel and floodplain development processes. Figure 5-1 is a timeline of the major climate trends of the Holocene and the seven periods of geomorphic channel evolution presented in the channel and floodplain development model of the lower Sycan River.

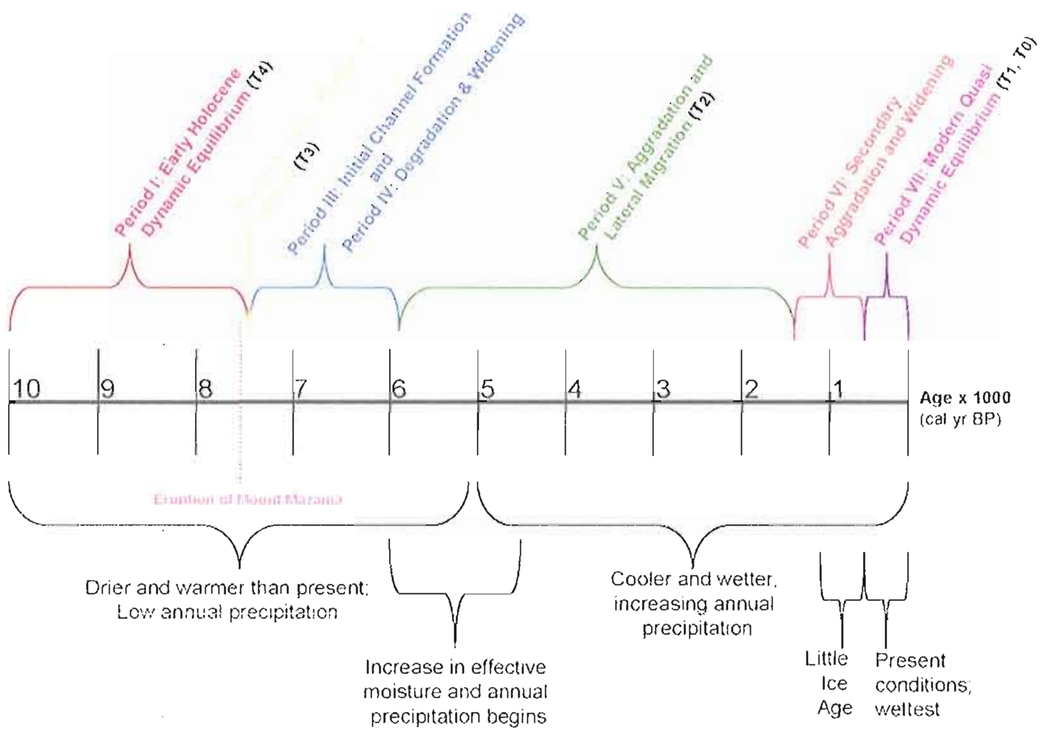

Figure 5-1. Timeline of major regional climate trends and the geomorphic periods of evolution of the lower Sycan River during the Holocene.

Of particular interest to this research are the influences climate conditions had on the creation of the dam that resulted in the Sycan Outburst Flood, and the potential role climate played in shifting the system from one geomorphic period to the next. This is important when evaluating the driving forces behind the channel and floodplain development model of the lower Sycan River. Also, it may prove useful for predicting the sensitivity of this system to future climate change.

Early Holocene

In general, the data on climate reconstruction indicate that the early Holocene was warmer and drier than present. This trend extended throughout the region from 10 ka to approximately 6 ka, at which time a cooler, wetter trend began. However, it was not until 5 – 4.5 ka yr BP that conditions approached precipitation rates and temperatures similar to present.

Based on climate reconstruction of the region it is assumed that the Sycan River watershed experienced a period of warm and dry, perhaps drought, conditions at the time of the Mazama eruption. I suggest that the warm and dry climatic environment of the early Holocene was further exacerbated in the Sycan River watershed by direct and indirect impacts from the eruption of Mount Mazama. A similar scenario was described at Dead Horse Lake, near the Sycan watershed. At Dead Horse Lake a noticeable alteration towards more arid-land vegetation is attributed to the input of Mazama airfall tephra resulting in dry low-nutrient soil (Minckley et al. 2007). Alterations in vegetation cover as a result of the direct inputs of Mazama pumice have yet to be studied in the Sycan River watershed. However, I speculated that an increase in the area's aridity occurred as a result of inputs of nutrient poor pumice across the landscape, further decreasing vegetation cover.

Unvegetated easily mobilized pumice and the strong winds that have been a feature of the region over the last 10 ka (Bradburgy et al. 2004) probably increased the potential for aeolian processes. This supports hypothesis of an aeolian-produced pumice dam in the upper Sycan Canyon and/or Sycan Marsh after the eruption of Mount

Mazama. The partially stabilized transverse pumice dunes atop the Miocene and Pliocene basalts along upper Sycan Canyon are evidence that active aeolian processes have redistributed Mazama pumice in the past. More calculations and modeling are needed to confirm that the time-span between the eruption of Mount Mazama (7660 cal *yr* BP) and the conservative maximum age of the Sycan Outburst Flood (7580 cal *yr* BP (Beta-252116)) was sufficient to support the hypothesis presented in this thesis.

Mid Holocene

The climate trend of the region towards wetter cooler conditions in the mid to later Holocene began approximately 6-5 ka. This trend probably resulted in a gradual increase of effective moisture in the Sycan River watershed that led to increased runoff and channel discharge. I propose that the trend towards a wetter, cooler climate was a factor in instigating Period V (~ 5920 – 1350 cal *yr* BP) of the channel and floodplain development model presented in this research. An increase in discharge would have increased the channel's capacity to reactivate the pumiceous sediment of unit T_3 in the valley and other sediment stored on the landscape. During this time, sediment delivery from the upland to the channel may have also increase, if climate and vegetation changes combined to increase surface runoff. It is during this period that the Late Holocene floodplain unit T_2 was developed. The oldest basal date associated with the development of floodplain unit T_2 (5920 cal *yr* BP (Beta-234715)) suggests that aggradation began fairly early-on in the climate shift.

An increase in runoff intensity is expected to generate rapid aggradation in the alluvial portions of a river system (Tucker and Slingerland 1997). The downstream aggradation is fed by an increase in upstream sediment supply as a consequence of the expansion of channel networks. Though the upstream channel network of the Sycan River is fairly limited, the quantity and type (easily transported pumice) of sediment stored on the landscape likely fed downstream floodplain development and channel evolution when reactivated by increased effective moisture.

Supporting evidence of mobilization of Mazama pumice-rich sediment as a result of increased precipitation and surface discharge during the mid Holocene is observed in the floodplain stratigraphy on the North Fork Sprague River. The North Fork Sprague is the third largest tributary in the Sprague River Basin (see Figure 2-1) with its confluence 23.3 river kilometers upstream (east) of the Sycan confluence. The pumice-rich North Fork Sprague floodplain unit has similar characteristics to the sand-rich T_2 floodplain unit of the lower Sycan River. A single wood fragment from the base of a pumice-rich bank exposure (located at GPS coordinates N: 4702279.262, E: 655270.548) in the North Fork Sprague returned a median age of 4327 cal *yr* BP (Beta-234716), which is broadly consistent with the mid-Holocene age of the Sycan River's T_2 unit. The correlation in style and timing of alleviation in these separate tributaries of the Sprague River suggests that the control of this behavior is climatic rather than some internal threshold within the Sycan River system.

Late Holocene

The Little Ice Age is reported to have influenced a dry period in Klamath Lake (Bradbury et al., 2004), the northwestern Great Basin (Wigand and Rhode 2002), and Siskiyou Mountains (Briles et al. 2008) from approximately 1 – 0.5 ka. The timing of the Little Ice Age corresponds somewhat to the period of secondary degradation in the lower Sycan River (Period VI ~ 1350 – 590 cal *yr* BP). However, it is not clear that the Little Ice Age was expressed as a climate change in the Sycan watershed. The shifts in geomorphic process that define Periods VI and VII of the evolutionary model of the lower Sycan River are likely a combination of internal channel processes and shifts in the regional climate of the late Holocene.

The variability of the climate record for the past 1 ka years makes direct correlation of climate and channel geomorphology difficult. The Little Ice Age is recognized in some climate reconstructions in the region around the Sycan watershed as a period of drier and cooler conditions starting about 1.2 to 1 ka and ending about 0.5 to 0.2 ka. But this episode is not recognized at climate reconstruction sites closest to the Sycan (Patterson, Lily and Dead Horse Lake in Minckley et al. 2007), which show wetter conditions during this period. Although the timing of the Little Ice Age roughly correlates with Period IV and V in the Sycan River chronology, it is not clear whether or how this climate interval was expressed in the Sycan watershed. While climate change may have triggered Periods VI and VII, these periods may also have been due to internal adjustments in the fluvial system.

The geomorphic response of the lower Sycan River during Period VI and VII are less extreme than Periods II-V. I propose that this is due to internal system relaxation in response to the inputs of Mazama tephra, the impacts of the Sycan Outburst Flood, and the more subtle external shifts in climate. Perhaps a slight decrease in precipitation related to the Little Ice Age was able to hasten the termination of Period V, which was already adjusting itself towards an internal geomorphic threshold towards a period of degradation. Period VI (~ 1350 -590 cal *yr* BP) was then dominated by degradation and widening. When discharge increased slightly at 0.5 ka yr BP, as suggested by Bradbury et al. (2004) and Grayson (1993), reactivation of sediment within the system may have initiated the modern dynamic equilibrium (Period VII) in which floodplain units T_1 and T_0 have developed.

Geomorphic Variables of Channel Evolution

The reconstructed history of the lower Sycan River depicts dynamic channel and floodplain evolution through the Holocene. The system evolution was instigated by both external and internal variables of environmental change. The model presented in this research for the Sycan River can serve for comparison with other fluvial systems of the area influenced by Mount Mazama eruption deposits and regional climate fluctuations of the Holocene.

The seven main periods of geomorphic evolution defined in the channel and floodplain development model for the Holocene are not equivalent in time or magnitude of change (Figure 5-1). While Period II (Sycan Outburst Flood) transformed the system with a massive deposit of sediment in a single event lasting only hours or days, Period V (Aggradation and Lateral Migration) is long. I propose that its longevity was a result of the channel's capacity, or lack thereof, to process the system's overabundant sediment supply without additional geomorphic thresholds beyond the gradual increase in effective moisture. It is also possible that the scale of this study missed subtle shifts in the geomorphic processes that would have identified separate periods of channel and floodplain evolution that are currently considered part of Period V.

Identifying Primary Extrinsic and Intrinsic Variables

System adjustments are instigated by the innate evolutionary process of landform change. According to Schumm (1979; 2005), intrinsically generated landform change is the result of the fluvial system's naturally evolving morphology (shifts in meander sinuosity, bank failure from incision induced shear stress, etc). Extrinsically generated landform change can also occur, triggered by external forces such as climate change, tectonics, sediment influx from a volcanic eruption, etc. Identifying which geomorphic threshold adjustments are intrinsic or extrinsic aids in interpreting the relative stability of the system during each period of the channel and floodplain development model. It is also an important component of predicting the system's susceptibility to adjust in response to future landform change.

The addition of Mount Mazama eruption material at 7660 cal *yr* BP was an extrinsic variable imposed on to the Sycan River Watershed. In the Sycan Valley, soil stratigraphy (T_4) indicates that the system quickly adjusted to the aerial deposition of ~5 cm of Mazama pumice. Pre-eruption floodplain soil development processes continued undisturbed in the relatively stable fluvial system of the lower Sycan River during the early Holocene (see Figure 4-9).

In contrast, the deposition of pumice over the upper Sycan watershed, and its transport and concentration resulted in a significant system response. The development and breach of a pumice dam in upper Sycan Canyon or Sycan Marsh are here considered extrinsic variables to the fluvial system of the lower Sycan River.

The catastrophic disturbance imposed on the landscape of the Sycan by the outburst flood transformed and destabilized the lower Sycan River. An extrinsic landscape transformation event, such as the Sycan Outburst Flood (Period II), is referred to by Schumm (1969, 2005) as a river metamorphosis. The lower Sycan River was forced to immediately adjust to the massive glut of sediment emplaced by the Sycan Outburst Flood.

The additionally imposed extrinsic variable of climate change influenced or initiated Periods V-VII in the lower Sycan River. Climate change that increased the system's overall hydrologic regime not only increased the lower Sycan River's capacity to rework outburst flood event deposits, it also may have mobilized the available sediment stored on the landscape. If the mobilized sediment from upstream initiated geomorphic threshold responses and induced processes downstream in the lower Sycan Valley, locally (at the reach scale), it can be considered an extrinsic variable. Likewise, a decrease in precipitation and therefore discharge would reduce the channel's capacity to transport coarse sediment, thus instigating intrinsic evolution of channel processes. This is the style of mixed intrinsic and extrinsic influences believed to have been imposed on the evolution of the lower Sycan River.

Substantial sediment stores of Mazama pumice exist today throughout the Sycan River watershed. In the Sycan Valley the pumice is stored in the flood deposit terraces and active floodplain. Dunes and sheets of Mazama pumice are visible atop the canyon basalts in the uplands. Within Sycan Canyon available pumice sands are present as colluvium and within floodplain sediments. All of these upstream stores of easily mobilized pumice-rich sediment may make the lower Sycan River sensitive to future geomorphic change, especially with regards to regional climate change.

Channel Relaxation and Response

The channel and floodplain development model of the lower Sycan River assumes that channel response and adjustments will result from geomorphic threshold exceedence. The channel adjustments are expected to initially be rapid and dramatic, and the scale (magnitude and duration) of adjustments are expected to correlate to the scale of the disturbance (Graf 1982; Knox 1972; Simon 1999).

Channel relaxation over time means that adjustment to a disturbance is greatest at first and then becomes progressively less over time (Graf 1977, Figure 1-1), as the system trends towards a new state of system equilibrium. This assumes the system is responding to a single disturbance. When external variables impose additional geomorphic threshold responses on to an already adjusting system, a channel's evolutionary trajectory towards equilibrium can be altered. Consequently the system's trajectory is no longer a single non-linear curve but a series of curves varying in degree of adjustment, depending on the system's stability and the scale of the geomorphic threshold exceedence. Figure 5-2 depicts this general concept in an arbitrary complex channel relaxation curve.

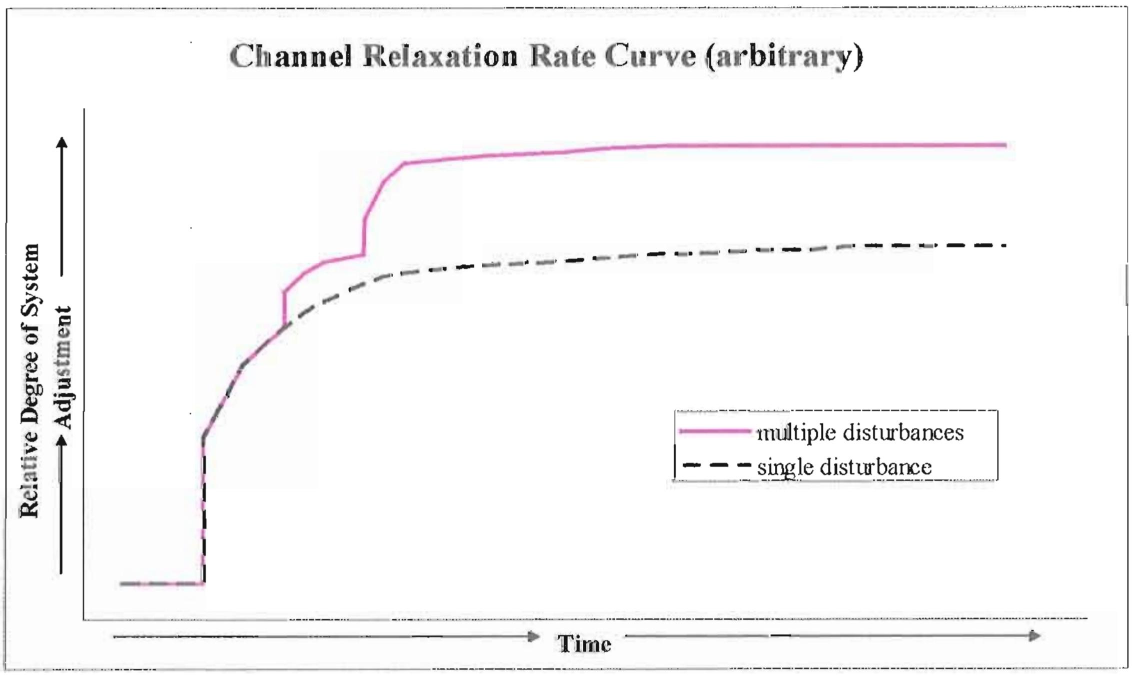

Figure 5-2. Arbitrary channel relaxation rate curve; representing a channel relaxation trajectory of channel response towards a new state of equilibrium -- imposed upon by additional geomorphic threshold disturbances.

I propose that the lower Sycan River's original relaxation trajectory in response to the impacts of the Sycan Outburst Flood was superimposed upon by additional extrinsic forcings from climate change. The additional variables pushed the system through geomorphic thresholds that redefined the original relaxation trajectory of the channel response. The primary additional extrinsic variable was climate change during the

Holocene. Determining the degree of trajectory alteration experienced by the system from each imposed variable is beyond the scope of this research. However, this study presents the concept of multiple or superimposed channel response trajectories as important when interpreting historic channel evolution, especially when the system has experienced large-scale environmental change.

Overall, the preserved floodplain stratigraphy of the lower Sycan River reveals a progressively diminished degree of adjustment in response to geomorphic threshold disturbances since the Sycan Outburst Flood. This is seen in the evolution of floodplain surface gradients in the lower Sycan River (Table 5-1 and Figure 4-1). A diminished degree of adjustment may reflect an increased stability of the system as it relaxes towards a new state of equilibrium. However, the entire system continues to process the sediment received from the eruption of Mount Mazama. Thus, evolution of the lower Sycan River remains susceptible to shifts in its hydrologic regime.

Lower Sycan River Floodplain Surface Slopes				
Floodplain Surface	**T4**	**T3**	**T2**	**T1**
Slope	0.00047	0.00053	0.00031	0.00033

Table 5-1. Slopes of floodplain surfaces.

Landscape

The lower Sycan River is a prime example of how fluvial systems are a legacy of the history of their landscape. Historic regional and local landscape characteristics such as geology, climate, vegetation, and topography shape the system we see today. For example, this research shows that the sediment inputs from the eruption of Mount Mazama have been a driving variable of channel and floodplain development in the Sycan River for over 7.5 ky. At the head and terminus of Sycan Valley are two other important landscape features that influence geomorphic processes of the lower Sycan River, the Coyote Bucket Section of Sycan Canyon and the confluence with the Sprague River.

Coyote Bucket

An obvious break in channel gradient from a steeper bedrock canyon section to the low gradient valley occurs where the Sycan River exits Sycan Canyon (Figure 2-2). This section is known as Coyote Bucket. Channel and floodplain development of the lower Sycan River was and is limited by the bedrock channel at Coyote Bucket.

The headward-migrating knick-zones of complex response extend throughout the entire lower Sycan River, but are limited geographically to the Sycan Valley. The basalt boulders and bedrock of the downstream section of Coyote Bucket halt up-canyon knick-zone migration. Thus upstream inputs of sediment from knick-zone migration are limited to below Coyote Bucket.

Confluence

The Sycan River flows through a complex floodplain near its confluence with the Sprague River. Observations of this complex stratigraphy raise the question as to whether the downstream-most modern floodplain was developed by flows from the Sycan or the Sprague River. Based on the pumice-sand dominated stratigraphy and paleo-channel scars, initial interpretation is that this area is an aggrading delta-like formation of the Sycan River. However, at modern flood stage the Sprague River appears to back water up the mouth of the Sycan River. Obviously there is a strong interaction between the low gradient Sprague and Sycan Rivers near their confluence. Perhaps both river systems contribute to modern floodplain accretion, depending on the discharge regime. More detailed data collection and analysis is needed to interpret the complex stratigraphy and historic channel processes of this part of the system.

CHAPTER VI

CONCLUSIONS AND MANAGEMENT IMPLICATIONS

Climate trends and historic geologic events influenced channel and floodplain development in the lower Sycan River. There has been seven main periods of channel and floodplain development in the lower Sycan River during the Holocene. Periods III-VII included sequential episodes of complex channel response (upstream degradation resulting in downstream aggradation) initiated by headward-migrating knick-zones. Floodplain development through aggradational processes dominated Periods I, II, V, and VII, while Periods III, IV, and VI were dominated by processes of incision and bed degradation. Period II (Sycan Outburst Flood) was a river metamorphosis-scale event that buried the floor of Sycan Valley.

The floodplain terrace of the Sycan Outburst Flood (T_3) was created from a single flood event deposit lasting only hours or a few days. The surface of the Sycan Outburst Flood terrace was never an active floodplain for the Sycan River. Immediate incision into the outburst flood deposits at the waning of the event resulted in relatively rapid abandonment of the terrace. Once abandoned, the terraces have not been inundated except at the mouth of the river, even by subsequent flood flows. The outburst flood terrace deposits (T_3) flank the inset active floodplain units (T_2, T_1, and T_0) throughout the Sycan Valley.

The lower Sycan River has currently evolved to a state of dynamic equilibrium where modern discharge regimes maintain a regular connectivity with active floodplain surfaces. The active floodplain surfaces of the modern channel include the three primary floodplain units (T_2, T_1, and T_0) developed after the Sycan Outburst Flood. These three surfaces are hydrologically and geomorphically connected to the channel, based on their regularity of inundation and evidence of vertical accretion. Seasonal high flows at a two year flood recurrence frequency inundate the active floodplain surfaces. The active floodplain units currently accumulate, store, and supply sediment to the lower Sycan River.

The sediment influx to the Sycan River watershed from the eruption of Mount Mazama (7660 cal *yr* BP) has been a driving force of channel evolution on the lower Sycan River. Beginning with the Sycan Outburst Flood, floodplain development has remained dominated by fluvially transported, pumice-rich Mazama tephra. Stores of the Mazama tephra within the terraces and floodplain, and as partially stabilized upland dunes, remain available sediment sources to this evolving system.

The composition of the outburst flood terraces and the active floodplain units make them vulnerable to anthropogenic land use practices. Bank failures from trampling or extensive vegetation removal were observed at sites where cattle access the channel. Unchecked, these impacts can lead to geomorphic alterations such as channel widening from bank failures, increased stream gradient, and bed degradation (incision) (Magilligan and McDowell, 1997). Incision often results in a lowered groundwater table and the abandonment of floodplain surfaces. Where off-channel watering for cattle and riparian fencing occurred, greater bank stability and channel form diversity was observed.

Restoration management decisions on the lower Sycan River should integrate the findings of this research. In particular, the Sycan Outburst Flood deposit terraces need to be managed as an abandoned terrace not as an active floodplain or wetland. Wetland and floodplain management need to be focused on the active inset floodplain surfaces and next to springs. Due to channel and floodplain development processes over the past 10 ky, the modern active floodplain surfaces of the lower Sycan River form a relatively narrow inset area on the valley floor.

The findings of this thesis leave several important questions unresolved. Identification of the location and damming mechanism of the Sycan Outburst Flood is needed for analyzing reservoir impoundment, flood hydraulics, and dam breach processes of the flood event. Further research on the immediate and continued influence of the Sycan Outburst Flood on the Sprague River and Upper Klamath Lake is important in reconstructing the geomorphic history of the Upper Klamath Lake Basin.

APPENDICES

APPENDIX A

PHOTO GALLERY

Figure A-1. Sycan Marsh – at outlet looking NE into the Marsh

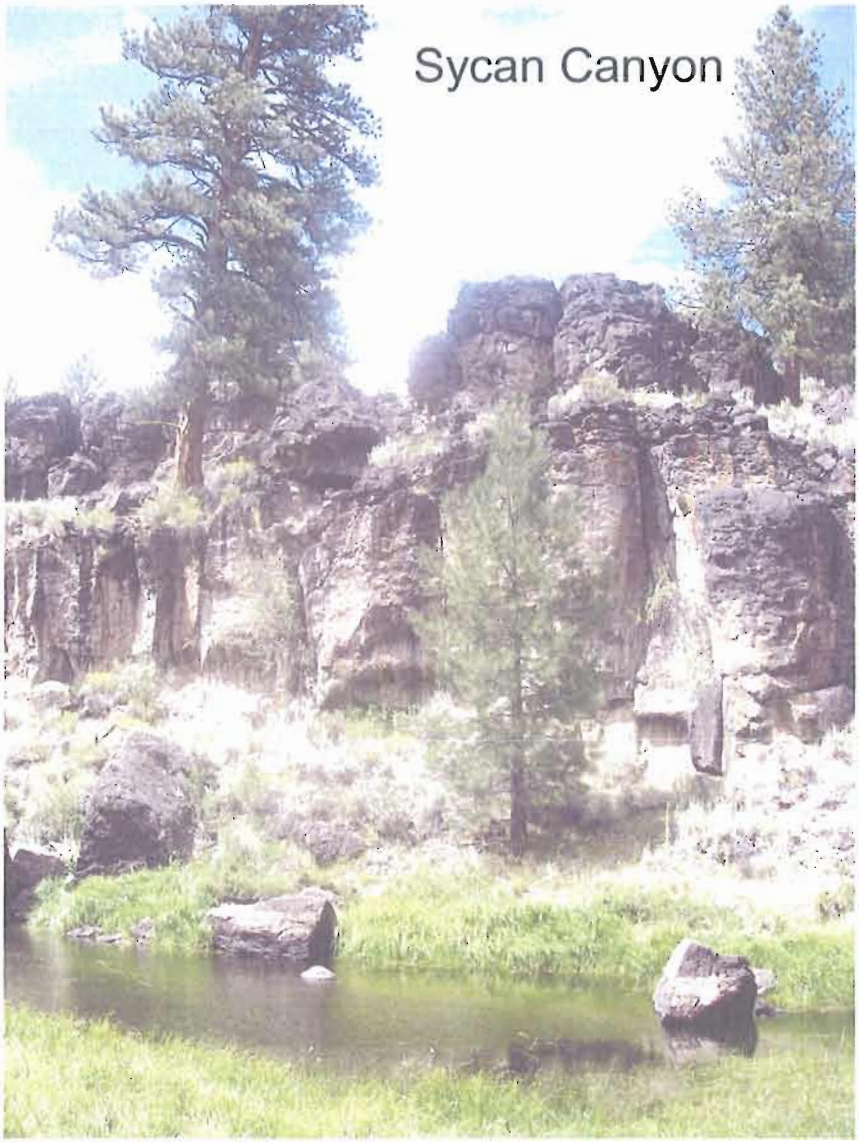

Figure A-2. Basalt canyon walls of Upper Sycan Canyon

Teddy Powers Meadow

Figure A-3. Teddy Powers Meadow -- at right bank looking north (upstream).

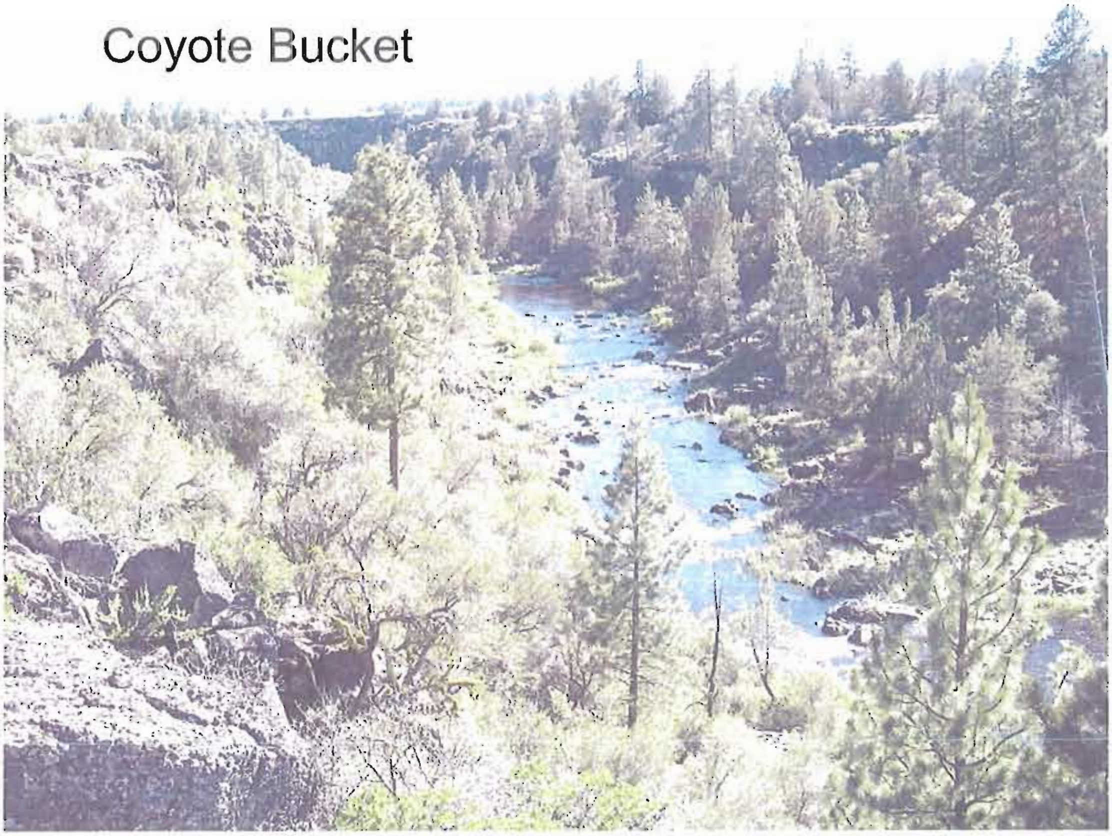

Figure A-4. Coyote Bucket -- lower Sycan Canyon from atop the left bank canyon wall looking south (downstream).

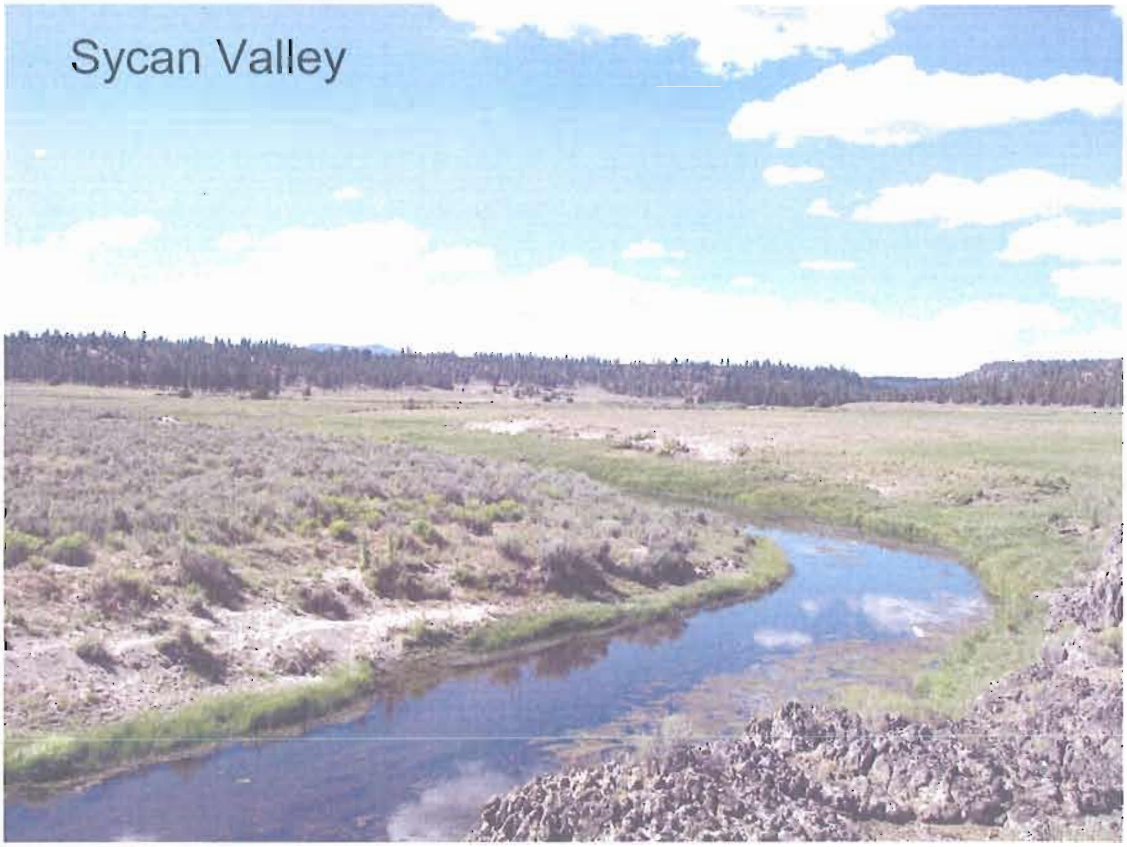

Figure A-5. Sycan Valley – mid-valley on left bank looking north (upstream).

APPENDIX B

STRATIGRAPHIC DIAGRAMS

Table B-1. Stratigraphic diagram of AUG-01

Date/Site: 7-24-07.07 Auger Hole: AUG-01

Location Description: (N: 4702491.102, E: 641693.175) auger hole summary description at most distal end of locally high surface; north of Sprague and east of Sycan confluence ~875m

LiDAR elevation at surface: 1314.44 (m)

Depth from surface (cm)	Profile Description	Geomorphic Interpretation
0	sandy loam with pumice grains up to very coarse, mixed mafics; brown (dry)	
at 101	silt loam; fines downward to silty clay loam; brown (dry)	
at 183	silty clay; orange and brown; common mottles and concretions	
at 196	very fine silty sand; green/blue	
at 205	sand (fine-medium), mixed lithics </= coarse sized grains; coarsens down to pebbly medium sand; green/blue	fluvially re-worked Sycan Outburst Flood deposits in a delta-like channel confluence setting
at 260	pebbly gravel with medium sand; wetted; green	

Table B-2. Stratigraphic diagram of AUG-02

Date/Site: 9-19-07.01 Auger Hole: AUG-02

Location Description: (N: 4730752.997, E: 649201.267) auger hole NW of Sycan/Sprague confluenc ~310m, N of plugged spring ~ 200m, on high floodplain terrace

LiDAR elevation at surface: 1314.49 (m)

Depth from surface (cm)	Profile Description	Geomorphic Interpretation
0-105	silty loam; rounded rare medium pumice grains; fining up sequence; pumice increases in size and % density up to coarse grains with depth; brown; subtle granular pedogenic structure	accrectionary overbank deposit; bioturbated; some soil development
105-134	pumiceous loamy sand that coarsens down to medium-coarse sand; sub-angular to sub-rounded grains; light brown at top;	loamy bioturbated Sycan flood deposit? (dry); no pure white pumice grains in this unit
134-146	silty loam; dark brown; black mottles, organic rich	weltand paleosol - pre Sycan Flood
146-150	loamy sand; medium grained well sorted angular pumice grains; brown	Mazama airfall
105+	clay loam; dark brown; strong blocky peds; orange mottling	paleosol - wetland soil - pre Mazama eruption

Table B-3. Stratigraphic diagram of AUG-03

Date/Site: 6-26-07.04 Auger Hole: AUG-03

Location Description: (N: 4708116.963, E: 638955.793) auger hole into Sycan Flood deposit between South Shields Creek and Brown Springs; between driveway and palagonitic rock outcrop

LiDAR elevation at surface: 1320.49 (m)

Depth from surface (cm)	Profile Description	Geomorphic Interpretation
0-45	silty with coarse pumice sand (loam); slight decrease in silt as pumice sand becomes more pure downward;	ENTIRE SITE: Appears to be Sycan Outburst Flood wash despoit; INTERPRETATION: fining up sequence over a fluvially influenced "wet" vegetated arear that was stable and accumulic until being burried by the pumice-rich Sycan Flood deposit
at 70	pumiceous sand; silt almost gone; ~90%+ pumice and incrases to 100% downward; granules </= 1 cm; yellowish-tan; % large grains increase downward	
at 139	100% Mazama pumice sand; poorly sorted; medium-very coarse with grain </= 1 cm; light tan; % of large grains increased	
at 147	meidum-coarse pumice sand with mixed mafics (lithic grains increase - hornblen or andesite); salt and pepper coloration;	
at 157-150	layer of silty-very fine sand; grey and salmon colored;	perhaps two layers of ash fines
at 157	medium-coarse pumiceous sand; salt and pepper coloration; increased dark colored mafics	
at 176	pumice sand coarsens </=1 cm diameter grains; tan; decrease in dark colored mafics;	
at 191	silty fine sand (loam) with medium sized pumice grains present; dark brown; soft; oxidized very coarse pumice sand and pebbles at base of Sycan Flood deposit - slightly indurated (1 cm diameter)	burried paleosol below Sycan Flood
at 194.5	silty sand with medium sized well sorted pumice grains (angular); wet	top of Mazama airfall layer
no depth recorded	clayey silty very fine sand; dark brown (wet); mottling present; some evidence of organics (veg fragments)	
at 227	coarsens to medium sand and rounded pebbles in clayey silt matrix; grains </= 1 cm diameter;	

continued:

AUG-03 (continued)

Depth from surface (cm)	Profile Description	Geomorphic Interpretation
at 260	fine-medium sand with rounded grains of ~2 mm diameter; brown; hint of orange mottling (from oxidation?); between 260-280cm depth sand fines downward and begins to get more dense	
at 281	fine-medium sand (clay loam) with sparse grains of 1-2 mm; Orange color increases at 281 cm depth; fines down to fine sand with some sparse organics (sedge remnants) and grains </= 1-2 mm	
at 320	slightly clayey very fine sand (clay loam); bluish grey; bluish grey; thin layer of < 1 cm gravels within sand; better sorted than unit above; silt/clay % fine sand increasing downward slightly - resulting in harder, less wetted sand; more compact than unit above; some organic fragments	
at 330	compacted clayey silty fine sand; sparse grains </=1mm; distinct greenish tint; evidence of organics (sedge, seeds, grass);	
at 341	clayey fine sand (compact); some grains </= 1 mm; sparse organics; stopped augering	

Table B-4. Stratigraphic diagram of AUG-04

Date/Site: 9-18-07.01 Auger Hole: AUG-04

Location Description: (N: 4708467.367, E: 639293.896) auger hole summary description; mid-Sycan Valley floodplain surface

LiDAR elevation at surface: 1318.02 (m)

Depth from surface (cm)	Profile Description	Geomorphic Interpretation
0-185	pumice -rich sitly to sandy loam coarsens downward gradually to fine-medium sand; brown; fining upward sequence; coarsened to med-coarse sands	OVERALL INTERPRETATION: aggrading, laterally active sand-rich period - post Sycan Outburst Flood
at 185	medium-coarse pumiceous sand	
at 260	very fine-medium pumiceous sand	
at 313	saturation, oscillating fining up sequences of pumice rich sands	

Table B-5. Stratigraphic diagram of AUG-05

Date/Site: 7-22-07.03 Auger Hole: AUG-05

Location Description: (N: 4708479.829, E: 639659.974) left bank auger hole on terrace surface; summary description

LiDAR elevation at surface: 1319.74 (m)

Depth from surface (cm)	Profile Description	Geomorphic Interpretation
0-110	sandy loam with medium-coarse pumice grains, coarsens downward	OVERALL INTERPRETATION: Sycan Flood deposit
at 110	medium-very coarse pumice-rich sand; mixed mafics (horneblend, feldspar, orangish cyrstals, and others - black and cinder); pure clean white and black (salt & pepper coloration); overall grain size coarsens downward	
at 210	medium-very coarse pure pumice sand; discontinous lense	
at 240	silty fine sandy loam with well sorted medium sized pumice grains; brown (wetted); loam that coarsens down to rounded pebbles and gravels (</= 2 cm diameter) of mixed mafics.	pre-Sycan Flood floodplain surface with mixed Mazama airfall
at 280	silty clay loam with significant quantity of very fine sand	paleosol
at 310	cemented sand	fluvial deposits from spring tributaries and hillslopes on east side of the valley
at 360	sandy gravel; brown (wet)	

Table B-6. Stratigraphic diagram of AUG-06

Date/Site: 7-22-07.02 Auger Hole: AUG-06

Location Description: (N: 4708556.936, E: 639539.063) auger on left bank -- summary description; inland ~175 m from channel

LiDAR elevation at surface: 1318.73 (m)

Depth from surface (cm)	Profile Description	Geomorphic Interpretation
0-176	Mixed sandy loam, grading down to pumice-rich sand with pebbles	overbank deposits
176-180	clay loam	probably a lense, not a paleosol
180-220	medium-very coarse pumice sands; cleans down to white Sycan Flood sands -- almost pure coarse/pebble pumice; lower boundary is sharp	Sycan Outburst Flood deposit
220-239	clay	pre-flood paleosol
239-260	medium pumice grains, well sorted	Mazama airfall ? - difficult to discern because loose pumice from upper units falling into the auger hole
260+	pumice (likely auger hole edge collapse from upper pure loose pumice unit)	stopped augering at 260 -- only getting pure pumice in each bucket.

Table B-7. Stratigraphic diagram of AUG-07
Date/Site: 7-01-05.01 Auger Hole: AUG-07
Location Description: (N: 4711963.201, E: 638683.444) highest floodplain terrace; NE of Hippy Village ~ 75m
LiDAR elevation at surface: 1322.89 (m)

Depth from surface (cm)	**Profile Description**	**Geomorphic Interpretation**
0 - 60	pumice sand with sparse root fragments; orangeish/light brown; slightly oxidized	Sycan Outburst Flood deposit
100	coarse pumice sand with isolated pebbles (rounded) of varied lithologies; fines upward;	
160	coarse pumice sand; coarsening down with intermitten large pebbles; obsidian flake present	
190	coarse pumice sand with inter-mitten thin layers of pumice; more lithic fragments in sand (black & glassy);	
201	sand-sized pumice grains; fines downward slightly;	
260	gradual change of % content of pumice to sand – pebble content and size decreased;	
295 - 290	clean pumice grains ~>/= 2mm diameter;	
302	silt sized tefra; 1cm thick bed; light baige in color	
312	coarse pumice sand; coarsens down to clean pumice with large clast grains >/= 1cm diameter;	
335	clayish silt; sand sized pumice grains in silt; brown; root or veg material; soil motteling	Pre-flood paleosol
340	clayish silt with sparse pumice grains; brown	
370	clayey silt; brownish	
425	clayey silt; brownish; wetness in soil; motteling continued; **charcoal fragment (adopted age of 11,640 cal yr BP)**	
440	clayey silt; motteling is gone	
485	soil saturated; water table	
500	last auger depth	

Table B-8. Stratigraphica diagram of BE-01

Date/Site: 7-23-07.01

Bank Exposure: BE-01

Location Description: (N: 4702653.729, E: 640887.5) right bank exposure with auger at base (starting at ~ 150 cm depth), on outside meander bend; floodplain is flat, extensive, and vegetated with grasses, forbes and minimal sage/rabbit brush – definitely grazed; surface of water is 145 cm below floodplain surface

LiDAR elevation at surface: 1314.32 (m)

Depth from surface (cm)	Profile Description	Geomorphic Interpretation
0-42	very fine sand and silt loam; light grey (dry); top 10 cm is sod layer; horiontal laminae; crumby structure; loose; lower boundary is horizontal and distinct; no visible mottling; very bioturbated withabundant modern roots, burrows, worm and root voids	overbank accrection floodplain deposits
42-64	clay loam; off white (dry), dark brown (wet); very subtle horizontal laminae of ~1 mm; appears massive but at point of breaking; hard; lower boundary is horizontal and visible across bank - gradataion over 3cm; few fine distinct orange mottles throughout; bioturbated with common root voids, worm holes and filled burrows </= 5 cm diameter, few modern roots	sequence of accrectionary over bank floodplain deposits on vegetated surface
64-112	silty clay loam; dark brown (moist), very light gray (dry); no bedding; massive, loose blocky structure; dried exposure surface expresses 1-2 cm wide vertical desication cracks along extent of exposure (40 m); friable, slightly hard; lower boundary is gradational over 4 cm and defined by darker coloration, descication cracks, and slightly firmer texture; many medium-large orange and black mottles; bioturbated with common root voids (</=3 cm) and common modern roots	vertical accrection sequence of fines on vegetated surfaces with soil development

continued:

BE-01 (continued)

Depth from surface (cm)	Profile Description	Geomorphic Interpretation
112-135	very fine sandy clay loam; brown (moist), light grey (dry); weak blocky pedogentic structure; friable; lower boundary is very wavy with relief of </=3 cm, distinct; many medium orange mottles and dark gray (organic stains?), mottling and organics increase from few to many in upper 10 cm; common root voids (</= 5 mm), modern roots present, top 10 cm of unit very bioturbated	accreting floodplain fines with some soil development over sandy more energetic unit
135-150+	very fine sand that coarsens up to coarse sand (pumice rich in upper 4 cm); light grey-blue (moist); very friable; few fine faint mottles of orange; few organics, modern roots present	unable to see bottom of unit but may be single event desposition of sand from high flow
at 160	medium sand with abundant pumice grains; overall moderately sorted; coarsens down to pebbly sand; blue-grey; fine distinct orange mottles and few common organic detritus;	AUGER -- likely bottom portion of unit above.
at 180	very coarse pebbly sand with mixed lithics; many fine roots (modern?)	AUGER
at 200	coarsens into sandy gravel; organ-brown hue to matrix (oxidation?)	AUGER -- sandy gravels continue below 2 m depth
at 260	sandy gravel infill	AUGER -- auger hole kept refilling with sandy gravel infill -- stopped augering

Table B-9. Stratigraphic diagram of BE-02

Date/Site: 7-24-07.02 & 03 Bank Exposure: BE-02

Location Description: (N: 4703127.717, E: 641205.926) right bank exposure description done in two sections to avoid unneccsary bank damage in the obviously eroding pumice units; exposure is ~ 100 m long; lower unit slopes upward in an upstream direction

LiDAR elevation at surface: 1314.57 (m)

Depth from surface (cm)	Profile Description	Geomorphic Interpretation
0-33	silt loam; top 5cm is sod layer; dark brown (wet), light brown (dry); fine laminea; very subtle subangular bed structure at bottom 10 cm; vertical desiccation cracks ~ 2 mm diameter; loose. very slightly friable; lower boundary is irregular over 4 cm; common medium faint orange mottling in lower 10 cm, no visible mottling in top 23 cm; very bioturbated, root and worm voids </= 1 cm, abundant modern roots, burrow and burrow fills </=5 cm	sequence of overbank accretionary deposist on aggrading floodplain
33-80	silt loam with coarse pumice grains; brown (moist), light grey (dry); no visible bedding; crumby peds; loose; lower boundary is gradational over 4cm; no visible mottling; bioturbated, many root voids, burrow holes </=8 cm (filled); expresses a vertical face on exposure	
80-120	5-10 cm thick alternating beds of loamy sand and silty loam; both bed sequences have coarse pumice grains </= 1.5 cm diameter (few); no defined ped structure; very friable; lower boundary is horizontal, gradational 2 cm; common medium faint mottles (orange); few dispersed black medium cemented clasts; sparse modern roots, burrow fills </= 8 cm diameter; unit expressed as protruding less erosive layer	sand bar, energetic bank deposits?, or active delta formation

continued:

BE-02 (continued)

Depth from surface (cm)	Profile Description	Geomorphic Interpretation
120-155	coarse pumice sand; granules </= 1.5 cm (pumice) in lower 20 cm; alternating beds ~5-6 cm thick; top 15 cm coarse pumice sand; pure white-off white pumice sand; salt and pepper (beds) from dark mafics; alternating beds with medium–very coarse sand; sub-horizontal bedding defined by grain size; loose sand no ped structure; between 10-6 cm of this unit - weakly cemented lense; black with orange horizons; lower boundary is sharp and horizontal	truncated remnant of Sycan Outburst Flood deposit, slightly worked top (flood delta?)
155-165	silty clay with few pumice grains; black (wet), very light brown (dry); massive; slightly hard (dry); lower boundary is horizontal, gradational </= 3 cm; rich in organics (vegetation fragments and seeeds); few fine mottles in top 3cm; **seeds (*polygonum*) from upper portion of unit (adopted age 7630 cal yr BP)**	vegetated wetland or marsh
165-170	medium pumice sand, grains are angular and well sorted; no pedogenic structure; matrix of silty clay - but grain supported; loose (dry); lower boundary is horizontal, slightly irregular (1-1.5 cm relief); no mottling; bioturbated with burrows and root voids </= 3.5 cm diameter; charcoal clast at 167 cm depth;	Mazama airfall tephra on wetland-like soils
170-194	clayey silt; black (wet); very light brown (dry); when dry vertical desiccation cracks </=1 cm; prismatic ped struct. (dry); massive; sticky when wet; hard (dry); lower boundary is horizontal and clear, gradational over 3 cm; no mottling; bioturbated with organics, few modern roots and voids (fine)	wetland soil -- cumulic
194-219	clay; black (wet), grey (dry); when dry desiccates into angular blocky peds 1-2 cm diameter; sticky (wet), hard (dry); lower boundary is gradational over 6cm; no visible mottling; bioturbated, modern roots (few)	wetland
219+ (230 is channel)	gravely sand; angular-sub-rounded; mixed mafics; loose and soft;	paleo-channel bed

Table B-10. Stratigraphic diagram of BE-03

Date/Site: 7-24-07.01 Bank Exposure: BE-03

Location Description: (N: 4703245.502, E: 641292.974) right bank exposure with auger at base (starting at ~ 152 cm depth); has downstream slightly dipping beds (3%) and is located at the up-stream end of a slight meander on the outside bank; channel bed is silty sand (sticky) and heavily vegetated with submerged aquatic vegetation; floodplain is 152 cm above water surface

LiDAR elevation at surface: 1313.84 (m)

Depth from surface (cm)	Profile Description	Geomorphic Interpretation
0-12	very fine sandy loam; sod layer occupies unit; fine laminea; no pedogenic structure; loose; lower boundary is irregular with reliefe of 3 cm, horizontal; no visible mottling; bio-turbated with many modern roots, root voids and worm holes </= 1 cm	sequence of overbank accretionary fines on aggrading floodplain surface
12-36	fine sandy clay loam; very dark brown (wet), grey (dry); laminea that become more fine at top; few vertical dessication cracks <= 2 mm, crumbly pedogenic structure; very hard peds; lower boundary is horizontal, gradational over 4cm - defined by increased root abudance, color, and unit structure; no visible mottling; very bioturbated – many root voids <= 1 cm, worm void fills </=1 cm, abundant modern roots	sequence of overbank accretionary fines on aggrading floodplain surface
36-90	fine sandy loam, fines up gradually; light brown (wet), off-white (dry); subtle laminea (bioturbated); vertical desiccation cracks <=3 mm, slightly loose blocky ped structure; hard; lower boundary is horizontal, gradational over 10 cm; many medium dark brown and orange mottles; heavily bioturbated, abundant root voids, worm holes and burrows up to 8 cm diameter, many fine modern roots in upper 30 cm unit	

continued:

BE-03 (continued)

Depth from surface (cm)	Profile Description	Geomorphic Interpretation
90-143	medium sand with grains ranging from fine to coarse, pumice rich, overall sequence fines upward, upper 20 cm expresses upward fining most clearly; brown; slight horizontal bedding, expressed in two 2 cm beds in lower 20 cm of unit, 2 inter-beds – silty very fine sand; no pedogenic structure; loose; lower boundary is horizontal and clear, gradational over 1cm; no visible mottling; few modern roots, few modern root voids – 3 mm diameter in upper 10 cm, 1 charcoal clast visible on exposure at 109 cm depth	series of relatively higher energy bank deposits (possible sand bar). Active surface?
143-152+	silt loam; dark brown (wet); no apparent bedding; loose (dry). non-slightly sicky (wet); top 5cm organic rich; no visible mottling; few modern roots; unit extends below water surface - water surface is at 152 cm depth	buried, vegetated, active floodplain surface
143-163 (AUG)	matched unit above (143-152	
at 163	gravely pebbly sand; clasts are mixed mafics (including pumice), angular-subrounded; clasts up to 2 cm diameter increase in size downward; many fine roots	AUGER -- active deposit (channel bed or gravel bar)
at 228	silty sand rich in coarse pumice grain and other mafics (</= 2cm diameter); few organics	
at 239	very find sandy clay loam; muted grey (wet); few organics (grass?); no visible mottling; near contact, some pebbles and sand grains	
at 250	same as above unit -- stopped augering at 250 cm depth	AUGER -- overall: buried vegetated surface or filled channel/oxbow that was reactivated

Table B-11. Stratigraphic diagram of BE-04

Date/Site: 6-23-07.02 Bank Exposure: BE-04

Location Description: (N: 4703379.205, E: 642104.354) left bank exposure at bend in Gadawa Spring Road; water surface at 2.1 m below top of floodplain; elsewhere along outcrop saw a pumice-rich sand outcropping ~ 0.5m above water level but did not find it at this bank exposure; augered at base of unit

LiDAR elevation at surface: 1315.24 (m)

Depth from surface (cm)	Profile Description	Geomorphic Interpretation
0-41	silty very fine sand (loamy); at 10-13cm below top is a zone with abundant 2 mm pumice grains; medium brown (moist) to light brown-grayish brown (dry); no evident bedding except fine laminae in upper 5cm; 0-3 cm is sod; weak angular peds up to 5 cm; some vertical cracks along weathered faces; lower boundary is gradational over 2 cm; no mottling; open and filled burrows up to 2-3 mm diameter; abundant modern roots	multiple overbank flood deposits
41-101	silt with some clay and a little sand; brown (moist), light gray (dry); no evident bedding; matrix supported mazama grains < 1mm with abundance increasing upward; slightly softer at base than underlying unit; friable, slightly hard angular peds <2 cm diam; denser network of vertical cracks than 101 – 172 cm; lower boundary is gradational over 10cm; no mottling; intensely bioturbated, filled burrow holes at base 1-15 cm diameter; abundant modern grass roots	slowly accumulating A-horizon
101-122	sandy clayey silt with abundant <1mm matrix supported Mazama pumice grains; no evident bedding; slightly finer and a little harder than unit below; weathered faces have vertical cracks spaced 20 cm apart and <1 cm wide, creates a subtle cliff along exposure; lower boundary is gradational over 10 cm, defined by a very subtle texture shift; a few modern roots, few open burrow voids </= 3 mm diameter, no mottling, sparse modern roots	slowly accumulating organic rich floodplain surface with bioturbation

continued:

BE-04 (continued)

Depth from surface (cm)	Profile Description	Geomorphic Interpretation
122-143	sandy clayey silt with abundant matrix-support pumice grains, mainly <1 mm but up to 3 mm diamter; no evident bedding; very weak angular peds; lower boundary is gradational over 10 cm; sparse modern roots, many open burrow voids all <3 mm - makes it softer than unit below;	cumulic A-horizon; organic-rich; intensely bioturbated
143-197	sandy clayey silt; abundant matrix-supported pumice grains up to 1mm in upper 30 cm; light brown (moist); no ped structure; lower boundary is gradational over 3cm, horizontal; two discontinuous insitu charcoal bands (burn horizons) < 2cm thick at 177 cm and at 160 cm; at 192-197 cm depth unit is indurated by iron cement; ~75% of unit contains orange mottles; mottling decreases but still evident up to ~177 cm depth; abundant < 5 mm diameter burrow fills throughout; modern root traces, some root and burrow voids in upper 30cm where color becomes medium gray (moist);	accreting surface, probably overbank floodplain deposits; vegetated; surface burned on occasion
197-210	clayey silt; saturated; brown (moist); no evident bedding; no ped structure; vertical open cracks; lower boundary not visible; some filled and open burrows up to 20 cm diameter; subtle mottling near top; some modern roots	low energy fluvial deposit - not organic enough to be a marsh
250-275	alternating coarse pumice sands and organics; ledgy-looking deposit with wood	pre-flood paleosol

Table B-12. Stratigraphic diagram of BE-05
Date/Site: 6-22-07.05 Bank Exposure: BE-05
Location Description: (N: 4704490.42, E: 641521.94) right bank exposure; downstream from sharp left bending meander;
LiDAR elevation at surface: 1316.17 (m)

Depth from surface (cm)	Profile Description	Geomorphic Interpretation
0-9	loam; sod layer; lower boundary is gradational over 5 cm;	vegetated surface on overbank accretionary fines
9-66	loam; si content; light brown; 18-20 cm thick beds of alternating or varying very fine sand; horizontal boundar is gradational over 1cm; lower boundary is gradational over 2 cm; intensely bioturbated; burrow ~30 cm diameter; worm and root holes; this contains the bottom of modern root zone	overbank flood deposits, ~3+ events
66-143	silt clay loam; isolated pumi grains </= 1 mm diameter; brown (moist); subtle sandier laminae (discontinous); weathers to a coarse prismatic structure with prismatic platings; soft to friable; lower boundary is sharp over ~1cm and dips a few degrees downstream; extensively bioturbated; abundant burrows less than or equal to 3mm diameter, abundant fine roots;	accumulated over bank floodplain accretion over a bar
143-178	sitly very-fine sand with rare pumice grains throughout; light brown; bedding dips very slighly downstream, subtle and horizontal, alternating between very fine sand and sandy silt in beds of 3-10 cm; lower boundary is sharp and horizontal with slight tongues of fines into underlying unit; charcoal layer at 170-175 cm depth, discontinuous; contains burrow fills up to 5 cm diameter; in upper 20 cm is orange-gold iron mottling; modern roots throughout; **charcoal at 174 cm depth (adopted age 5920 cal *yr* BP)**	fluvial vertical accretion; charcoal indicates cumulic floodplain surface

continued:

BE-05 (continued)

Depth from surface (cm)	Profile Description	Geomorphic Interpretation
178-220	medium to very coarse pumice sand; well sorted; top 2 cm are medium to coarse sand; cream colored; one tan silty fine sand bed in middle of unit at 194-197 cm horizontal and even; lower boundary is not exposed, but where we penetrated with soil probe it seemd sharp	Sycan Outburst Flood deposit
194-197	silty find sand horizon in unit above; tan; unit boundary top is sharp, bottom is gradataion over 1 cm;	slack water deposit in Sycan Outburst Flood deposit
2.26	clay loam; continuous downward >10-15 cm; dark gray; unit forms a 2-m wide ledge at base of bank; lots of water seeping out here (cold!) and too wet to dig.	pre-flood paleosol

Table B-13. Stratigraphic diagram of BE-06

Date/Site: 6-22-07.04 Bank Exposure: BE-06

Location Description: (N: 4704607.412, E: 641493.803) right bank exposure; water surface 183cm below floodplain surface; base innundated with hyperiec flow

LiDAR elevation at surface: 1314.98 (m)

Depth from surface (cm)	Profile Description	Geomorphic Interpretation
0-9	silt loam; dark brown; no evident bedding; medium-weak granular structure; dense root network of modern grass that forms ledge	overbank accretion fines
9-41	silt loam; at ~15-25 cm depth silt loam has higher content of medium pumice sand grains; light brown (dry); no evident bedding; weak, fine, blocky ped structure; lower boundary is gradational and clear over 3-4cm; bioturbated; has pores and burrows; common fine roots of living grass	same as underlying unit with more bioturbation; overbank floodplain deposits
41-93	silt clay loam; isolated pumi grains </= 1 mm diameter; brown (moist); subtle sandier laminae (discontinous); weathers to a coarse prismatic structure with prismatic platings; soft to friable; lower boundary is sharp over ~1cm and dips a few degrees downstream; extensively bioturbated; abundant burrows less than or equal to 3mm diameter, abundant fine roots;	accumulated over bank floodplain accretion over a bar
93-139	Medium to coarse pumiceous sand with silty fine sand lenses; upper 20 cm contains more silt in sand matrix (slightly indurated); mostly grey (moist) to light grey (dry); sand lenses </= 3cm thick; sand is cross bedded with ~30% dip; lower boundary is sharp over ~2 cm; local abundant detrital charcoal frags; upper 20 cm dry; lower 20 cm strongly mottled with a basal 2 cm iron cemented orange sub-horizontal band	Downstream end of sand bar that starts 10-15 m upstream with less than or equal to 1 m relief. Dwnstream of description point doesn't appear to include this sand unit.
139-146	Interbedded silty fine pumiceous sand and silty clay loam; grayish-brown (moist); sand lenses are 1-3 cm thick and contain granula less than or equal to 3 mm; laminea are generally sub-horizontal (wavy); lower boundary is gradational ~3 cm; oxidized orange at contacts; fine roots;	related to unit below; separated because of oxidation orange color and increased sand quantities

continued:

BE-06 (continued)

Depth from surface (cm)	Profile Description	Geomorphic Interpretation
146-211	silt loam to silty clay loam with laminea of very fine sand; dark brown, color lightens upward (dark grey/brown at bottom to light/medium gray brown); laminea of very fine sand that decrease upward, becoming thinner and less frequent; subhorizontal and slightly dipping; thin black lamina in silts, especially visible in upper 30 cm; no evident pedigenic structure; lower boundary is gradual over 4-5 cm; roots and orange mottling along root traces; apparent sedge fragments; overall fines upward; **willow stem sample collected from below water surface (adopted age 1350 cal *yr* BP).**	low energy fluvial deposition, likely heavily vegetated
211-221+	gravely coarse pumiceous sand with gravel clasts </= 1 cm; gravels are mixed lithics; (angular – rounded) dominantly subangular; pumice granules up to 3 mm coarse to very coarse sand sized pumice grains; auger refusal at 2.38m because of gravels, from probing in water, we determined sand and gravel extends down to 55 cm below water surface	original or reworked Sycan Outburst Flood deposit

Table B-14. Stratigraphic diagram of BE-07

Date/Site: 6-28-07.01 Bank Exposure: BE-07

Location Description: (N: 4705183.565, E: 641503.168) left bank exposure ~75 m upstream from Drews Road bridge

LiDAR elevation at surface: 1318.02 (m)

Depth from surface (cm)	Profile Description	Geomorphic Interpretation
0-23	silty sand and pebbles/cobles, angular gravel capped by 10 cm of loose sandy sod; multiple layers of road gravel; alternating layers of silty sand and pebbles	
23-33	silty very fine sand with abundant pumice grains; isolated lithic clasts </= 1 cm that are angular (may be from burrows above); dark grey; may express laminar bedding with sandy partings; weathers distinctly to 1mm thick horizontal platy structure; lower boundary is sharp over < 1 cm, marked by color change and texture, subhorizontal and wavy with about 15 cm of relief over length of outcrop; abundant modern roots near top; open and filled burrows </= 5 cm diameter	possibly recent overbank flooding but overprinted by organics (likely bottom of O-horizon given it's dark color); vertical accretion
33-120	very fine sand with abundant granules </= 1.5 mm; max clast size increases systematically from 5-8 mm to 1.5 mm, fines up; light brown with hint of orange (moist), grey (dry), upper 10 cm is slightly darker; bottom 30 cm has visible bedding of subtle cross bedding - indistinct in upper part of unit; breaks into soft sub-angular blocks; lower portion is loose, upper portion is slightly indurated and friable; lower boundary is subtle and difficult to see but marked by distinct difference in outcrop weathering character, contact marked by large 5x5 obsidian flake; few modern roots; few large open burrows </= 30 cm diameter, particularly along base	Sycan Flood equivalent – much less well sorted than classic Sycan Outburst Flood

continued:

BE-07 (continued)

Depth from surface (cm)	Profile Description	Geomorphic Interpretation
120-205	gravelly silty-sand, poorly sorted, max clast ~2 cm at base and 1.5 cm at top; most gravels are angular to sub-angular but abundant subrounded to rounded silt clasts; gravels are seemingly randomly oriented; brown (moist), grey (dry); unable to determine if unit is clast or matrix supported (likely clast), forms massive appearing resistant ledge in exposure with modern sage and rabbitbrush rooted at top; fresh exposures breaks into soft sub-angular blocky texture, no evident sed structure or depositional hiatus; weathered faces have a friable texture; lower boundary is sharp but irregular and primarily indicated by increased silt content and weathering of unit into a prominent "rounded" face; sage and rabbitbrush at top; some fine modern roots within upper 30 cm; bioturbated with abundant filled burrows ~ 1 cm diameter, open and filled root traces – plentiful	perhaps a very muddy flood deposit or maybe even debris flow. Abundant pumice content may indicate post-Mazama and thus may display another aspect of Sycan Outburst Flood – pumice needs to be analyzed and i.d. as Mazama. This pumice unit differs from other Sycan-Mazama flood units because it has other lithic materials and pebbles
205-242	Sandy gravel, max clast size decreases from ~2 cm at base to </= 1 cm at top; greyish brown (moist), light grey (dry); thin (<5 cm) thick discontinuous sand lenses, sub-horizontal bedding indicated by grain size variation - especially on weathered faces; no strongly developed ped structure; compact - although sandy horizons are slightly loose; lower boundary is sharp but wavy with ~20-30 cm of relief; common burrows and burrow fills (especially in upper 20 cm), no modern roots, perhaps some organic staining in upper 10 cm	another channel gravel -- uncomforably overlying soil developed on underlying unit

continued:

BE-07 (continued)

Depth from surface (cm)	Profile Description	Geomorphic Interpretation
242-297	sandy silt; brown (moist), light grey (dry); 3 discontinuous 2-4 cm thick beds of very fine to fine sand, including one at the top (242 – 245 cm) - ; no obvious sed structures; weathers to a slightly hard–hard angular blocky structure; compact; lower boundary is gradational over ~ 20 cm and based on subtle change in sed texture and intensity of bio-turbation; abundant filled burrows – intensly burrowed, local Fe mottling and perhaps charcoal staining; upper 20 cm slightly darker (organics?); no modern roots -- sand lenses are sub-horiontal but with irregular boundaries and brownish grey in color, composed of diverse lithics (abundant feldspar crystals), perhaps some pumi grains, sand lenses are slightly looser and form subtle notches on face of exposure	continual episodic vertical floodplain accretion over-printed by cumulic soil formation and bioturbation
297-360	Fine-medium sand, fining upward to a silty very fine sand, generally well sorted; golden brown (moist), greyish tan-grey (dry); lenses of medium-coarse sand in lower 30 cm; prominent 2 cm thick silty lamina (horizontal) at 3.29 m; no ped structure; compact; horizontal for at least 30 m and is sharp over </= 1 cm but with about 10 cm relief – apparently conformable; upper 30 cm has common filled hummus </= 1 cm diameter with burrow density increasing towards the top; abundant sed structures preserved, predominantly horizontal-sub-horizontal fines; laminations, but some of coarser sand lenses show crossbedding;	vertically accreted sandbar or low floodplain experiencing relatively rapid agradation; could have been formed in one or few episodes
360-492+	sandy pebbles/gravels that fine upward from 3-5 cm diameter to 1-2 cm daimeter, angular to well rounded (dominantly subangular to subrounded), diverse lithologies; deposited in sub-horizontal packages 10-30 cm thick that individually fine up slightly; compact locally indurated; lower boundary is not visible (note – channel bed substrate is gravel equivalent); few modern roots but otherwise no apparent bio-turbation	water emerging from basically the top of the unit (irrigation currently occurring up-slope); channel bed is made up of this unit that erodes in conglomeratic blocks and is ~50 cm deep

Table B-15. Stratigrahic diagram of BE-08

Date/Site: 6-25-07.01 Bank Exposure: BE-08

Location Description: (N: 4705730.534, E: 640776.32) right bank exposure after left-curving meander downstream of Brown Springs inlet ~ 450m; ~75 m downstream from BE-09; channel bed appears to be clay substrate with sand and gravels; water level at 288 cm below top of section

LiDAR elevation at surface: 1316.39 (m)

Depth from surface (cm)	Profile Description	Geomorphic Interpretation
0-10	pumiceous medium sandy loam; tan (dry); sublte horizontal - wavy laminea; no ped structure; (dry) soft and loose; lower boundary is irregular and sharp; plentiful bioturbation; upper 3-5 cm is sod; unit fills burrow holes of unit below;	recent overbank flood deposits
10-79	silty loam with some very fine sand and abudant coarse pumice grains; brown (dry); no bedding or ped structure; hard; vertical cracks on dry face (extends into unit below); lower boundary is gradual over 3 cm, smooth; biotrubated, modern roots, some burrow fills, some worm holes	vertical accretion
79-126	sandy loam with fine-medium sand; brown (dry at top and moist at bottom); no bedding or ped structure; lower boundary is gradual over 1 cm, wavy; plentiful bioturbation; modern Equisetum and other roots, some small root voids; coarse pumice grains dispersed throughout, increasing in frequency towards the top of unit;	vertical accretion
126-173	sandy loam with fine-medium sand and plentiful medium-coarse pumice grains; brown (slightly moist); very faint suggestion of horizontal lamination; no ped structure; lower boundary is wavy (up to 5 cm) and sharp; biotrubation: root voids, modern equisetum roots, filled burrows 4-5cm diameter; very subtle, fine, common organic mottling;	vertical accretion

continued:

BE-08 (continued)

Depth from surface (cm)	Profile Description	Geomorphic Interpretation
173-238	silty fine sand; brown (moist); sublte horizontal laminations 1-2 cm thick, differentiated by color and some slight textural differences; no ped structure; lower boundary is horizontal and gradational over 1cm; faint fine common orange mottles; bioturbated with small root voids (<3mm) and pumice sand filled burrows </= 6-7cm diameter, fiew live roots (woody); in-situ burn horizon at 212 cm	vertical accretion of a vegetated surface
238- below water surface	coarse pumice sand with interbeds of silt loam with coare pumice sand and organics; sand = grey-tan (moist); finer interbeds are dark gray (saturated below ~2.8 & moist above); dark slim beds expressed at 2.96, 2.82 and 2.69 with thicknesses of 4-5+cm; interbeds have sharp-grad over 1cm boundary; lowest interbed contains wood sticks and detritus; mid and top interbed has small grain fragments; similar bedding continues below water level - some beds have plentiful wood; pumice units between interbeds are 10cm (bottom), 12cm, and 30cm thick; at 246 cm is a moist orange band 3 cm thick, hard clayey coarse sand at base of orange band appears to be an Fe-cemented horizon with light yellow-orange color and hard dark orange concretions; pumice units fines up from very coarse sand to clayey coarse sand; above orange band is coarse pumice sand with some fines uppwe pumicw bed fines up to medium sand; lower boundary is sharp; **plant material at 313 cm depth (adopted age 1980 cal *yr* BP)**	below water level is lateral accretion or sand bar environment
332	clay sand with granules; blue; probe at base of unit found pebbles (thin layer) and then blue clay (erosional contact);	unit is a scarred surface 44 cm below water surface that rises towards the middle of the channel
348	gravels	indurated gravels below blue clay in channel pool ~60cm below water surface

Table B-16. Stratigraphic diagram of BE-09

Date/Site: 6-25-07.02 Bank Exposure: BE-09

Location Description: (N: 4705691.941, E: 640764.224) right bank exposure; ~ 75 upstream from BE-08; at same bank exposure

LiDAR elevation at surface: 1316.58 (m)

Depth from surface (cm)	Profile Description	Geomorphic Interpretation
0-57	silty sand with abundant pumice and sand granular clasts </= 3 mm; fining up to sitly fine sand in upper 10 cm; grey (dry); loose (relative to unit below); lower boundary is gradational over ~5 cm; extensively bioturbed with sage, rabbitbrush, and equisetum roots; open cavities (5-10 cm diameter) some occupied with swallow nests; upper 5 cm is sod;	multiple over bank deposits with slightly higher energy than underlying unit
57-146	silty sand grading up to silty very fine sand; abundant pumice grains and coarse sand granules in lower 30 cm; light brown (moist), grey (dry); interbedded with thick silty-fine sand beds; little evidence of bedding except lower 30cm; weathers to a coarse prismatic structure; forms prominent vertical face along the length of the exposure; abundant vertical cracks; lower boundary is sharp over <1/2 cm but irregular and appears to dip east; exensively bio-turbated by roots and burrows especially in upper 50 cm, abundant small voids < 2 mm especially in upper 30 cm, 1 cm diameter open burrows present, abundant equisetum roots;	accumulic floodplain vertically accreting surface
146-207	poorly sorted coarse sand; granular rich with coarse sand and gravels, 100% pumice grains; fines up to silty fine-med pumice sand; within lower 40cm - subtle horizontal bedding defined by particle size variations; local cross stratifcation at 176 cm of silty fine sand lense is inter-bed with coarse pumice sand; lower boundary is sharp over <1 cm, planar but slightly irregular; abundant root voids throughout as well as some modern equisetum and other roots; upper 20 cm intensly bioturbated with filled burrows </= 6 cm daimeter and abundant </= 1 cm burrow fills; isolated charcoal clasts; **charcoal clast at 186 cm (adopted age 5540 ca *yr* BP)**	Sycan Flood deposit (original or slightly reworked) with perhaps some ped development and/or revealing of upper 30cm

continued:

BE-09 (continued)

Depth from surface (cm)	Profile Description	Geomorphic Interpretation
207-211	silty clay; dark grey; no evident sedimentary structure; lower boundary is sharp over 1/2 cm but irregular with ~3 cm of relief over planar horizontal surface; upper 2 cm with 50% Fe mottling -- assuming along root traces; upper 1/2 cm dark grey (perhaps effected by charcoal stain); some filled burrows < 3 mm diameter especially in top 3 cm	organic-rich marsh deposit on-top of Mazama airfall tephra
211-214	well sorted medium-sand, angular pumice clasts with minor feldspar and mafic smaller minerals and very small unknown redish minerals; thickness of unit varies from 1.5-5 cm; no evident sedimentary structure; lower boundary is sharp </= 1/2 cm, irregular with about 2 cm relief on planar horizon surface	Mazama airfall
214-225+	silty clay; dark grey -- upper 1 cm slightly darker; weathers to a light grey slightly hard fine angular blocky structure; vertical dessication cracks near top; moist and dense; lower boundary is not visible but extends below water surface and is likely the channel bed; bare root trace fills and modern equisetum roots	organic rich active floodplain at time of mazama eruption; fining-up fluvial section from pebbles to clay that temrinated in marshy environment

Table B-17. Stratigraphic diagram of BE-10

Date/Site: 6-19-08.01 Bank Exposure: BE-10

Location Description: (N: 4707654.429, E: 640048.91) right bank exposure description at left bending meander near mid-valley; irrigated floodplain; groundwater seepage at 238 cm depth along bank exposure

LiDAR elevation at surface: 1316.73 (m)

Depth from surface (cm)	Profile Description	Geomorphic Interpretation
0-10	silt loam with pumice grains up to 2 mm diameter (rare); tan (dry); laminae defined by larger sand grains; weak platey structure; friable; lower boundary is horizontal and clear; abundant modern roots; surface vegetated with grass, sage, rabbitbrush	sequence of accreting overbank deposits
10-46	loam with sand grains of coarse-fine, pumice rich; tan (dry); weak blocky structure; firable, slightly hard; common vertical and horizontal dessicration cracks up to 1 cm wide on vertical face; exposure displays slight overhang at this unit; lower boundary is horizontal and gradational over 3 cm; bioturbated, burrow holes up to 5 cm diameter, abundant modern roots (live), common root voids </= 1 cm diameter	overbank accretionary deposits
46-83	loam, sands are fine, rare coarse-medium pumice grains; tan (dry), brown (moist); very weak blocky structure; friable; there are common vertical dessication cracks >/= 2 mm wide on vertical face; lower boundary is gradiational over 2 cm and horizontal; abundant root voids 1-3 mm diameter, common live roots	despositional unit, likely related to lower unit
83-195	sandy loam that coarsens to fine pumice rich sand; brown (moist); friable, loose; lower boundary is gradual, likely related to lower unit; rare black and rust colored mottles of 2 cm, mottles more visible on top halfof unit; root and root voids </= 2 cm diameter throughout; rare modern live roots;	sandy aggradational unit (perhaps vegetated)

continued:

BE-10 (continued)

Depth from surface (cm)	Profile Description	Geomorphic Interpretation
195-229	very coarse-medium pumice sand; unit fines up from very coarse pumice sand; some horizontal lenses 5-15 cm long - sandy loam (medium-fine sand); loose; lower boundary is slightly irregular; horizontal, and clear; localized charcoal between 212-223 cm depth	oscillating sand and fine deposits, likely upper bar development
229-233	clay loam with medium-fine sand grains; grey/brown (wet); unit dips towards channel at ~25 degrees; weak platey structure; friable; lower boundary is horizontal, slightly wavey, and clear; rare small light orange mottles; rare fine roots	fluvial fines deposited on erroded surface of lower boundary
233-245+	very coarse-medium pumice sand, pumice rich with mixed lithics, grain size >/= 0.5 cm, fining up of sand grain size; creamy white -- pumice rich semi-rounded pumice; this unit dips towards channel at ~25 degrees; grain supported, loose; bottom portion of unit is saturated; lower boundary is not visible; groundwater saturation at 238 cm, groundwater very cold	Sycan Outburst Flood deposit or early re-distribution of flood material
~ 293-299 - in channel (55-61cm below water surface)	clay; organic rich; lower boundary is distinct; in-channel, organic rich dark clay; saturated; makes psuedo-ledge bedform	temporarily abandoned channel infilling after Sycan Outburst Flood event
~299-308 - in channel (61-70cm below water surface	pumice rich unit below modern water surface level	Sycan Outburst Flood deposit or early re-distribution of flood material

Table B-18. Stratigrahic diagram of BE-11

Date/Site: 6-25-07.04 Bank Exposure: BE-11

Location Description: (N: 4708204.782, E: 639473.607) right bank exposure on top of bedrock exposure; near 1911 gaging station; surface vegetated with sage, pine, juniper; floodplain elevation above water surface - 434 cm; section cut into 3 profiles

LiDAR elevation at surface: 1318.72 (m)

Depth from surface (cm)	Profile Description	Geomorphic Interpretation
0-9	silty very fine - fine sand; light brown (dry); sublte thin laminea 1-2 grains thick; loose - no obvious ped structure; lower boundary is gradational over ~3 cm; abundant shrub and grass roots;	eolian reworking, trampling of top of Sycan Outburst Flood deposit
9-88	very fine - coarse sand (predominately pumice grains) with sparse lithics and mineral frags; brown (moist); grey (dry); angular and rounded grains; fines up with increasing % of very fine - fine sand; some sublte gradation of higher % of coarse pumice grains; loose - no pedogenic structure; lower boundary is gradational over ~10 cm; abundant modern shrub and ponderosa pine roots;	upper part of Sycan Outburst Flood deposit; slightly finer and more bioturbed; minor silt near top.
88-163	fine - coarse sand with granules-pebbles up to 1 cm diameter; predominantly pumice but lithics are present (<1%); light grey (dry); fines upward with increasing fine-medium sand content; no sedimentary structure; minor alternating gradation defined by grainsize and sorting variation; loose; lower boundary is sharp (<1cm), planar, and slightly irregular with 2-3 cm of relief; modern roots; some filled (pumice) burows and root traces	lower, less bioturbated component of Sycan Outburst Flood deposit (no evidence of depositional hiatus)
163-185+	silty fine sandy loam with isolated matrix supported pumice pebbles </= 2 cm diameter; larger pebbles are subangular to sub rounded; orange-brown (moist); subhorizontal dark colored lenses of FE or Mn oxidization; no evident sedimentary structure; very compact; lower boundary is not visible; abundant modern ponderosa pine roots; pumice filled burrows; root traces	weathered bedrock surface with perhaps minor (weathered?) overbank deposits.

Table B-19. Stratigrahic diagram of BE-12

Date/Site: 9-12-06.02 Bank Exposure: BE-12

Location Description: (N: 4708754.674, E: 639363.998) right bank exposure at outer bend of meander; bank exposure cut into high floodplain terrace of Sycan Valley; surface water is 5.2 m depth below the floodplain surface; NOTE: necessary cut into bank ~ 1.5m to achieve vertical exposure

LiDAR elevation at surface: 1319.59 (m)

Depth from surface (cm)	Profile Description	Geomorphic Interpretation
0-5	sod; vegetated with grasses, rabbit brush, sage & thistle	
5-223	locally granular-rich coarse to fine pumice sand; yellowish to white; lower 50cm is coarser and bedded; structurally very loose, grades upward, less sorted with more fine sand and silt near top; lower boundary is sharp and planar; lower 30cm is strongly oxidized with local manganese concrections, upper 1m has abundant roots; **single charcoal clast at 110cm depth (adopted age 1300 cal *yr* BP) - sample discarded**	Sycan Outburst Flood deposit
223-235	silty sand w/ abundant pumice grains </= 1mm diam.; light grey; 1cm thick laminated silt cap; no visible sedimentary structure; lower boundary gradational over ~3cm; likely air-fall Mazama mixed/bio-turbated and perhaps capped by a thin over-bank flood deposit.	Likely air-fall Mazama mixed/bio-turbated and perhaps capped by a thin over-bank flood deposit.
235-312	sandy silt; brown; little preserved sed strucutres; lower boundary gradational over ~20cm; adundant iron (Fe) mottling	unit represents vertical floodplain accretion of silts, some clay and very find sands (similar to unit below)
312-382(+)	clayish silt; brown; saturated, water trickeling out of root traces; some sandy fine sand laminea near base; some reduced zones around root traces (grey/blue reduction zones); roots exposed on base of unit; abudant equisetum roots;	gradual floodplain accretion

Table B-20. Stratigraphic diagram of BE-13

Date/Site: 9-12-06.03 Bank Exposure: BE-13

Location Description: (N: 4708693.277, E: 639408.511) left bank verticle cut bank; water surface is 2.3 m below floodplain surface; top of floodplain has flood debris from 2006 high flows at least 55 cm above top of soil profile

LiDAR elevation at surface: 1317.09 (m)

Depth from surface (cm)	Profile Description	Geomorphic Interpretation
0-80	sandy silt; light brown; no obvious bedding; coarse prismatic texture on weathered face; lower boundary gradational; abundant roots, insect burrows & root traces; capped by 2006 flood debris	overbank deposits
80-107	clayey sandy silt; light grey; no obvious bedding; prominent open vertical cracks; lower boundary planar and gradational over 3cm	sequential overbank deposits.
107-141	sandy silt; tan; locally horizontally bedded; weathers to sub-angular blocky; abundant root traces (including live equisetum); some burrow fills; capped by 3-5cm slightly darker silt (may be burned organic/charcoal horizon)	multiple over-bank deposits.
145-141	charcoal rich horizon - traceable several meters horizontally along bnk exposure; locally light colored ashy matrix with locally light-orange oxidized zones; charcoal ash matrix; lower boundary gradational ~2cm	burned surface capping underlying unit
145-192	sands & silts; grey-brownish; horizontally but locally wavy beds of sand and silt, 2-10cm thick sand lenses (discontinuous in lower 30cm of unit), upper is fine bedded silts and sandy silts; lower boundary sharp and wavy; abudant burrows and root traces	represetns episodic point bar/floodplain vertical accretion
192-209	sandy silt; strongly mottled; lower boundary sharp and sub-planar; abudant fine roots; isolated charcoal clasts; FE-rich nodules	
209-230(+)	fine-medium sand with abundant pumice grains </= 1mm diameter; mostly reduced but some oxidization in coarser layers and along burrow and root traces	likely a point bar or channel deposit

Table B-21. Stratigraphic diagram of BE-14

Date/Site: 9-12-06.01A&B Bank Exposure: BE-14

Location Description: (N: 4709052.128, E: 639296.609) right bank, due east from Teepee camp at Shields Ranch; profile described in two sections approximately 15 m apart due to soil layering on an incline from upstream to downstream end of valley; downstream upper portion of soil profile completed first; water level at 3.37m below floodplain surface

LiDAR elevation at surface: 1317.79 (m)

9-12-06.01A

Depth from Surface (cm)	Profile Description	Geomorphic Interpretation
0 - 35	silty pumiceous sand; Pumice grains < 1.5mm diameter; poorly sorted; local hints of planar bedding; very soft unit; extensively burrowed; capped by 3cm thick sod-layer with grass, thistle, rabbit brush; extensively bio-turbated	may represent a single large over-topping flood event (visible up and downstream in bank cut).
35 - 80	silty fine sand; some slightly darker horizons; brown; isolated < 1mm diameter pumice grains; no apparent bedding; slightly “softer” than unit below; lower boundary is gradational over ~ 10cm; abundant root and insect burrows; slightly mottled	likely vertically accreted floodplain deposits; slightly darker horizons that may represent developing A horizons that are buried
80 - 244	silty fine sand alternating with siltier horizons; brown; lower boundary is sharp and planer; extensively mottled and burrowed; isolated charcoal fragments present; dark, organic rich and charcoal rich horizons at 2.6, 1.9, 1.6, 1.43m depth and <1m wide where exposured on bank cut; perhaps representing localized floodplain fires; upper 60cm of unit is less mottled and massive;	likely cumulative floodplain processes resulting in vertical accretion
244 - 271	pumiceous medium to coarse sand; upper most portion of unit dominated by coarse pumice sand; locally wavy bedding defined by grain size variation; lower boundary is wavy and sharp, distinguished by grain size variation and charcoal content; charcoal rich (content = 3.4%); upper portion of unit contains greater charcoal; 2.59-2.64m depth- mottled and bio turbated	represents numerous depositional events that likely occurred after a major burn event in the Sycan; determined by charcoal content

continued:

BE-14 (continued)

Depth from Surface (cm)	Profile Description	Geomorphic Interpretation
271 - 302	pumice granules fining up to pumiceous medium to coarse sand; yellowish; 2.83-2.88m depth silty fine to medium pumiceous sand interbedded; open matrix; lower boundary is wavy, unconformable and sharp; some isolated charcoal clasts, especially notable in 3-4cm of unit base;	probably 2 or 3 depositional events
302 - 331	sand bedded grey medium sand alternating with yellowish pumiceous coarse sand; pumice clasts < 5mm diameter; yellow to grey; generally fines upward; nicely inter-bedded; lower boundary is sharp and planer, distinguished by pumice content of upper unit; isolated charcoal clasts in upper 5cm	may be single deposit event
331 - 365+	sandy gravel; pumice not evident in this unit; grey; well rounded to angular	

9/12/06.1B — Continuation of soil profile description. Approx. 15m upstream of 9/12/06.1A on right bank of Syan. Followed evident pumice layer equivalent to 1A unit at 2.11-2.71m depth. **NOTE**: 1m on tape is 1m above water surface. Considering 1A water level at 3.37 below FP surface, wl elev = 1314.42. 1m on tape above water surface at 1B = 1315.42 m elev.

72-86	medium to coarse pumiceous sand; lower boundary is sharp and wavy; charcoal rich (equivalent to 1A unit at 2.44-2.71m depth);	
86-96	silty sand; fining up to silty very fine sand; brown; lower boundary is gradational over ~2cm; mottled; root traces;	likely a floodplain over-bank deposit, not perserved or deposited in section 1A
96-110	coarse pumice sand - grading from 2-3mm at base, up to medium sand at the top; lower boundary is sharp and planer (equivalent to 1A unit 2.71-3.02m depth); abundant charcoal clasts	likely one depositional event
110-145	coarse pumice sand, grading up to medium to fine sand; grey to dark grey; planer bedding (especially in lower 20 cm); lower boundary contact is sharp; some iron staining in lower 15cm; abundant burrow fills in upper ~20cm; isolated charcoal clasts	likely represents one or more overbank or point bar deposits that were bio-turbated prior to being overtopped by pumice sand.
145-180+	medium to coarse pumiceous sand; medium sand alternating with grey or silty sands; fines up to medium pumice sand alternating with greyer silty sands; locally capped with 2-3cm thick charcoal/wood detritus horizon;	

Table B-22. Stratigraphic diagram of BE-15

Date/Site: 7-20-07.04 Bank Exposure: BE-15

Location Description: (N: 4709839.096, E: 639235.547) left bank exposure upstream of fence line; bank is ~ 6 m high, exposure is primary in the upper 1.3 m

LiDAR elevation at surface: 1315.0 (m)

Depth from surface (cm)	Profile Description	Geomorphic Interpretation
18 - 0	silt loam wth abundant pumice grains up to 3 mm, no grading; light tan; subtle laminae, horizontal, defined by larger pumice grains; no pedogenic structure; loose; lower boundary is gradational over 4 cm; no mottles; common modern roots, fines up to coarse roots and woody, some root voids, 0.5 cm diameter; upper 4 cm. is a sod layer	COMBINED INTERPRETATION: thinnish Sycan Outburst Flood deposit on pre-Mazama terrace; described as four units but they were in quick succession and really only sedimentary variation in one event
54 - 18	very find sandy loam with abundant pumice grains of very coarse sand, poorly-sorted, with very fine-granule size sand; light tan; no bedding or grading; no pedogenic structure; loose; lower boundary is gradational over 5 cm; no mottles; bioturbated around modern roots, no evident root voids but likely filled; burrow holes up to 10 cm to left and right of section	
78 - 54	fine to very coarse sand, fines upward slightly; light tan (slight salt and pepper); slightly better sorted (less very fine sand) than unit above; no bedding; no pedogenic structure; loose; lower boundary is gradational over 4 cm; no mottles; bioturbated, burrow holes up to 4 cm diameter, abundant modern roots, no root voids evident, as in overlying unit	
130 - 78	medium to coarse sand, well sorted; salt and pepper, color shifts to light tan towards top as pumice grains increase; increase in frequency and size of coarse pumice grains going upward; no bedding; no pedogenic structure; loose; lower boundary is irregular and very sharp < 1 cm horizontal; no mottles; bioturbated, sparse modern roots, one large filled burrow (~8 cm diam) at base of unit; several subangular med-fine gravels found sitting on the underlying surface (paleosol surface)	

continued:

BE-15 (continued)

Depth from surface (cm)	Profile Description	Geomorphic Interpretation
145 - 130	sandy loam, contains pumice grains and sand worked down from above; brown, includes lighter brown patches; weak blocky structure; friable; lower boundary is not visible; few faint fine pale-orange mottles; few root voids and few modern woody roots; some sand filled burrows	upper portion of pre-Mazama paleosol

Table B-23. Stratigraphic diagram of BE-16

Date/Site: 7-02-05.01 Bank Exposure: BE-16

Location Description: (N: 4711697.866, E: 638833.61) right bank nearest entry road and lava flow to the west; SE of Hippy Village site

LiDAR elevation at surface: 1319.51 (m)

Depth from surface (cm)	Profile Description	Geomorphic Interpretation
0 - 10	silty sand; poorly sorted; sand grains and granulars are pumice and mixed lithics; grey-light brown; no visible bedding; breaks down into soft platy peds; lower boundary is planar, defined by pedogenic structures; abundant fine rootlets	weak A horizon
10 - 56	gradational; silty (med - coarse) sand; abundant granulas =/< 4mm; larger grains are rounded lithics; sand is dominated by pumic grains (<10% lithics); grayish brown; no obvious soil structure; lower boundary is gradational for 5cm, planar, and primarily defined by silt content; roots and burrows (filled & open)	rapid sand aggradation, probably continuous with unit below but with an increased silt content (reflecting fine grained deposition or pedogenic silt penetration)
56 - 86	medium to coarse sand (~5% granules); fines up from granular coarse sand to medium sand; grains > 1mm are yellow pumice subrounded to round; finer grains are feldspar crystals, angular horneblends & pyroxenes, and other sparce rounded lithics; no apparent bedding; lower boundary is gradational for 2cm, defined on basis of grain size	rapid deposition of Mazama pumice and probably volcanic crystals
86 - 98	silt; composed entirely of glass frags with sparse mafic mineral crystals that are discontinuous and >/= 2 cm diameter; pinkish orange; hint of sub-planar lamination; no apparent sedimentary structure; lower boundary is sharp, defined by grain size difference	slack water deposition of tefra laden water; no evidence of significant time; clearly represents a period of lower energy deposition
98 - 124	sandy gravel that fines up to coarse sand; basal part composed of granules </= 5mm; all coarse grains & granules are rounded pumice; abundant feldspar, horneblend & pyroxene angular crystals from medium sand-sized grains; lower boundary is sharp, planar, defined by grain size; lower 3 cm strongly stained with iron and magnesium oxides;	fluvially transported Mazama eruption products; Sycan Outburst Flood deposits

continued:

BE-16 (continued)

Depth from surface (cm)	Profile Description	Geomorphic Interpretation
114 - 124	silty fine to medium sand with maximum clasts size = 1mm; coarsens up from medium sand to sandy silt (upper 2cm); no grains > 2mm; all grains > 1mm are sub-rounded pumice clasts; all grains > ½ mm are sub-rounded pumice grains; yellowish brown; lower boundary is irregular over ~ 5cm; motteled; sparse fine rootlets	it appears that pumic grains filled animal burrows in underlying unit. Airfall Mazama product. Perhaps contaminated by flood plain silts in upper 2cm. Landed on a vegetated flood plain surface
124 - 231	clayish silt; mostly brown; some subtle coarser horizons (perhaps with fine sand content); weathers into fine angular 2-3cm blocks; lower boundary is gradational over ~ 20cm, defined by weathering texture; mottels of iron staining (perhaps charcoal fragment stains); abundant roots and pumice sand filled animal burrows;	episodically created floodplain soil formed by vertical aggredation; extensively bio-turbated; likely actively forming at the time of the Mazama deposition
231 - 268	clayish slit (~1% matrix supported – granules of lithic clasts); orangish-brown; lower boundary is sharp but highly irregular with relief of at least 30cm, defined by 2cm thick silty very-fine sand; mottled with iron and/or charcoal staining; abundant root traces;	accumulic floodplain soil formed on deposits laid on top of bank edge or other "high relief surface"
268 - 334	silty, very-fine sand to silt clay; brown; no apparent sedimentary structures; lower boundary is not exposed; mottled with iron and charcoal staining; some modern and paleo roots; some clay filled burrows	floodplain overbank deposits; perhaps silty material was a more energetic facies than layer above

Table B-24. Stratigraphic diagram of BE-17
Date/Site: 7-19-07.07 Bank Exposure: BE-17
Location Description: (N: 4711916.864, E: 638844.84) right bank exposure description; water level is at 277 cm
LiDAR elevation at surface: 1318.40 (m)

Depth from surface (cm)	Profile Description	Geomorphic Interpretation
42 - 0	sandy loam with silt, medium-coarse sand grains, pumiceous, fines upward slightly; laminated in top 8 cm; no pedogenic structure; loose; lower boundary is horizontal, clear; bioturbation: root voids, burrow fills, modern roots up to 4 cm diameter, abundant modern roots 2 mm maximum diameter; no mottles	cumulic overbank deposits on a vegetated surface
96 - 42	sandy loam and silty in beds. bottom 15 cm has coarse sand pumice in it and rest of it has some finer pumice in sandy loam beds; bedding is disrupted by bioturbation, dominant silt to sand beds are horizontal, slightly wavy (ripples?); one horizontal laminae has humus and fine organic fragments (probably graminoid detritus deposited with or buried by sediment); no pedogenic structure; friable (silt loam) to loose (sandy loam); lower boundary is horizontal, gradational over 3-4 cm; common 5-10 cm burrows; some dessication cracks extend down from overlying unit; other bioturbation: root voids, modern roots; no mottling	cumulic overbank deposits on a vegetated surface
138 - 96	pumiceous sandy loam, poorly sorted throughout, very fine-very coarse sand; silt content increases in upper 3 cm; tan; no evident bedding; no pedogenic structure; friable; lower boundary is wavy, sharp; bioturbation: large krotovinas up to 10 cm diameter; root voids, worm burrows, some modern roots, few scattered charcoal pieces up to 3 mm diameter	overbank flood deposit rich in pumice

continued:

BE-17 (continued)

Depth from surface (cm)	Profile Description	Geomorphic Interpretation
198 - 138	silt loam; light brown (dry); laminae of tan, medium brown with differences in silt content; also several prominent dark brown laminae, 1 cm thick, subhorizontal to wavy, continue >1 m; fine laminae are disrupted in upper 10 cm; no pedogenic structure; slightly hard (dry); lower boundary is horizontal, gradational over 3-4 cm; charcoal fragments; some modern roots; few fine faint orange mottles; dry bank face shows prominent vertical dessication cracks starting at top of this unit and extending to 216 cm; bioturbation above 161 cm: a filled burrow 3 cm diameter, many fine root voids; bioturbation below 162 cm: many fine root voids, few modern roots; at 161-162 cm is a prominent lamina rich in fine charcoal fragments (up to 1 cm) and pumice very coarse sand grains, this laminae extends about 3 m in bank	depositional events (overbank) rich in charcoal and pumice
210 - 198	very fine sandy loam; faint horizontal laminae that are slightly darker and lighter brown, with higher silt content in darker laminae, laminae are disrupted in places; no pedogenic structure; soft consistency; lower boundary is slightly wavy, gradational over 2 cm; common fine distinct rusty red mottles; few to common charcoal pieces throughout; bioturbation: few fine modern roots (live), few root voids;	cumulic deposition on a vegetated surface, finer bar top deposit or initial floodplain deposit, probably vertical accretion.
216 - 210	poorly sorted pumice sand, very fine to coarse; not 100% pumice but rich in pumice; all coarse sand grains are pumice, well rounded; fines upward; light brown with “salt” (Mazama tephra); no evident bedding; upper surface dips slightly downstream; no pedogenic structure; loose (moist) consistence; lower boundary is horizontal, sharp; no evident bioturbation	sandy bar deposit

continued:

BE-17 (continued)

Depth from surface (cm)	Profile Description	Geomorphic Interpretation
250 - 216	sandy gravels (coarse sand); gravels well-rounded, up to 2.5 cm, slight fining up in gravel size; sand may have pumice in it; brown; no apparent bedding; matrix supported; cementation is extremely firm (moist), very hard; lower boundary is sub-horizontal, dipping slightly downstream, clear; cemented oxidized; distinctly coarser and more cemented than underlying unit; orange and red in mottles and horizontal bands, many mottles, medium prominent orange; no bioturbation; pieces of charcoal (2-4 mm) at upper boundary of this unit; this unit is capped by 1-2 cm thick bed of fine sandy loam, no cementation, no gravels, light brown	gravel bar deposit, lateral extent ~20m
277+ - 250	gravelly coarse sand, well rounded gravels up to 2.5 cm, mixed lithology; fines upward to coarse sand at top; gravels decrease in size and abundance going up; sands appear to include pumice; salt-and-pepper (brown) wet; no apparent bedding; matrix supported; no evident cementation; orange-stained zone at very top, 1-2 cm thick; no bioturbation	gravel bar deposit, lateral extent ~20m

Table B-25. Stratigraphic diagram of BE-18

Date/Site: 7-01-05.02 Bank Exposure: BE-18

Location Description: (N: 4711980.316, E: 638875.982) left bank; upper Sycan Valley; summarized bank exposure description; top of bank is 2.6 m to surface of water

LiDAR elevation at surface: 1319.19 (m)

Depth from surface (cm)	Profile Description	Geomorphic Interpretation
0 - 260	Sandy gravel that fines up to silty sandy loam throughout the section;	Post-Mazama vertical floodplain aggradation sequence; capped by fine grained historic flood deposits
270	carbon sample below water surface elevation; **2 cm diameter wood sample (adopted age 590 cal yr BP)**	

Table B-26. Stratigraphic diagram of BE-19

Date/Site: 7-21-07.03 Bank Exposure: BE-19

Location Description: (N: 4713257.271, E: 637577.212) left bank -- upper Sycan Canyon on inset floodplain surface; summary bank exposure description; floodplain surface is approximately 225 cm above water surface

GPS elevation at surface: 1502.35 (m)

Depth from surface (cm)	Profile Description	Geomorphic Interpretation
0 - 70	Silty loam with coarse pumice grains, an overall fining up sequence; light brown; subtle laminae separated by larger pumice grains; no pedogenic structure; loose (friable); lower boundary is horizontal and sharp (~ 2 cm); very bioturbated with roots, burrows, and voids;	over bank floodplain accretion -- post Sycan Outburst Flood
70 - 108	Sand and loam, 3-6 cm thick alternating beds, sequence fines upward, sand is coarse at base and pumice rich; alternating beds have different structures (sand = no structure, loam = very subtle blocky); lower boundary is horizontal and sharp; fine orange mottling and charcoal pieces in loamy beds; roots and worm voids present throughout;	sequence of overbank (accretionary) deposits on vegetated developing floodplain - post Sycan Outburst Flood
108 - 120	sandy loam, coarse pumice grains sparsely present throughout; brown; no apparent bedding; very subtle blocky pedogenic structure; soft; lower boundary is wavy and gradational over 3 cm; few orange mottles in upper 10 cm ; charcoal clast present; moder roots and voids	sequence of accreting floodplain deposits (evidence of lateral migration within this confined canyon section? -- or change in sediment load and transport capacity?) -- post Sycan Outburst Flood
120 - 125	fine-coarse sand	deposit fines up from underlying sandy gravel
125+	sandy gravels (well rounded), clasts </= 3 cm	channel bed or active bar

Table B-27. Stratigraphic diagram of PIT-01

Date/Site: 9-19-07.02 Soil Pit: PIT-01

Location Description: (N: 4708155.57, E: 638959.241) soil pit dug at western side of mid-Sycan Valley between Shields driveway and rock outcrop, south of South Shields Creek

LiDAR elevation at surface: 1320.57 (m)

Depth from surface (cm)	Profile Description	Geomorphic Interpretation
0-65	pumiceous sandy loam; fining up sequence; brown; loose, friable; lower boundary is gradational; heavily bioturbated, many fine roots and filled burrow holes;	bioturbated and soil development in upper sequence of Sycan Outburst Flood deposit
65-165	medium-very coarse pumice rich sand, grain </= 1 cm diameter, subangular to subrounded; fines up to very fine-coarse sand, poorly sorted; cream colored at base, brown at top; lower boundary is clear and horizontal; prominent dark brown sand filled burrows throughout (burrow fills </=15 cm diameter);	bioturbated upper sequence of Sycan Outburst Flood deposit
165-170	fine-coarse pumice-rich sand; salt and pepper (peper dominated) coloration; grain supported; unit is discontinuous in exposure but is horizontal; burrow fills and other boiturbation present	
170-190	medium-coarse pumice-rich sand; salt and pepper (pepper dominated) coloration; yellowish color band at 174-185 cm depth; contains two thin horizontal beds (at 170-170.2 cm and 190-192 cm depth)	Second flood pulse of Sycan Outburst Flood with slight oxidation occurring
170-170.2	very fine silty sand; dark grey with paper-thin yellowish band at base;	slack-water deposits during flood event
190-192	silt; grey and salmon; horizontally bedded - slightly irregular in shape; irregular shape of bedding likely due to irregular surface at deposition; grey is more predominantly on top - althout it is mixed in areas;	slack-water deposits during flood event

continued:

PIT-01 (continued)

Depth from surface (cm)	Profile Description	Geomorphic Interpretation
192-216	very coarse (1cm diameter grains) pumice sand and pebbles; subangular to subrounded grains; top is poorly sorted; grain supported, fining up sequence; bottom 5 cm is pure pumice; cream at base, salt and pepper coloration increases at top; loose; lower boundary is horizontal, abrupt and slightly irregular with 1cm horizontal variance; base of unit has a slightly yellowish tint (~1 cm thick) expresses slight cementation; no bioturbation	base of Sycan Outburst Flood deposit
216+	silty loam with pumice sand grains of fine-coarse (angular to subrounded); dark brown (wet); massive; weak; no visible mottles; grounwater inundation at 236cm	pre-Sycan Outburst Flood paleosol

Table B-28. Stratigraphic diagram of PIT-02

Date/Site: 6-27-07.03 Soil Pit: PIT-02

Location Description: (N: 4730718.15, E: 649189.474) soil pit profile description at upper Sycan River ~ 1 mile downstream from Sycan Marsh outlet bridge; left bank; flat terrace between channel and tallis canyon walls

GPS elevation at surface: 1516.03 (m)

Depth from surface (cm)	Profile Description	Geomorphic Interpretation
0-8	organic rich sandy silt; very soft crumbly texture; no obvious sed structure; lower boundary is gradational over 5 cm; abundant pine needles and modern fine roots	forest floor soil 0-horizon; post Sycan Outburst Flood soil development
8-80	feldspar and mafic crystal fragments; silt content increases towards top of unit; locally (at base of unit) is an ashy silt-very fine sand </= 1.5 cm thick – discontinuous but mostly present; grey (dry), pale yellowish orange (moist); lower 30 cm has subtle bedding that is subhorizontal, defined on basis of grain size variation and sorting; lower boundary is base is irrigular but sharp throughout, ranging from 50-80 cm from unit top to base; abundant modern roots in upper 60 cm; abundant charcoal staining and clasts (probably mostly from burned roots); abundant filled burrows and root traces </= 5 cm diameter	fluvially deposited pumiceous sand deposit; single event over an irregular surface; Sycan Outburst Flood deposit
80-112+	sandy silt; coarsening up to a silty, very fine sand with matrix supported sub-rounded pebbles </= 2 cm diameter; as well as large "pit-controlling" boulders; several 1-2 cm rounded pebbles near top of unit; "purplish" grey -- dusty lavender (moist); no obvious sed structures, breaks into soft angular blocks (base); upper portion is softer, lesss compact; base is unexposed – unable to describe lower contact; some orange FE mottling (especially near base); some roots, sand filled burrows and root traces </= 4 cm diameter; some charcoal present (perhaps mostly burned roots)	low energy fluvial deposit that infills talis from basalt cliff 50 m to west; based on sample composition appears to post-date Mazama eruption and Sycan Outburst Flood

APPENDIX C

CALIBRATION PROBABILITY CURVES OF RADIOCARBON SAMPLES

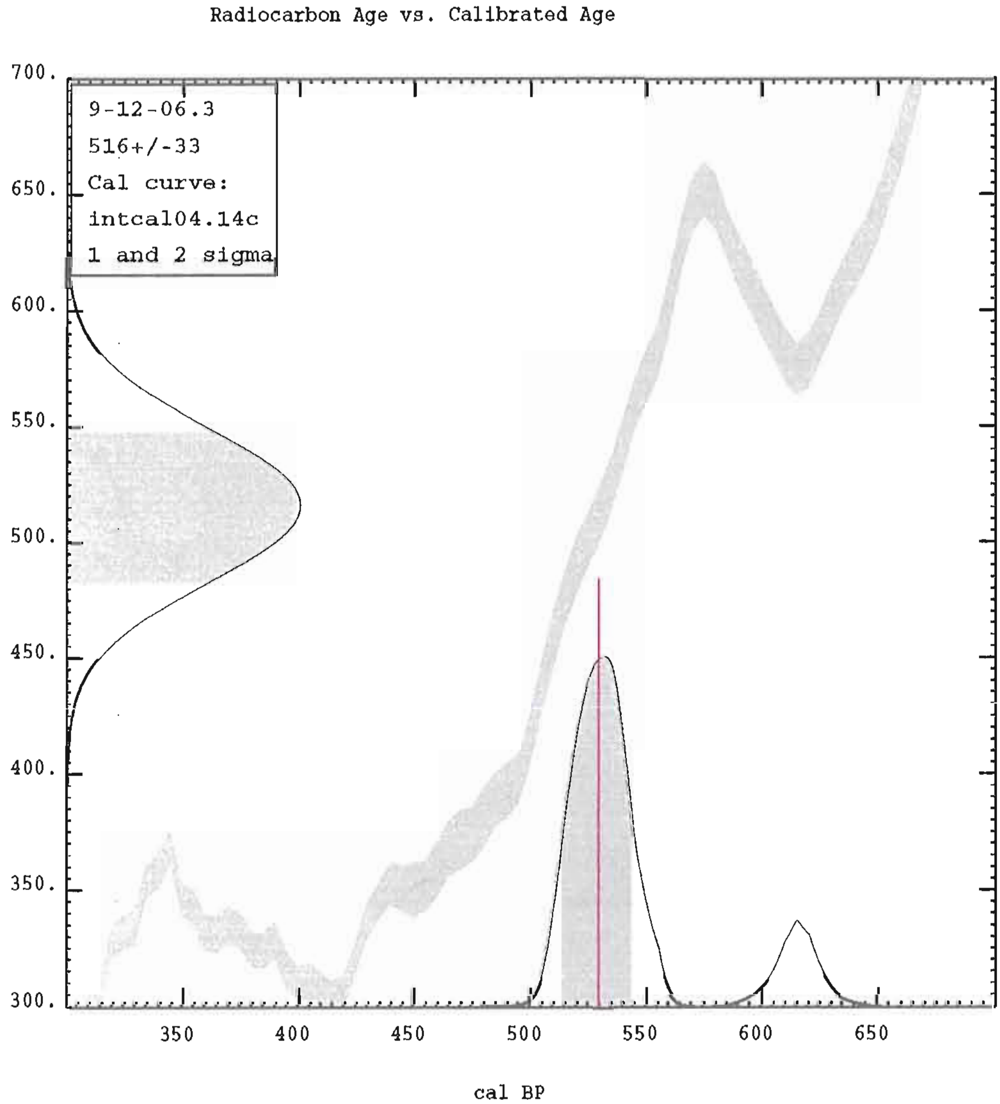

Figure C-1. Calibration curve of carbon sample at BE-13
Site: BE-13 Lab Sample Code: WW6097
Median Age (p50), cal *yr* BP: 534
Adopted Age, cal *yr* BP: 530

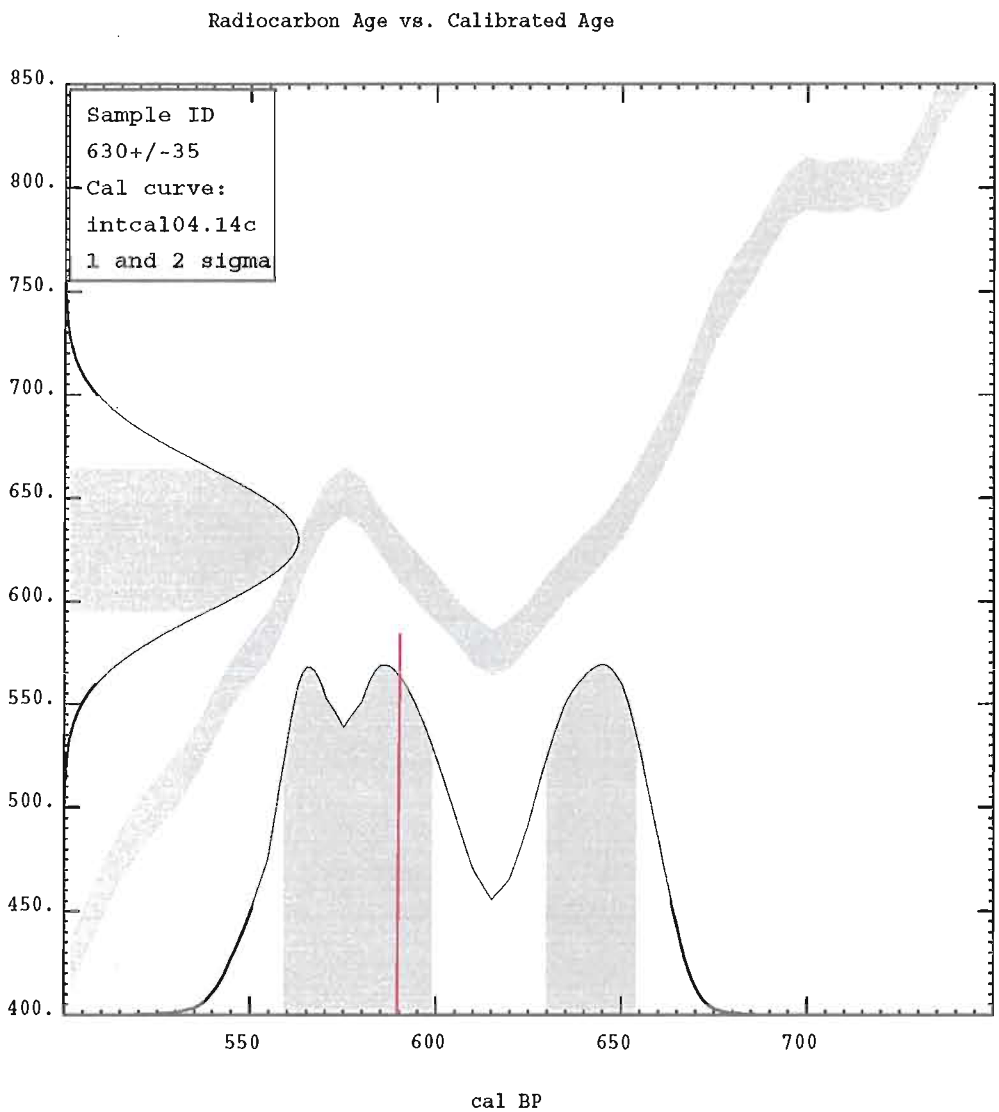

Figure C-2. Calibration curve of carbon sample at BE-18
Site: BE-18 Lab Sample Code: WW5422
Median Age (p50), cal *yr* BP: 601
Adopted Age, cal *yr* BP: 590

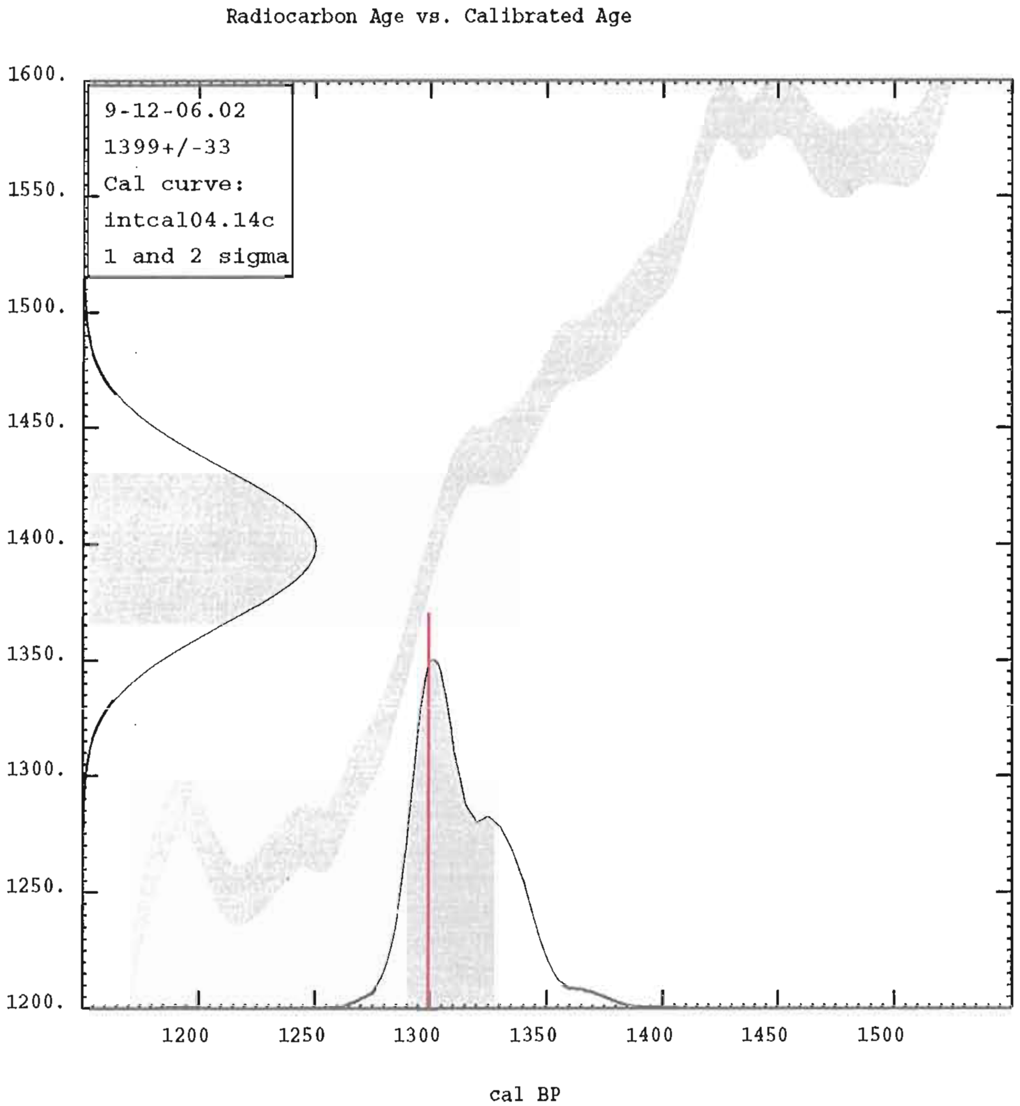

Figure C-3. Calibration curve of carbon sample at BE-12
Site: BE-12 Lab Sample Code: WW6096
Median Age (p50), cal *yr* BP: 1311
Adopted Age, cal *yr* BP: 1300

Note: Sample discarded due to incongruence of calibrated age range to related stratigraphy and the high likelihood of bioturbation emplacement of the sample by burrowing animals.

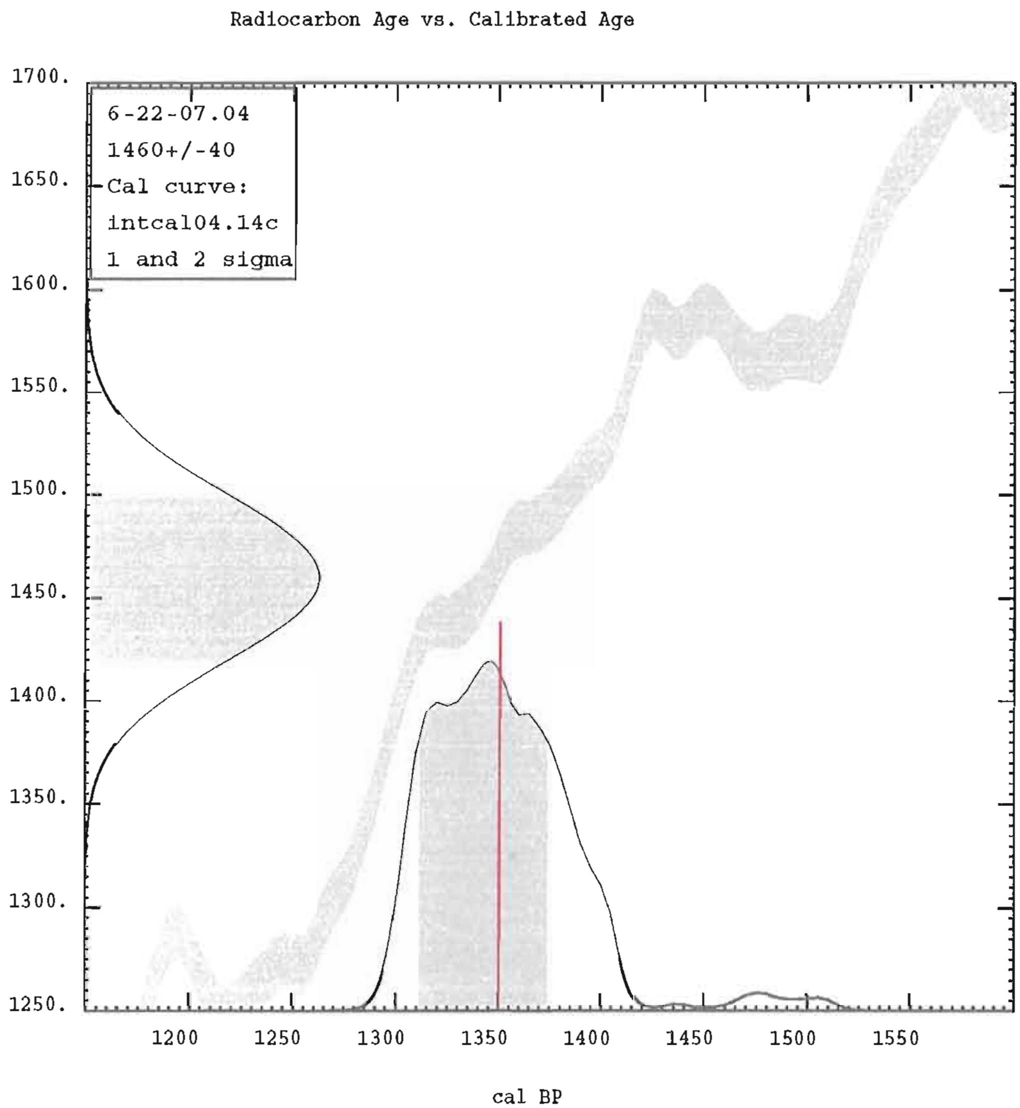

Figure C-4. Calibration curve of carbon sample at BE-06
Site: BE-06 Lab Sample Code: Beta-234718
Median Age (p50), cal *yr* BP: 1350
Adopted Age, cal *yr* BP: 1350

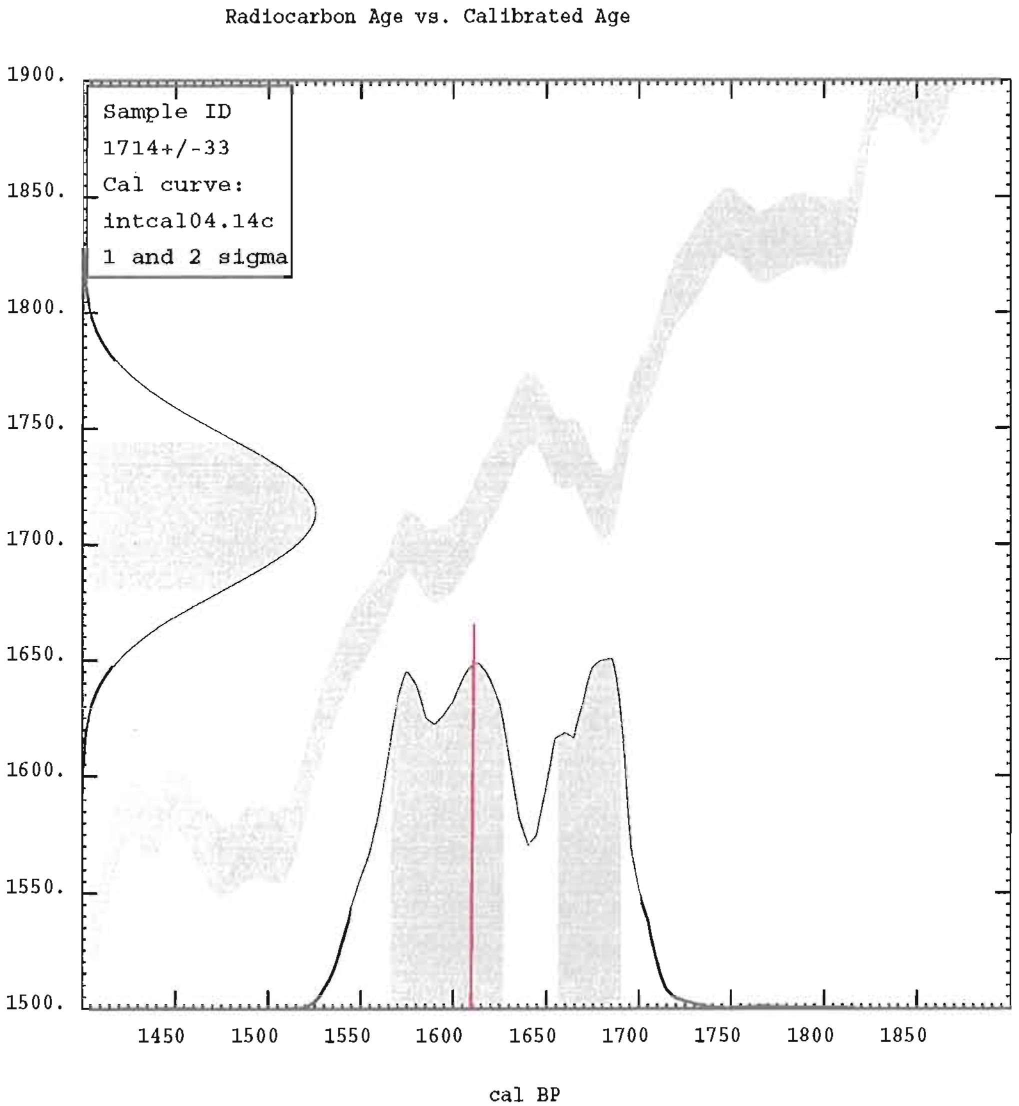

Figure C-5. Calibration curve of carbon sample at BE-14
Site: BE-14 Lab Sample Code: WW6095
Median Age (p50), cal *yr* BP: 1622
Adopted Age, cal *yr* BP: 1610

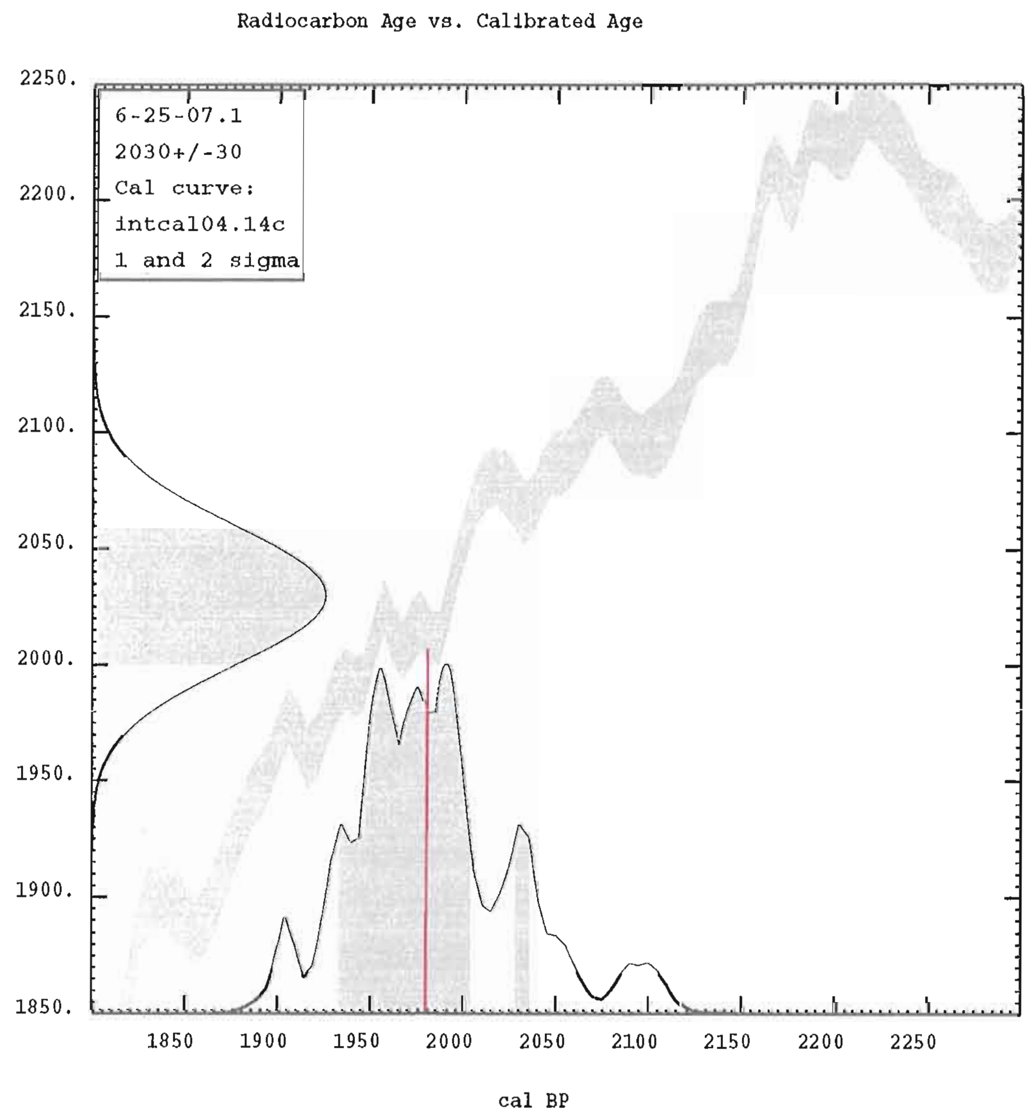

Figure C-6. Calibration curve of carbon sample at BE-08
Site: BE-08 Lab Sample Code: WW6419
Median Age (p50), cal *yr* BP: 1980
Adopted Age, cal *yr* BP: 1980

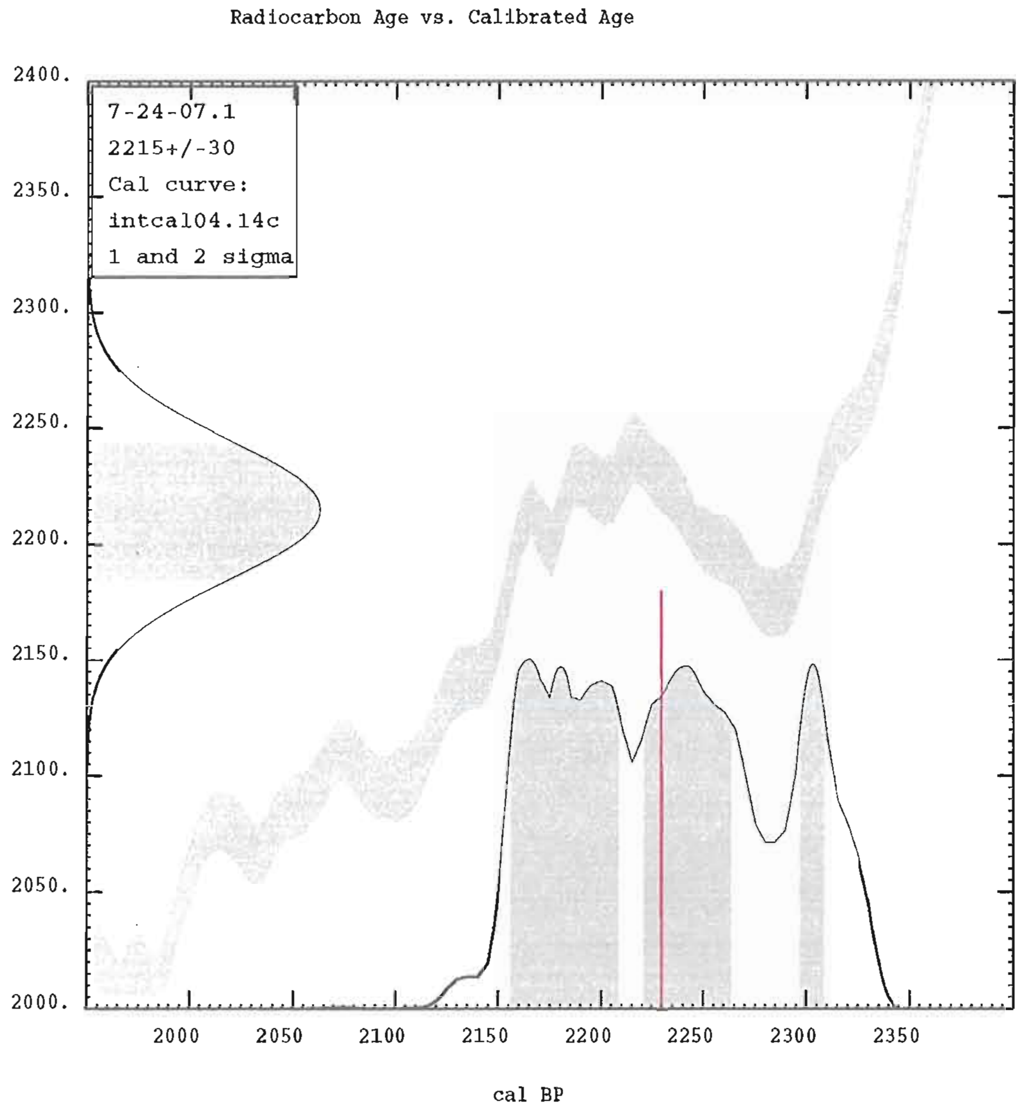

Figure C-7. Calibration curve of carbon sample at BE-03
Site: BE-03 Lab Sample Code: WW6420
Median Age (p50), cal *yr* BP: 2232
Adopted Age, cal *yr* BP: 2230

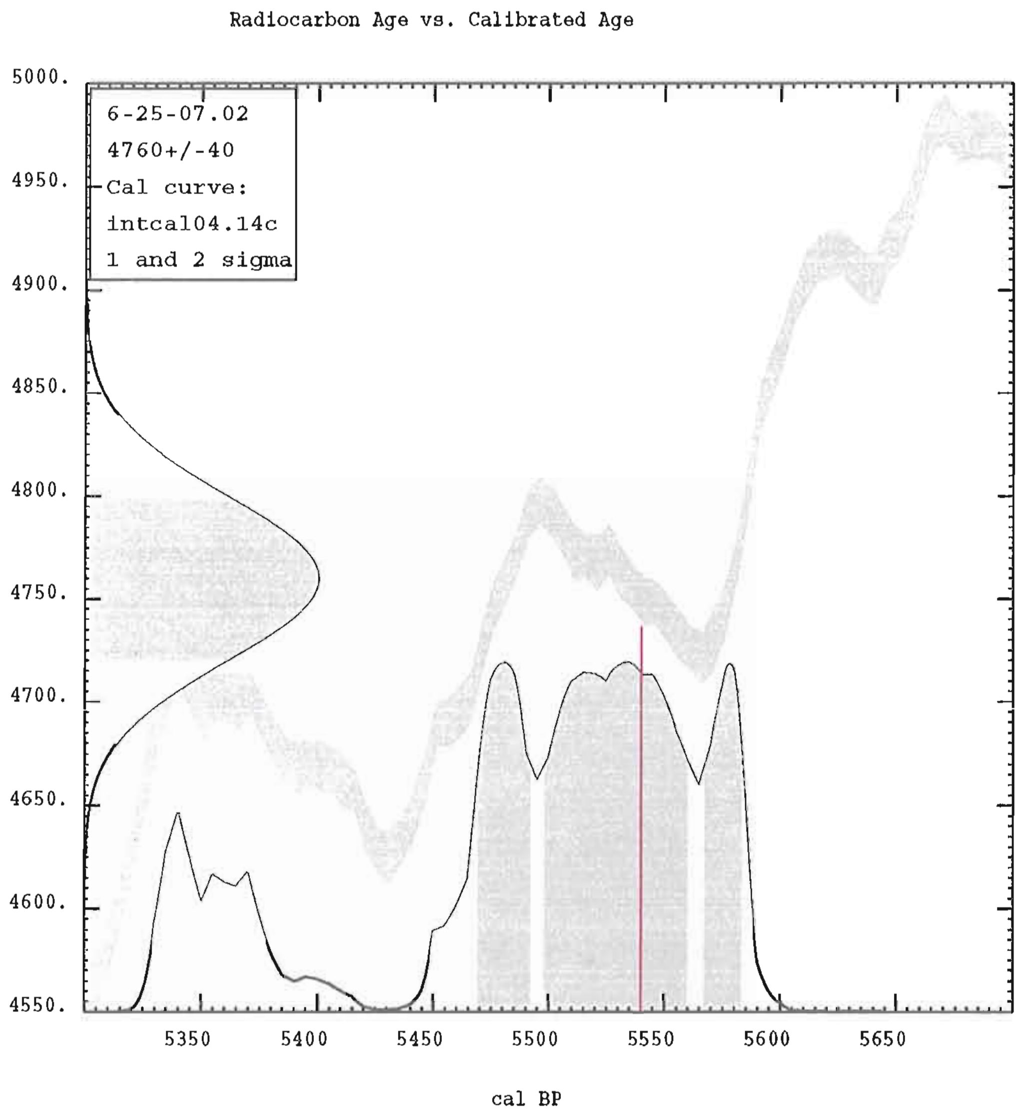

Figure C-8. Calibration curve of carbon sample at BE-09
Site: BE-09 Lab Sample Code: Beta-234714
Median Age (p50), cal *yr* BP: 5513
Adopted Age, cal *yr* BP: 5540

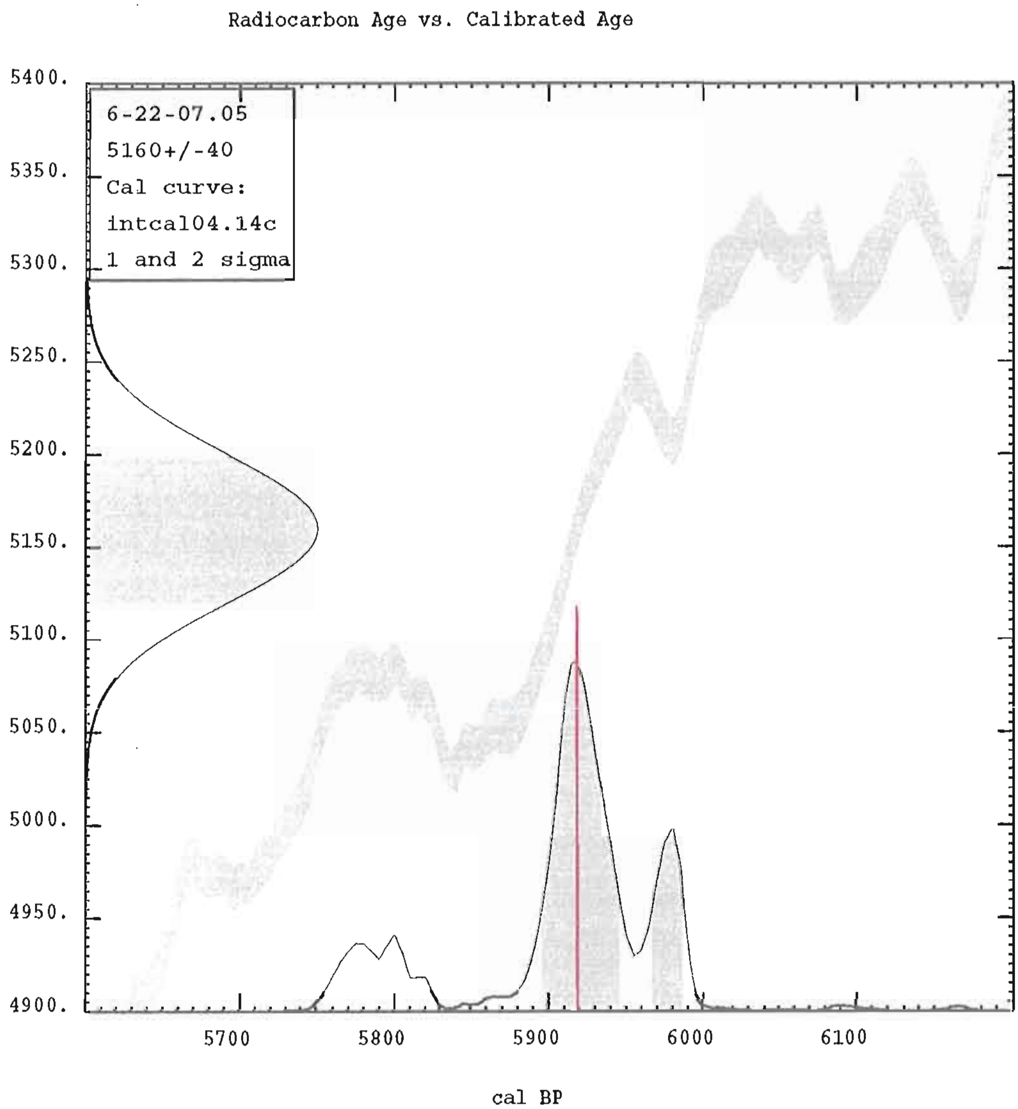

Figure C-9. Calibration curve of carbon sample at BE-05
Site: BE-05 Lab Sample Code: Beta-234715
Median Age (p50), cal *yr* BP: 5921
Adopted Age, cal *yr* BP: 5920

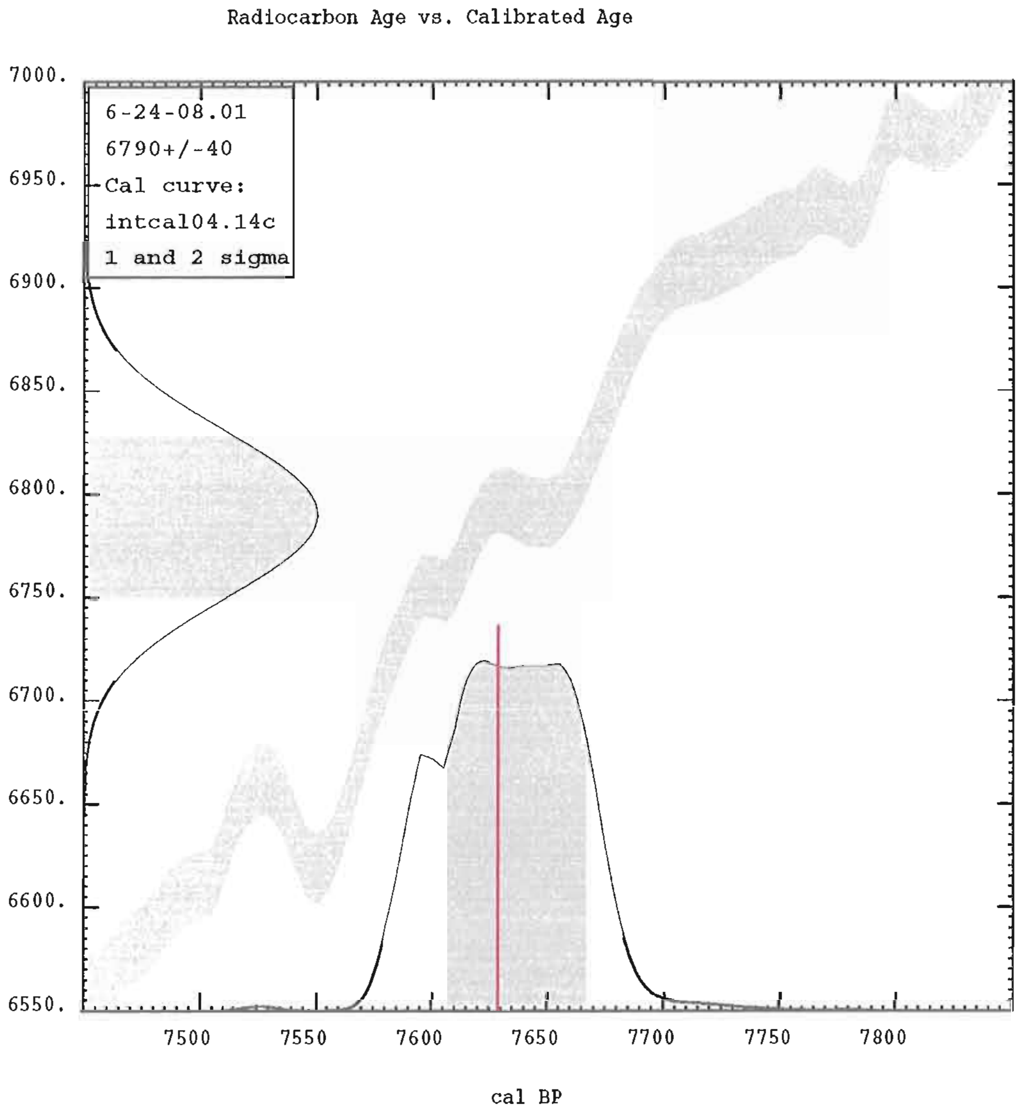

Figure C-10. Calibration curve of carbon sample at BE-02
Site: BE-02 Lab Sample Code: Beta-252116
Median Age (p50), cal *yr* BP: 7634
Adopted Age, cal *yr* BP: 7630

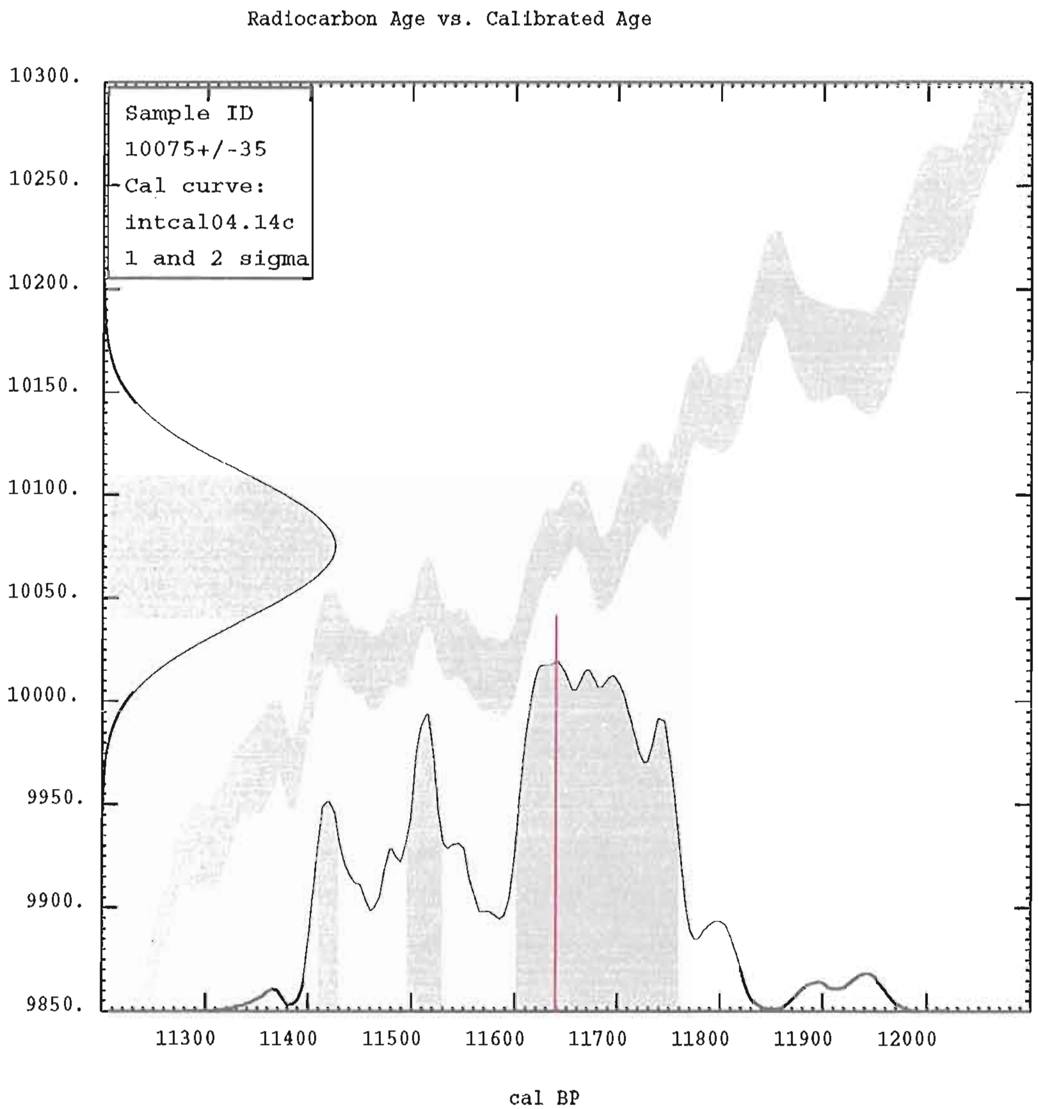

Figure C-11. Calibration curve of carbon sample at AUG-07
Site: AUG-07 Lab Sample Code: WW5421
Median Age (p50), cal *yr* BP: 11640
Adopted Age, cal *yr* BP: 11640

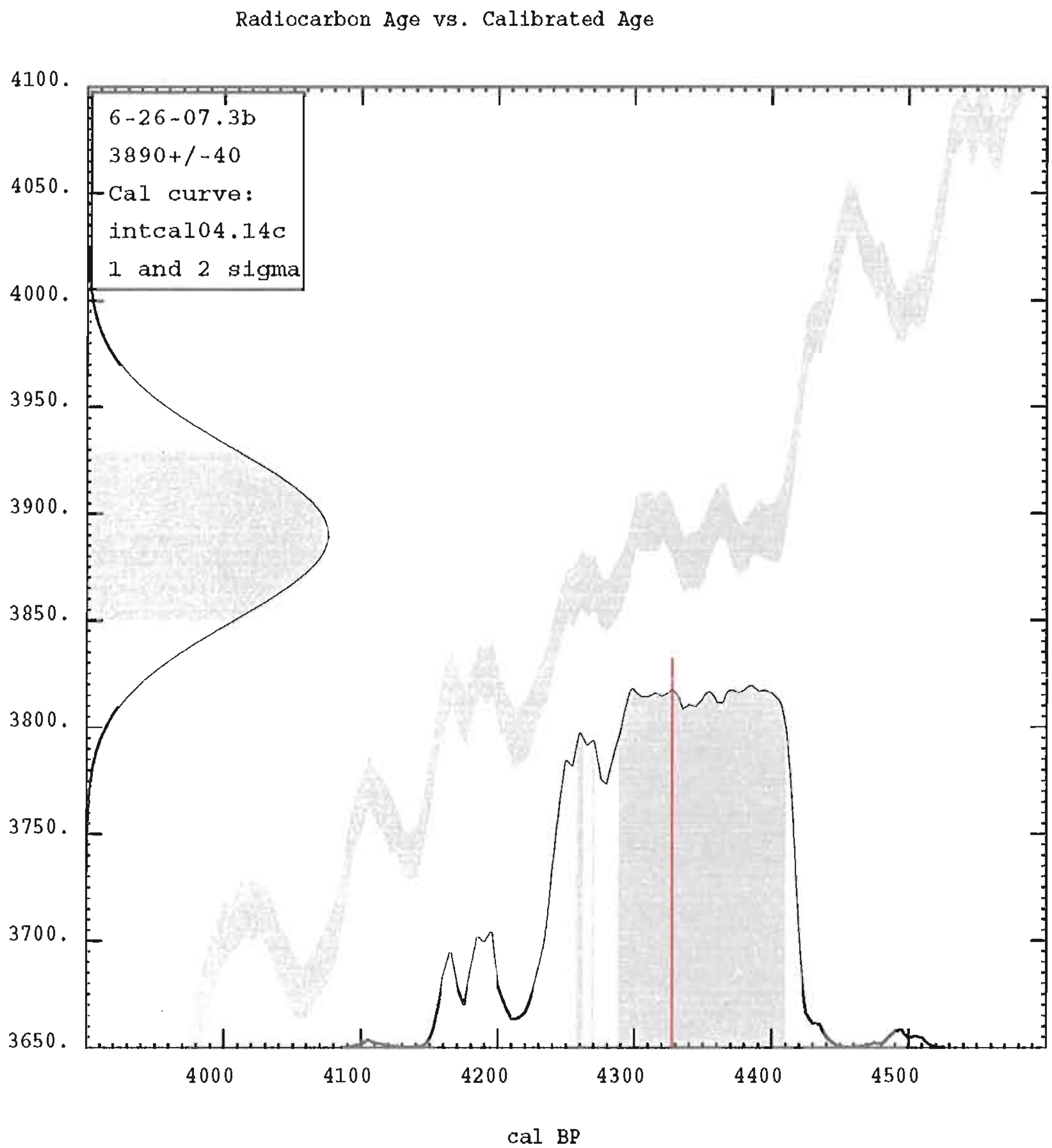

Figure C-12. Calibration curve of carbon sample at N Fork Sprague
Site: N Fork Sprague Lab Sample Code: Beta-234716
Median Age (p50), cal *yr* BP: 4327
Adopted Age, cal *yr* BP: 4330

APPENDIX D

GEOMORPHOLOGY MAP AND PLATES

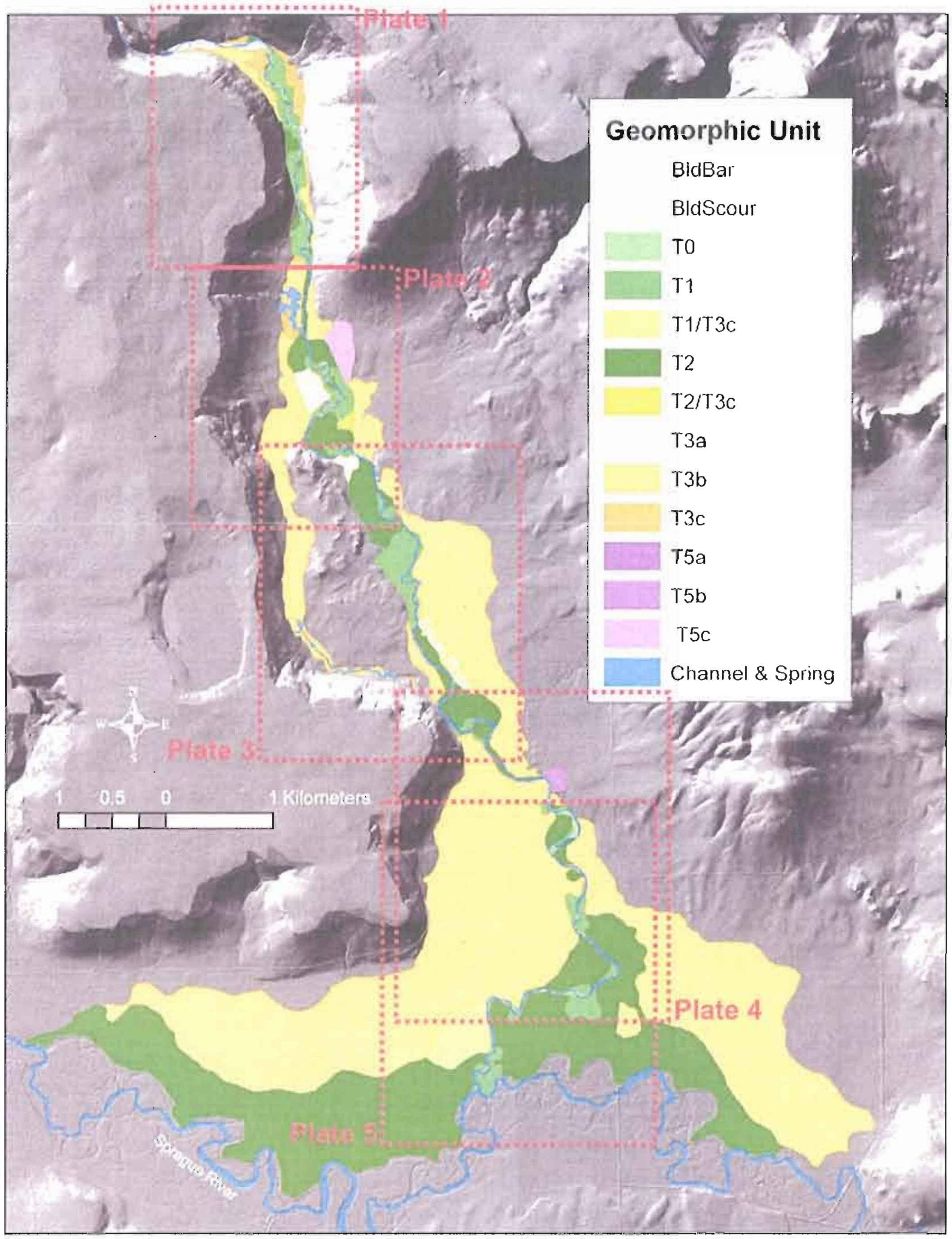

D-1. Geomorphic Surface map of the Sycan Valley

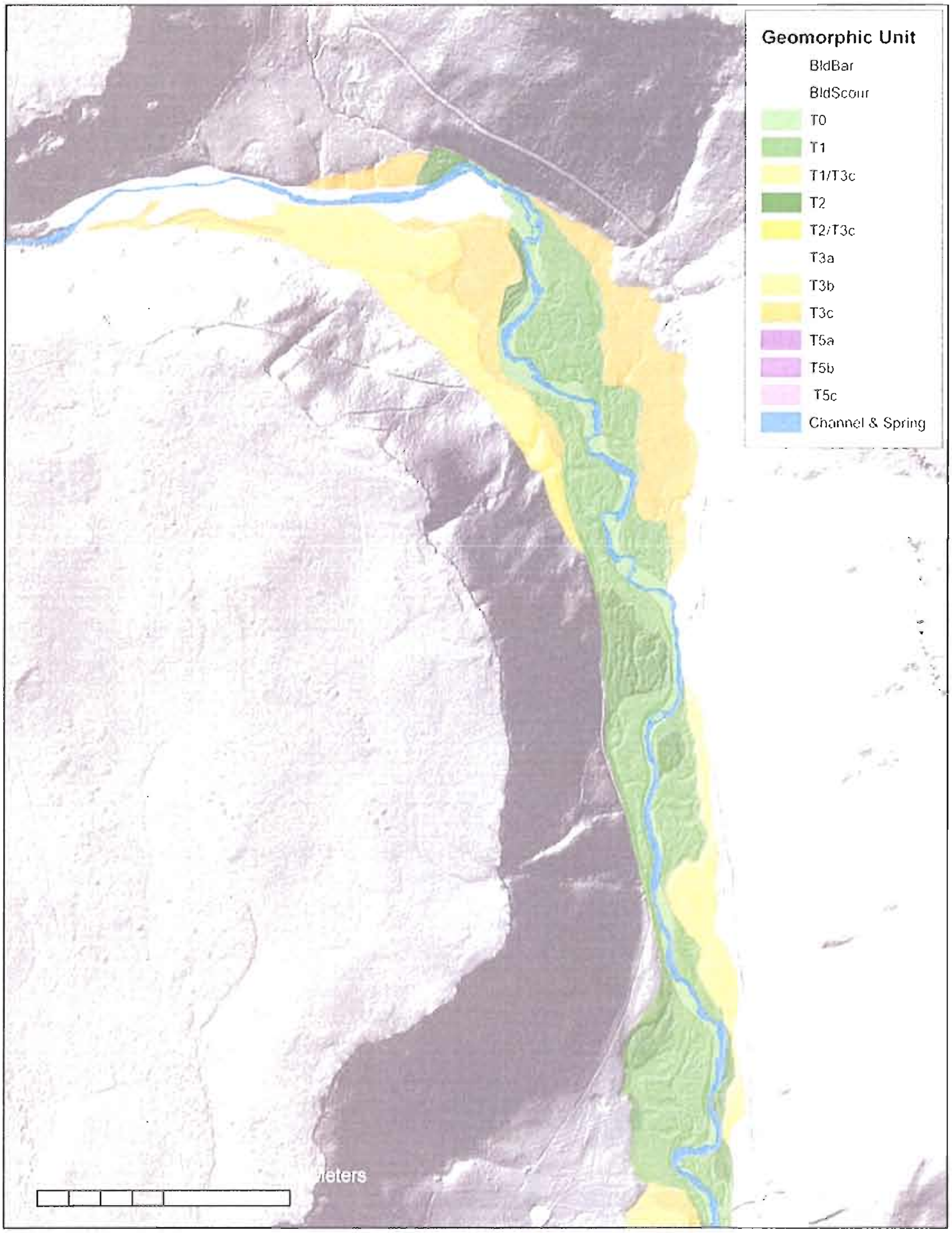

D-2. Plate 1 – Geomorphic surface map

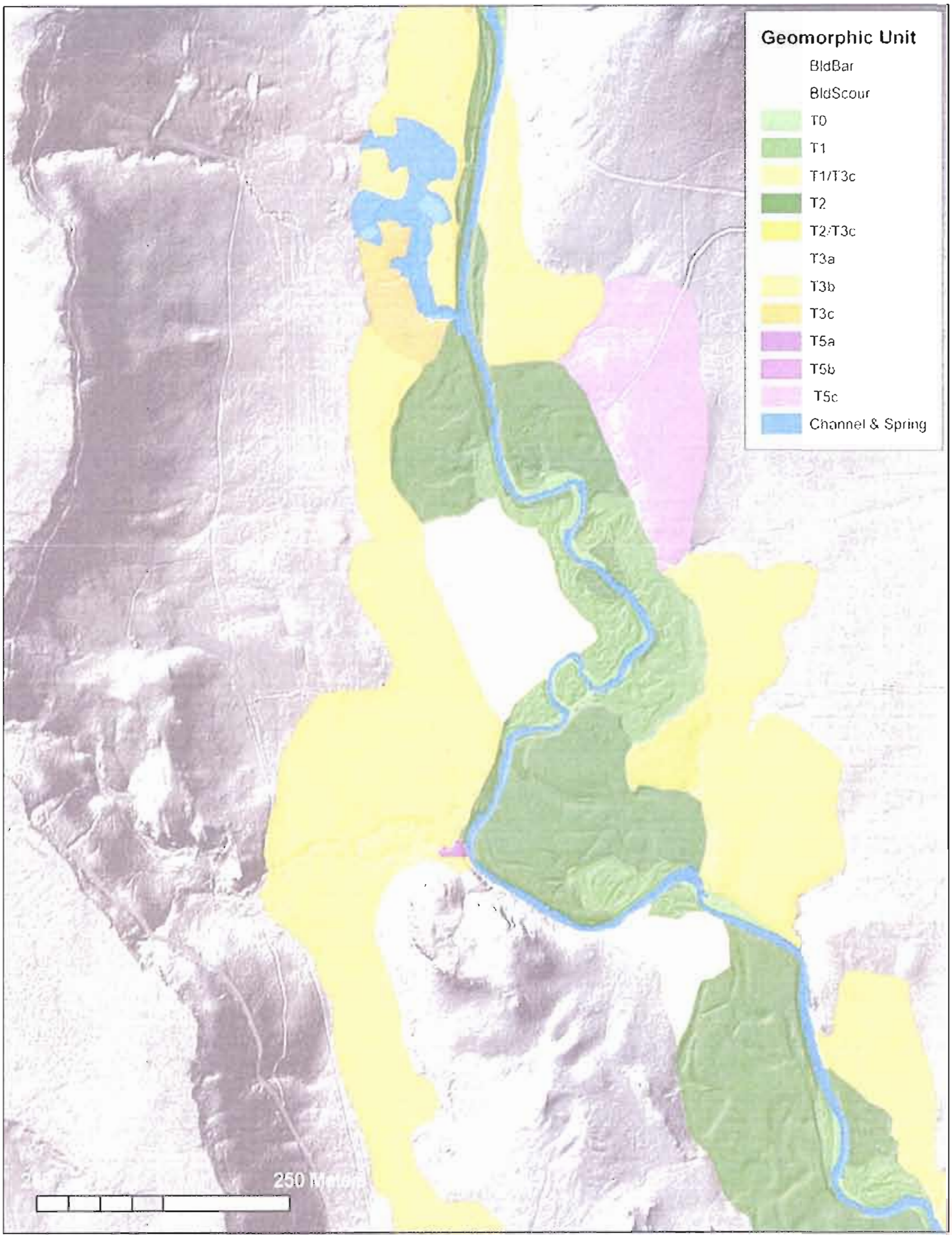

D-3. Plate 2 – Geomorphic surface map

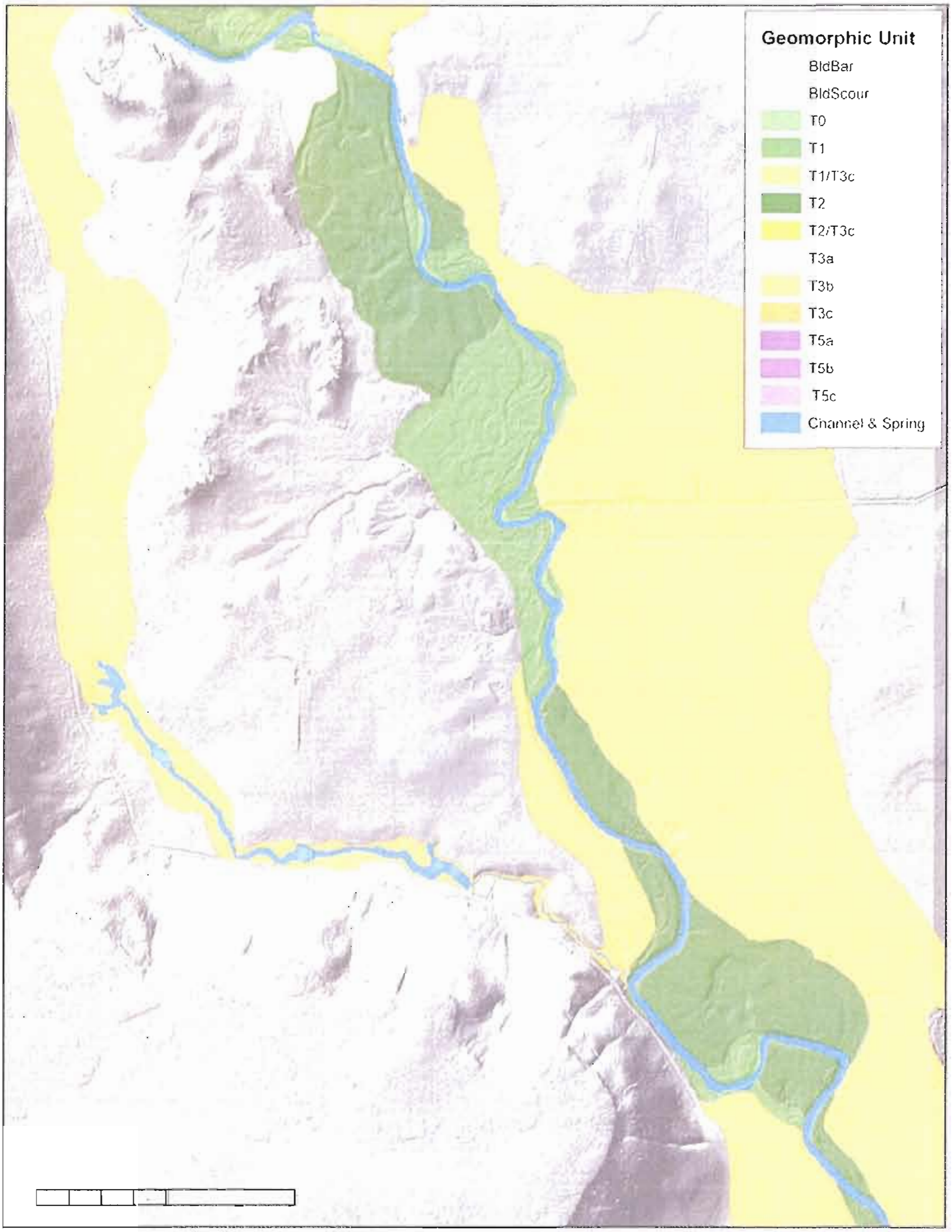

D-4. Plate 3 – Geomorphic surface map

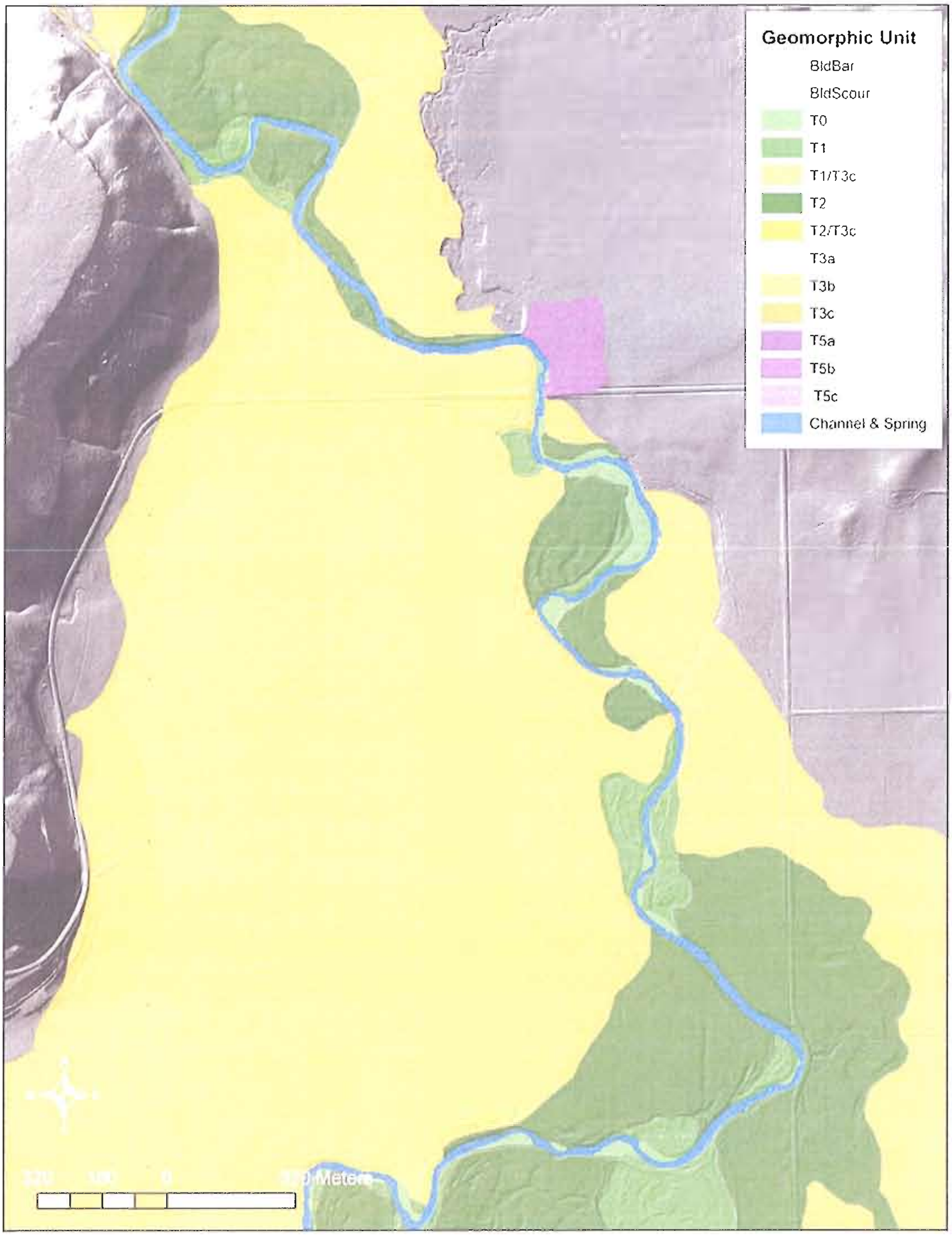

D-5. Plate 4 – Geomorphic surface map

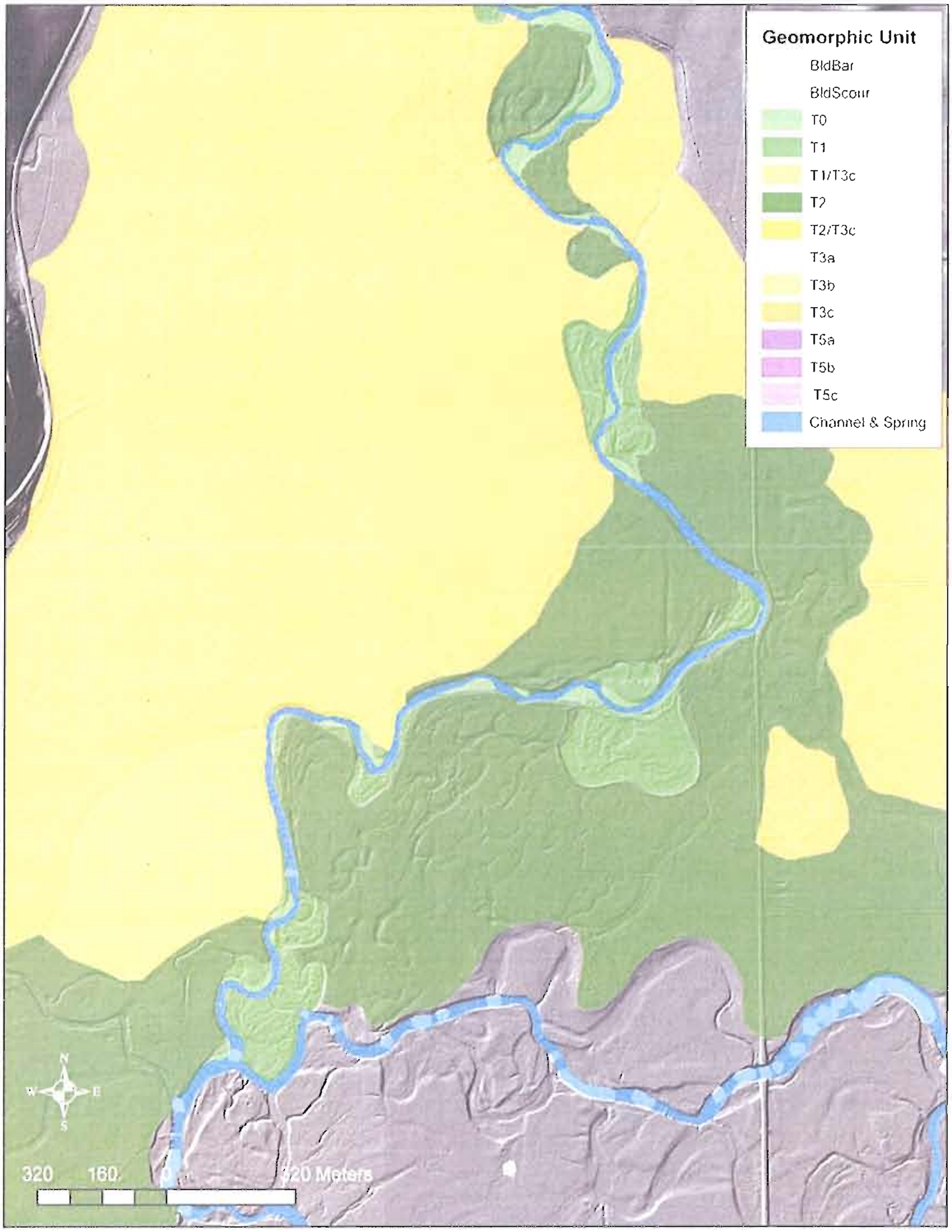

D-6. Plate 5 – Geomorphic surface map

REFERENCES

Bacon, C. R. 1983. Eruptive history of Mount Mazama and Crater Lakes caldera, Cascade Range, U.S.A. *Journal of Volcanology and Geothermal Research* 18, 57-115.

Bacon, C. R., and Lanphere, M. A. 2006. Eruptive history and geochronology of Mount Mazama and the Crater Lake region, Oregon. *Geological Society of America Bulletin* 118, 1331-1359.

Baker, V. R. 1988. Flood erosion. In *Flood Geomorphology*, ed. Victor R. Baker, R. Craig Kochel, and Peter C. Patton, 81-95. New York, NY: Wiley and Sons, Inc.

Baker, V. R. 2002. High-energy megafloods: planetary settings and sedimentary dynamics. *Special Publication of the International Association of Sedimentologists* 32, 3-15.

Baker, V. R., and Bunker, R. C. 1985. Cataclysmic late Pleistocene flooding from glacial Lake Missoula. *Quaternary Science Reviews* 4, 1-41.

Beebee, R. A. 2003. Snowmelt hydrology, paleohydrology, and landslide dams in the Deschutes River Basin, Oregon. PhD diss., University of Oregon.

Benvenuti, M., and Martini, I. P. 2002. Analysis of terrestrial hyperconcentrated flows and their deposits. *Special Publication of the International Association of Sedimentologists* 32, 167-193.

Blair, T. C. 1987. Sedimentary processes, vertical stratification sequences, and geomorphology of the Roaring River alluvial fans, Rocky Mountain National Park, Colorado. *Journal of Sedimentary Petrology* 57, 1-18.

Blair, T. C. 2001. Outburst flood sedimentation of the proglacial Tuttle Canyon alluvial fan, Owens Valley, California, U.S.A. *Journal of Sedimentary Research* 71, 657-679.

Blair, T. C. 2002. Alluvial-fan sedimentation from a glacial-outburst flood, Lone Pine, California, and contrasts with meteorological flood deposits. *Special Publication of the International Association of Sedimentologists* 32, 113-140.

Boggs, S. 2001. *Principles of sedimentology and stratigraphy*, 3rd ed. Upper Saddle River, New Jersey: Prentice Hall.

Bradbury, J. P., Colman, S. M., and Dean, W. E. 2004. Limnological and climatic environments at Upper Klamath Lake, Oregon during the past 45,000 years. *Journal of Paleolimnology* 31, 167-188.

Brakenridge, G. R. 1988. River flood regime and floodplain stratigraphy. In *Flood Geomorphology*, ed. Victor R. Baker, R. Craig Kochel, and Peter C. Patton, 139-156. New York, NY: Wiley and Sons, Inc.

Brierley, G .J., and Fryirs, K. A. 2005. *Geomorphology and river management, applications of the river styles framework.* Malden, MA: Blackwell Publishing.

Briles, C. E., Whitlock, C., Bartlein, P. J., and Higuera, P. 2008. Regional and local controls on postglacial vegetation and fire in the Siskiyou Mountains, northern California, USA. *Palaeogeography, Palaeoclimatology, Palaeoecology* 265, 159-169.

Conaway, J. S. 2000. Hydrogeology and paleohydrology in the Williamson River Basin, Klamath County, Oregon. Master's thesis, Portland State University.

Cornwell, K. 1998. Quaternary break-out flood sediments in the Peshawar basin of northern Pakistan. *Geomorphology* 25, 225-248.

Costa, J. E. 1988. Flood from dam failures. In *Flood Geomorphology*, ed. Victor R. Baker, R. Craig Kochel, and Peter C. Patton, 439-463. New York, NY: Wiley and Sons, Inc.

Costa, J. E., and Schuster, R. L. 1988. The formation and failure of natural dams. *Geological Society of America Bulletin* 100, 1054-1068.

Cressman, L. S., Hagg, W. G., and Laughlin, W. S. 1956. *Klamath Prehistory, the prehistory of the culture of the Klamath Lake area, Oregon.* Transactions of the American Philosophical Society, n.s., 46, pt. 4, 375 -513. Philadephia.

Doerner, J. P., and Carrara, P. E. 2001. Late Quaternary vegetation and climate history of the Long Valley area, west-central Idaho, U.S.A. *Quaternary Research* 56, 103-111.

Donnelly-Nolan, J. M., and Nolan, K. M. Catastrophic flooding and eruption of ash-flow tuff at Medicine Lake Volcano, California. *Geology* 14, 875-878.

Doyle, M. W., and Harbor, J. M. 2003. Modeling the effect of form and profile adjustments on channel equilibrium timescales. *Earth Surface Processes and Landforms* 28, 1271-1287.

Enzel, Y., Ely, L. L., Martinez-Goytre, J., and Vivian, R. G. 1994. Paleofloods and a dam-failure flood on the Virgin River, Utah and Arizona. *Journal of Hydrology* 153, 291-315.

Gaylord, D. R., Foit, F. F. Jr., Schatz, J. K., and Coleman, A. J. 2001. Smith Canyon dune field, Washington, U.S.A.: relation to glacial outburst floods, the Mazama eruption, and Holocene paleoclimate. *Journal of Arid Environments* 47, 403-424.

Geological Survey of Canada (GSC). 1971. *Radiocarbon geochronology of southern British Columbia*, by Fulton. R. J. Report 71-37.

Gerrard, J. 1992. *Soil geomorphology: an integration of pedology and geomorphology.* London, UK: Chapman & Hall.

Graf, W. L. 1977. The rate law in fluvial geomorphology. *American Journal of Science* 277, 178-191.

Graf, W. L. 1982. Distance decay and arroyo development in the Henry Mountains region, Utah. *American Journal of Science* 282, 1541-1554.

Graf. W. L. 1985. *The Colorado River, instability and basin management.* Washington, DC: Association of American Geographers.

Graf, W. L. 1988a. Definition of flood plains along arid-region rivers. In *Flood Geomorphology*, ed. Victor R. Baker, R. Craig Kochel, and Peter C. Patton, 231-242. New York, NY: Wiley and Sons, Inc.

Graf, W.L. 1988b. Fluvial processes in dryland rivers. Berlin, Germany: Springer-Verlag.

Grayson, D. K. 1993. *The desert's past: a natural history of the Great Basin.* Washington, DC: Smithsonian Institution Press.

Hagedorn, J., and Rother, N. 1992. Holocene floodplain evolution of small rivers in the uplands of Lower Saxony, Germany. *Geomorphology* 4, 423-432.

Hallett, D. J., Hills, L. V., and Clague, J. J. 1997. New accelerator mass spectrometry radiocarbon ages for the Mazama tephra layer from Kootenay National Park, British Columbia, Canada. *Canadian Journal of Earth Sciences* 34, 1202-1209.

Hodgson, K. A., and Nairn, I. A. 2005. The c. AD 1315 syn-eruption and AD 1904 post-eruption breakout floods from Lake Tarawera, Haroharo Caldera, North Island, New Zealand. *New Zealand Journal of Geology and Geophysics* 48, 491-506.

Hoffman, M. H. 2005. Rapid late Pleistocene and Holocene climate changes in NW-USA revealed by glacial lobe fluctuations and lake level changes of Flathead Lake, Montana. Paper presentation at the Geological Society of America annual meeting, Salt Lake City, Utah. October 17.

Houben, P. 2007. Geomorphological facies reconstruction of Late Quaternary alluvia by the application of fluvial architecture concepts. *Geomorphology* 86, 94-114.

Hughes, M. J., McDowell, P. F., and Marcus, A. 2006. Accuracy assessment of georectified aerial photographs: Implications for measuring lateral channel movement in a GIS. *Geomorphology* 74, 1-16.

Knighton, D. 1998. *Fluvial forms and processes*. New York, NY: Oxford University Press Inc.

Knox, J. C. 1972. Valley alleviation in southwestern Wisconsin. *Annals of the Association of American Geographers* 62, 401-410.

Knox, J. C. 2006. Floodplain sedimentation in the upper Mississippi Valley: natural versus human accelerated. *Geomorphology* 79, 286-310.

Knudsen, K. L., Sowers, J. M., Ostenaa, D. A., and Levish, D. R. 2002. Evaluation of glacial outburst flood hypothesis for the Big Lost River, Idaho. *Water Science and Application* 5, 217-235.

Lane, S. N., and Richards, K. S. 1997. Linking river channel form and process: time, space and causality revisited. *Earth Surface Processes and Landforms* 22, 249 – 260.

Lavee, H., Imeson, A. C., and Sarah, P. 1998. The impact of climate change on geomorphology and desertification along a Mediterranean-arid transect. *Land Degradation and Development* 9, 407-422.

Loy, W. G., Allan, S., Buckley, A. R., Meacham, J. E., Andreas, L. J., Martin, G. E., and West, R. 2001. *Atlas of Oregon, 2nd ed.*, ed. William Loy. Eugene, OR: University of Oregon Press.

Mack, G. H., McIntosh, W. C., Leeder, M. R., and Monger, H. C. 1996. Plio-Pleistocene pumice floods in the ancestral Rio Grande, southern Rio Grande Rift, USA. *Sedimentary Geology* 103, 1-8.

Magilligan, F. J., and McDowell, P. F. 1997. Stream channel adjustments following elimination of cattle grazing. *Journal of the American Water Resources Association* 32, 867-878.

Manville, V., Segschneider, B., and White, J. D. L. 2002. Hydrodynamic behavior of Taupo 1800a pumice: implications for the sedimentology of remobilized pyroclasts. *Sedimentology* 49, 955-976.

Manville, V., Newton, E. H., and White, J. D. L. 2005. Fluvial response of volcanism: resedimentation of the 1800a Taupo ignimbrite eruption in the Rangitaiki River catchment, North Island, New Zealand. *Geomorphology* 65, 49-70.

Martin, A. C., and Barkley, W. D. 1961. *Seed identification manual.* Berkeley, CA: University of California Press.

Massingill, C. 2008. Monitoring Floodplain Cover Change in South Central Oregon from 1940 to 2000 with GIS Mapping. Poster presented at Maryland Water Monitoring Council Annual Meeting, Baltimore, MD. December 4.

McDowell, P. F. 1983. Evidence of stream response to Holocene climatic change in a small Wisconsin watershed. *Quaternary Research* 19, 100-116.

Minckley, T. A., Whitlock, C., and Bartlein, P. J. 2007. Vegetation, fire, and climate history of the northwestern Great Basin during the last 14,000 years. *Quaternary Sciences Review* 26, 2167-2184.

Mohr, J. A., Whitlock, C., and Skinner, C. N. 2000. Postglacial vegetation and fire history, eastern Klamath Mountains, California, USA. *The Holocene* 10, 587-601.

Nanson, G.C., and Croke, J. C. 1992. A genetic classification of floodplains. *Geomorphology* 4, 459-486.

Native Plant Society of Oregon - Klamath Basin Chapter and Rabe Consulting (NPSO). 2007. *Common Plants of Upper Klamath Basin.* Klamath Falls, OR: Koko 2008. Graphix Design ~ Printing.

Natural Resources Conservation Service (NRCS). 2005. *Sprague – 18010202 Description.* U.S. Department of Agriculture. ftp://ftp-fc.sc.egov.usda.gov/OR/HUC/basins/highdesert/18010202_10-21-05.pdf [accessed December 10, 2008].

O'Connor, J. E. 1993. Hydrology, hydraulics, and geomorphology of the Bonneville Flood. *Geological Society of America*, Special Paper 274.

O'Connor, J. E., and Baker, V. R. 1992. Magnitudes and implications of peak discharge from glacial Lake Missoula. *Geological Society of America Bulletin*, v. 104, p. 267-279.

O'Connor, J. E., and Beebee, R. A. 2008. Floods from natural rock-material dams. In *Megafloods on Earth and Mars*, ed. D. Burr, P. Carling, and V. Baker, V. New York, NY: Cambridge University Press.

O'Connor, J. E., Grant, G. E., amd Costa, J. E. 2002. The geology and geography of floods. In Ancient floods, modern hazards: principles and applications of paleoflood hydrology. *Water Science and Application* 5, 359-385.

Ogden, R., Spooner, N., Reid, M., and Head, J. 2001. Sediment dates with implications for the age of the conversion from paleochannel to modern fluvial activity on the Murray River and tributaries. *Quaternary International* 83-85, 195-209.

Passmore, D. G., and Macklin, M. G. 2000. Late Holocene channel and floodplain development in a wandering gravel-bed river: the river South Tyne at Lambley, Northern England. *Earth Surfaces Processes and Landforms* 25, 1237-1256.

Richards, K. 1982. *Rivers, form and process in alluvial channels*. New York, NY: Methuen & Co. Ltd.

Schumm, S. A. 1969. River metamorphosis. *Journal of the Hydraulics Division* 95, 255-273.

Schumm, S. A. 1973. Geomorphic thresholds and complex response of drainage systems. In *Fluvial geomorphology*, ed. M. Morisawa, 299-310. Binghamton: State University of New York, Publications in Geomorphology.

Schumm, S. A. 1979. Geomorphic thresholds: the concept and its applications. *Transactions of the Institute of British Geographers*, new series 4, 485-515.

Schumm, S. A. 1985. Patterns of alluvial rivers. *Annual Review of Earth Planetary Sciences* 13, 5-27.

Schumm. S. A. 2005. *River variability and complexity*. Cambridge, NY: Cambridge University Press.

Schumm, S. A., Mosley, M. P., and Weaver, W. E. 1987. *Experimental fluvial geomorphology*. New York, NY: John Wiley & Sons, Inc.

Sherrod, D. R., and Pickthorn, L. B. G. 1992. *Geologic map of the west half of the Klamath Falls 1° by 2° quadrangle, south-central Oregon.* 1:250,000. U.S. Geologic Survey, Map 1-2182.

Simon, A. 1989. A model of channel response in disturbed alluvial channels. *Earth Surface Processes and Landforms* 14, 11-26.

Simon, A. 1992. Energy, time, and channel evolution in catastrophically disturbed fluvial systems. *Geomorphology* 5, 345-372.

Simon, A., Curini, A., Darby, S. E., and Langendoen, E. J. 2000. Bank and near-bank processes in an incised channel. *Geomorphology* 35, 193-217.

Simon, A., and Darby, S. 1999. The nature and significance of incised river channels. In *Incised River Channels: processes, forms, engineering and management,* ed. Stephen E. Darby and Andrew Simon, 3-18. West Sussex, England: John Wiley & Sons.

Simon, A., and Downs, P. W. 1995. An interdisciplinary approach to evaluation of potential instability in alluvial channels. *Geomorphology* 12, 215-232.

Simon, A., and Hupp, C. R. 1986. Channel evolution in modified Tennessee channels. Proceedings of the Fourth Federal Interagency Sedimentation Conference, Las Vegas, NV. March 24-27.

Simon, A., and Rinaldi, M. 2006. Disturbance, stream incision, and channel evolution: the roles of excess transport capacity and boundary materials in controlling channel response. *Geomorphology* 79, 361-383.

Simon, A., and Thomas, R. E. 2002. Processes and forms of an unstable alluvial system with resistant, cohesive streambeds. *Earth Surface Processes and Landforms* 27, 699-718.

Smith, G. A. 1993. Missoula flood dynamics and magnitudes inferred from sedimentology of slack-water deposits on the Columbia Plateau, Washington. *Geological Society of America Bulletin* 105, 77-100.

Starratt, S. W., Barron, J. A., Kneeshaw, T., Phillips, R. L., Bischoff, J. L., Lowenstern, J. B., and Wanket, J. A. 2002. A Holocene record from Medicine Lake, Siskiyou County, California: preliminary diatom, pollen, geochemical, and sedimentological data. Proceedings of the 19th Pacific Climate Workshop, Pacific Grove, CA. March 3-6.

Stuvier, M., and Reimer, P. J. 1993. Extended C-14 data-base and revised CALIB 3.0 C-14 age calibration program. *Radiocarbon* 35, 215-230.

Thorne, C. R., Allen, R. G., and Simon, A. 1996. Geomorphological river channel reconnaissance for river analysis, engineering and management. *Transactions of the Institute of British Geographers* 21, 469-483.

Tucker, G. E., and Slingerland, R. 1997. Drainage basin responses to climate change. *Water Resources Research* 33, 2031-2047.

U.S. Geological Survey (USGS). Surface-Water Data for the Nation. National Water Information System: Web Interface. http://nwis.waterdata.usgs.gov [accessed December 20, 2008].

U.S. Geological Survey (USGS). 1999. *Channel and drainage-basin response of the Toutle River system in the aftermath of the 1980 eruption of Mount St. Helens, Washington*, by Simon, A. Open-file report 96-633.

U.S. Geological Survey (USGS). 2007. *Ground-water hydrology of the Upper Klamath Basin, Oregon and California,* by Gannett, M. W., Lite, K. E. Jr., La Marche, J. L., Fisher, B. J., and Polette, D. J. Scientific Investigation report 2007-5050.

Watershed Sciences and ZM MaxDepth Aquatics (WS/ZM). 2005. *Sprague River LiDAR Remote Sensing and data collection.* Chiloquin, OR: The Klamath Tribes.

Welcher, K. E. 1993. Holocene channel changes of Camp Creek, an arroyo in eastern Oregon. Master's thesis, University of Oregon.

Wigand, P. E., and Rhode, D. 2002. Great basin vegetation history and aquatic systems: the last 150,000 years. In Great Basin Aquatic Systems History, Smithsonian Contributions to Earth Sciences, vol. 33, ed. R. Hershler, D.B. Madsen, and D.R. Currey, 309-367. Washington, DC: Smithsonian Institution Press.

Williams, G. P., and Costa, J. E. 1988. Geomorphic measurements after a flood. Flood Geomorphology. In *Flood Geomorphology*, ed. Victor R. Baker, R. Craig Kochel, and Peter C. Patton, 65-80. New York, NY: Wiley and Sons, Inc.

Womack, W. R., and Schumm, S. A. 1977. Terraces of Douglas Creek, northwestern Colorado: an example of episodic erosion. *Geology* 5, 72-76.

Zdanowicz, C.M., Zielinski, G.A., and Germani, M.S. 1999. Mount Mazama eruption: calendrical age verified and atmospheric impact assessed. *Geology* 27, 621-624.